INFORMATION TO USERS

This manuscript has been reproduced from the microfilm master. UMI films the text directly from the original or copy submitted. Thus, some thesis and dissertation copies are in typewriter face, while others may be from any type of computer printer.

The quality of this reproduction is dependent upon the quality of the copy submitted. Broken or indistinct print, colored or poor quality illustrations and photographs, print bleedthrough, substandard margins, and improper alignment can adversely affect reproduction.

In the unlikely event that the author did not send UMI a complete manuscript and there are missing pages, these will be noted. Also, if unauthorized copyright material had to be removed, a note will indicate the deletion.

Oversize materials (e.g., maps, drawings, charts) are reproduced by sectioning the original, beginning at the upper left-hand corner and continuing from left to right in equal sections with small overlaps. Each original is also photographed in one exposure and is included in reduced form at the back of the book.

Photographs included in the original manuscript have been reproduced xerographically in this copy. Higher quality 6" x 9" black and white photographic prints are available for any photographs or illustrations appearing in this copy for an additional charge. Contact UMI directly to order.

University Microfilms International
A Bell & Howell Information Company
300 North Zeeb Road, Ann Arbor, MI 48106-1346 USA
313/761-4700 800/521-0600

Order Number 9116949

Hydrothermal reaction of lime with fly ash to produce calcium silicates for dry flue gas desulfurization

Peterson, Joseph Roger, Ph.D.

The University of Texas at Austin, 1990

Copyright ©1990 by Peterson, Joseph Roger. All rights reserved.

U·M·I
300 N. Zeeb Rd.
Ann Arbor, MI 48106

NOTE TO USERS

THE ORIGINAL DOCUMENT RECEIVED BY U.M.I. CONTAINED PAGES WITH BLACK MARKS AND POOR PRINT. PAGES WERE FILMED AS RECEIVED.

THIS REPRODUCTION IS THE BEST AVAILABLE COPY.

HYDROTHERMAL REACTION OF LIME WITH FLY ASH TO PRODUCE CALCIUM SILICATES FOR DRY FLUE GAS DESULFURIZATION

by

JOSEPH ROGER PETERSON, B.S., M.S.

DISSERTATION

Presented to the Faculty of the Graduate School of

The University of Texas at Austin

in Partial Fulfillment

of the Requirements

for the Degree of

DOCTOR OF PHILOSOPHY

THE UNIVERSITY OF TEXAS AT AUSTIN

December, 1990

HYDROTHERMAL REACTION OF LIME WITH FLY ASH TO PRODUCE CALCIUM SILICATES FOR DRY FLUE GAS DESULFURIZATION

APPROVED BY
SUPERVISORY COMMITTEE:

Gary T. Rochelle

Hugo Steinfink

Joel Barlow

Ramon Carrasquillo

Howard Liljestrand

Copyright
by
Joseph Roger Peterson

1990

To Annick

ACKNOWLEDGEMENTS

I am deeply indebted to Dr. Gary Rochelle. He is an excellent instructor, in the classroom as well as in our weekly meetings. I greatly admire his technical expertise and his down-to-earth personality. I also appreciate the guidance and support of my committee, Professors Joel Barlow, Ramon Carrasquillo, Howard Liljestrand, and Hugo Steinfink. Dr. Carrasquillo has also provided financial support for a portion of the research described in this dissertation.

I would like to thank Dr. Ingemar Bjerle for giving me the chance to live and work in Sweden. My wife and I had a wonderful time with all of our friends and truly enjoyed the entire experience. Dr. Bjerle and his secretary, Anna-Stina, handled a lot of the beauraucratic details which would have been impossible for my wife and I to handle alone. Dr. Bjerle and his wife, Ingrid, were also excellent hosts for our families when they came to visit us in Sweden.

I thank Tom Petersen and Hans Karlsson, at the University of Lund, for their help and companionship while I worked in Sweden. They made me feel like I belonged to the group, even though I could barely speak their language and I was a long way from home. I will always remember the discussions with Hans over a glass of "stor stark öl" at the pizzaria and all of the card games with Tom and his wife, Ulrika.

I would also like to thank the other members of Dr. Rochelle's research group, present and past for all of the good times. I hope that life will be good to all of them. Special thanks go to Will White and Dave Austgen for unique views on world events and admirable personal and professional qualities, respectively.

I have received financial support through the Texas Advanced Technology Program, Acurex Corporation, the U.S. EPA, and through the various industrial sponsors of Dr. Rochelle's FGD program.

I have also received a great deal of support, both financial and technical, from Radian Corporation. I have learned about the practical side of FGD and engineering from Charlie Brown and Gary Blythe. I also appreciate the efforts of Pat Thompson to find small projects to keep me busy and financially stable.

I owe a great deal to my friends Dale Johnson and Kevin Hess. In times of crisis or overload, they were always there to provide a couch to veg-out on, baseball or football on the TV, and beer to drink. Come to think of it, it was just the couch and the sports, since I always bought the beer.

I am deeply indebted to my family. I don't think that my father really knows what chemical engineers do, but he has always supported my goals and pushed me to to excel at whatever I choose to do in life. My mother and my brothers and sisters have also been only a phone call away, whenever I needed support and guidance in my life.

Finally, I owe the most to my wife, Annick. She has been more than supportive and understanding through all of the late nights of research, even though our children were trying her patience. She is an excellent mother and friend and I am very lucky to have her for my wife.

HYDROTHERMAL REACTION OF LIME WITH FLY ASH TO PRODUCE CALCIUM SILICATES FOR DRY FLUE GAS DESULFURIZATION

Publication No. _____

Joseph Roger Peterson, Ph.D.
The University of Texas at Austin, 1990

Supervising Professor : Gary T. Rochelle

Experimental work was performed to determine the important chemical interactions involved in the formation of lime/fly ash solids for flue gas desulfurization. Three types of experiments were used: fly ash dissolution experiments, where the fly ash dissolution rate was measured in the absence of any precipitation reactions which may alter the dissolution rate; lime/fly ash reaction experiments, where hydrated lime was reacted with various sources of fly ash to determine the effect of fly ash type on the lime/fly ash reaction; and reagent chemical experiments, where the major components of fly ash were simulated with reagent chemicals to determine the relative importance of the various components of the fly ash. A significant amount of work was also performed to determine the effects of recycle (i.e. sulfite and sulfate) on the reaction of hydrated lime with fly ash.

The fly ash dissolution experiments showed that the high-calcium fly ashes were much more reactive than the low- and medium-calcium fly ashes. A significant fraction of the high-calcium fly ashes dissolved instantly, while the other fly ashes dissolved uniformly. The aluminum present in the high-calcium fly ashes

was much more reactive than the aluminum present in the low- and medium-calcium fly ashes.

The dissolution rate of silica from the low-calcium fly ash was found to be first-order in the hydroxide concentration of the solution. The activation energy for silica dissolution was determined to be 20.5 kcal/mol, comparable to previous results with the dissolution of quartz and amorphous silica. The dissolution rate of silica from the high calcium fly ash was much more sensitive to the hydroxide concentration in the solution because the glass present in the fly ash is much different than that present in the low-calcium fly ash.

The data from the lime/fly ash experiments showed a clear effect of fly ash type on the reaction of hydrated lime with fly ash. The solids produced with the high-calcium fly ash had a lower surface area and reactivity towards SO_2 than the solids produced from the low- and medium-calcium fly ashes.

The data from the reagent chemical experiments showed that the reason for the low reactivity of the solids from the high-calcium fly ash is due to the very reactive aluminum content of the fly ash. The reagent chemical experiments showed that the calcium-silicates produced by the reaction of hydrated lime with silica fume were amorphous and had a high surface area. These solids were very reactive towards SO_2. In contrast, the calcium-aluminate solids formed by reacting hydrated lime with $Al(OH)_3$ were very crystalline, had a low surface area, and were unreactive towards SO_2.

The experiments investigating the effect of recycle materials showed that the addition of gypsum to the slurry inhibited the formation of the unreactive calcium-aluminate materials, but had no effect on the formation of the calcium-silicate solids. The addition of calcium sulfite hemihydrate to the slurry changed the calcium-aluminate product, but the new product also had a low surface area and was unreactive towards SO_2.

TABLE OF CONTENTS

Acknowledgements v

Abstract vii

List of Tables xiii

List of Figures xiv

Chapter I : Flue Gas Desulfurization with Lime/Fly Ash Solids 1

1.1 Use of Coal to Produce Electricity 1

1.2 The Need for Flue Gas Desulfurization 2
- 1.2.1 Limestone Slurry Scrubbing 3
- 1.2.2 Spray-Dry Scrubbing 4
- 1.2.3 Dry FGD Alternatives 6
  - 1.2.3.1 Boiler Injection Processes 7
  - 1.2.3.2 Duct Injection Processes 8

1.3 Objectives and Scope of this Work 10

Chapter II : Lime/Fly Ash Solids for FGD : Literature Review 12

2.1 Bench-Scale Data 12
- 2.1.1 Effect of slurry temperature 13
- 2.1.2 Effect of fly ash:lime ratio 15
- 2.1.3 Effect of fly ash type 16
- 2.1.4 Effect of recycle materials 17
- 2.1.5 Effect of fly ash particle size 20
- 2.1.6 Effect of additives for fly ash dissolution 21
- 2.1.7 Investigations with other materials 22
- 2.1.8 Reactivation of boiler injection solids 23

2.2 Pilot-Scale Data 24
- 2.2.1 Effect of process variables 25
- 2.2.2 Effect of solids water content 25

2.3 Summary of Lime/Fly Ash for FGD 26

Chapter III : Chemistry and Mineralogy of Pozzolans 28

3.1 Introduction to Pozzolanic Materials 28

3.2 Chemistry and Mineralogy of Fly Ash 29
3.2.1 Origin of fly ash 29
3.2.2 Chemical composition of fly ash 30
3.2.3 Crystalline species in fly ash 31

3.3 Chemistry and Structure of the Glassy Fraction of the Fly Ash 33

3.4 Summary 42

Chapter IV : Chemical Reactions in the $Ca(OH)_2$-Pozzolan System 43

4.1 Introduction 43

4.2 Reactivities of silica and alumina 43

4.3 The CaO-SiO_2-H_2O system 48

4.4 The CaO-Al_2O_3-H_2O system 51

4.5 Other considerations 52

4.6 Summary of pozzolanic reactions 53

Chapter V : Experimental Apparatus and Procedure 54

5.1 Fly ash dissolution experiments 54

5.2 Solids Preparation 58

5.3 Solids characterization experiments 60
5.3.1 Solids reactivity experiments - equipment and procedure 61
5.3.2 Solids reactivity experiments - data analysis 64
5.3.3 Sugar Dissolution of Fly Ash/Lime Solids 64
5.3.4 Selective Dissolution Experiments 69

Chapter VI : Fly Ash Dissolution Experiments 72

6.1 Effect of fly ash type 72

6.2 Effect of NaOH concentration 78

6.3 Effect of slurry temperature 89

6.4 Effect of fly ash grinding 90

Chapter VII : Experiments Using Reagent Chemicals 96

7.1 Reaction of $Ca(OH)_2$ with silica 97

7.2 Reaction of $Ca(OH)_2$ with aluminum 106

7.3 Reaction of $Ca(OH)_2$ with mixtures of silica and aluminum 111

7.3 Effects of recycle materials 117

Chapter VIII : Experiments Using Lime/Fly Ash Solids 126

8.1 Effect of fly ash type 126
8.1.1 Solution analyses 127
8.1.2 Solids analyses 132
8.1.3 Chemical and mineralogical characterization of solids 141
8.1.4 Comparing reaction with fly ash dissolution 145

8.2 Effect of recycle materials 153
8.2.1 Effect of gypsum 153
8.2.2 Effect of calcium sulfite hemihydrate 160

8.3 Effect of fly ash grinding 162

Chapter IX : Summary, Conclusions, and Recommendations 169

9.1 Summary 169

9.2 Conclusions 170
9.2.1 Fly ash dissolution experiments 170
9.2.2 Reagent chemical experiments 171
9.2.3 Lime/fly ash experiments 173

9.3 Recommendations 174

Appendix A. Analytical Techniques 177

A.1 Atomic absorption 177

A.2 BET surface area 180

A.3 X-ray powder diffraction 181

Appendix B. Mathematical Treatment of Fly Ash Dissolution Data 183

B.1 Surface area analysis 184

B.2 Effect of hydroxide concentration 185

References Cited 188

LIST OF TABLES

Table 3.1 Effect of coal type on the chemical composition of fly ash. 31
Table 5.1 Chemical compositions of fly ashes 58
Table 7.1 Characterization of reagent chemicals. 97
Table 8.1 Determination of reactive calcium content of several fly ashes 135
Table 8.2 Summary of the X-ray diffraction analyses for some lime/fly ash solids. 146
Table A.1 Summary of parameters for atomic absorption analysis. 179

LIST OF FIGURES

Figure 1.1 Schematic of spray drying process for flue gas desulfurization.... 5

Figure 1.2 Schematic of duct-injection system : slurry injection 9

Figure 1.3 Schematic of duct-injection system : dry solids injection with separate humidification 10

Figure 2.1 Effect of slurry temperature on reactivity of lime/fly ash solids ... 14

Figure 2.2 Process concept for flue gas desulfurization using lime/fly ash solids..... 18

Figure 3.1 Electron microprobe chemical analyses for a low-calcium fly ash obtained from a bituminous coal..... 32

Figure 3.2 Electron microprobe chemical analyses for a high-calcium fly ash obtained from a lignite coal..... 33

Figure 3.3 Electron microprobe chemical analyses for a high-calcium fly ash obtained from a subbituminous coal. 34

Figure 3.4 Schematic representation in two dimensions of the structure of silica..... 35

Figure 3.5 Proposed structural differences between fly ash glass types..... 37

Figure 3.6 Use of x-ray diffraction for the detection of the "amorphous hump" present in fly ash..... 38

Figure 3.7 X-ray diffraction patterns for Na_2O-SiO_2 model glasses..... 39

Figure 3.8 Effect of modifier content on 2qmax for Na_2O-SiO_2 model glasses 41

Figure 4.1 Mechanism for the dissolution of silica in the presence of the hydroxide ion..... 45

Figure 4.2 Effect of solution pH and temperature on the solubility of amorphous silica in water.....46

Figure 4.3 Effect of solution pH on the dissolution rate of amorphous silica.....47

Figure 4.4 Equilibria between hydrous calcium silicates and solutions.....50

Figure 5.1. Apparatus used for fly ash dissolution experiments and solids preparation experiments.....57

Figure 5.2 Effect of EDTA on the dissolution rate of fly ash.....59

Figure 5.3. Packed bed reactor system.....62

Figure 5.4 Typical data from packed bed reactor experiments.....65

Figure 5.5 Determination of the time required for sugar dissolution tests.....68

Figure 5.6 Results from sugar dissolution tests on calcium silicate solids.....70

Figure 6.1 Effect of fly ash type on aluminum dissolution from the fly ash..74

Figure 6.2 Effect of fly ash type on silica dissolution from the fly ash.....75

Figure 6.3 Effect of fly ash type on the position of the amorphous hump determined by x-ray diffraction.....77

Figure 6.4 Effect of NaOH on the dissolution of silica from a low-calcium fly ash.....79

Figure 6.5 Collapsing the data for the effect of NaOH on the dissolution of silica from a low-calcium fly ash.....81

Figure 6.6 Determining the order of fly ash dissolution with respect to NaOH.....82

Figure 6.7 Comparing the rates of silicon and aluminum dissolution for low- and high-calcium fly ashes.....83

Figure 6.8 Effect of NaOH concentration on high-calcium fly ash dissolution.....85

Figure 6.9 Collapsing the data for the effect of NaOH on the dissolution of silica from a high-calcium fly ash.....86

Figure 6.10 Determining the order of fly ash dissolution with respect to NaOH.....87

Figure 6.11 Proposed mechanism for the dissolution of amorphous silica under alkaline conditions.....88

Figure 6.12 Effect of temperature on the dissolution of silica from a low-calcium fly ash.....91

Figure 6.13 Arrhenius plots for the dissolution of low calcium fly ash.....92

Figure 6.14 Effect of grinding on the dissolution rate of silica from a low-calcium fly ash.....94

Figure 6.15 Effect of grinding on the dissolution rate of aluminum from a low-calcium fly ash.....95

Figure 7.1 Comparing the dissolution rates of reagent aluminum sources....98

Figure 7.2 Filtrate analyses for silica fume reacting with $Ca(OH)_2$..... 100

Figure 7.3 Silica fume reacting with $Ca(OH)_2$, sugar titration for residual $Ca(OH)_2$..... 101

Figure 7.4 Powder x-ray diffraction pattern for solids produced by slurrying silica fume with $Ca(OH)_2$ for 0.5 hours..... 102

Figure 7.5 Powder x-ray diffraction pattern for solids produced by slurrying silica fume with $Ca(OH)_2$ for 7.5 hours..... 103

Figure 7.6 Reactivity and surface area of solids produced by reacting silica fume with $Ca(OH)_2$..... 104

Figure 7.7 Solution composition for $Ca(OH)_2$ reacting with $Al(OH)_3$..... 107

Figure 7.8 Effect of slurry temperature on solids free $Ca(OH)_2$ content.... 108

Figure 7.9 Powder x-ray diffraction pattern for solids produced by slurrying $Al(OH)_3$ with $Ca(OH)_2$ for 0.5 hours..... 109

Figure 7.10 Powder x-ray diffraction pattern for solids produced by slurrying $Al(OH)_3$ with $Ca(OH)_2$ for 7.5 hours..... 110

Figure 7.11 Results from surface area and solids reactivity experiments..... 112

Figure 7.12 Effect of slurry time on solids surface area..... 114

Figure 7.13 Reactivity of mixture solids towards SO_2..... 115

Figure 7.14 Powder x-ray diffraction pattern for solids produced by slurrying a mixture of $Al(OH)_3$ and silica fume with $Ca(OH)_2$ for 5 hours..... 116

Figure 7.15 Effect of recycle materials on the solution composition for slurries of $Ca(OH)_2$ and $Al(OH)_3$..... 118

Figure 7.16 Effect of recycle materials on the reaction of $Ca(OH)_2$ with $Al(OH)_3$..... 120

Figure 7.17 Effect of recycle materials on the development of surface area for calcium aluminate solids..... 121

Figure 7.18 Powder x-ray diffraction pattern for solids produced by slurrying a mixture of $Al(OH)_3$, $CaSO_3 \cdot 0.5H_2O$, and $Ca(OH)_2$ for 5 hours..... 122

Figure 7.19 Effect of gypsum on the reaction of $Ca(OH)_2$ with a mixture of $Al(OH)_3$ and silica fume..... 124

Figure 7.20 Effect of gypsum on the reaction of $Ca(OH)_2$ with a mixture of $Al(OH)_3$ and silica fume..... 125

Figure 8.1 Effect of fly ash type on the dissolved calcium concentration in the slurry..... 128

Figure 8.2 Effect of fly ash type on the solution pH for slurries of $Ca(OH)_2$ and fly ash..... 129

Figure 8.3 Solution composition for slurry of high calcium fly ash with $Ca(OH)_2$..... 130

Figure 8.4 Determining the relative saturation with respect to $Ca(OH)_2$ for the lime/fly ash slurries..... 131

Figure 8.5 Effect of fly ash type on its reactivity towards $Ca(OH)_2$..... 133

Figure 8.6 Effect of fly ash chemical composition on its reactivity towards $Ca(OH)_2$. 134

Figure 8.7 Effect of fly ash type on its reactivity towards $Ca(OH)_2$..... 136

Figure 8.8 Effect of fly ash type on surface area development of lime/fly ash solids..... 138

Figure 8.9 Effect of fly ash type on lime/fly ash solids reactivity towards SO_2. 139

Figure 8.10 Effect of fly ash type on the reactivity of lime/fly ash solids towards SO_2.. 140

Figure 8.11 Approximation of the chemical composition of the lime/fly ash products..... 142

Figure 8.12 SEM photograph of low-calcium fly ash/$Ca(OH)_2$ mixture after 0.25 hours of slurrying..... 143

Figure 8.13 SEM photograph of low-calcium fly ash/$Ca(OH)_2$ mixture after 8 hours of slurrying..... 144

Figure 8.14 SEM photograph of high-calcium fly ash/$Ca(OH)_2$ mixture after 0.25 hours of slurrying..... 147

Figure 8.15 SEM photograph of high-calcium fly ash/$Ca(OH)_2$ mixture after 8 hours of slurrying..... 148

Figure 8.16 Effect of fly ash type on the chemical composition of the lime/fly ash solids..... 149

Figure 8.17 Comparison of reaction with dissolution for a low-calcium fly ash..... 151

Figure 8.18 Comparison of reaction with dissolution for a high-calcium fly ash. 152

Figure 8.19 Effect of gypsum on the solution composition of lime/fly ash slurry for a high-calcium fly ash. 155

Figure 8.20 Effect of gypsum on the reaction between fly ash and $Ca(OH)_2$ 156

Figure 8.21 Effect of gypsum on the surface areas of lime/fly ash solids. ... 157

Figure 8.22 Effect of gypsum on the surface areas of lime/fly ash solids. ... 158

Figure 8.23 Effect of gypsum on the reactivity of lime/fly ash solids towards SO_2. 159

Figure 8.24 Effect of $CaSO_3 \cdot 0.5H_2O$ on lime/fly ash solids reactivity towards SO_2. 161

Figure 8.25 Effect of fly ash grinding on the reaction of fly ash with $Ca(OH)_2$ 163

Figure 8.26 Effect of fly ash grinding on the reaction of fly ash with $Ca(OH)_2$ 164

Figure 8.27 Effect of fly ash grinding on the surface area of the lime/fly ash solids 165

Figure 8.28 Effect of fly ash grinding on the surface area of the lime/fly ash solids 166

Figure 8.29 Effect of fly ash grinding on the reactivity of the lime/fly ash solids towards SO_2. 168

Figure B.1 Effect of initial surface area of the fly ash on the initial dissolution rate of silica from a low-calcium fly ash 186

Figure B.2 Graphical analysis of effect of fly ash surface area. 187

Chapter I

Flue Gas Desulfurization with Lime/Fly Ash Solids

This dissertation examines various reactions which take place when hydrated lime is mixed with fly ash and water at high temperature. These reactions are of interest because they produce solids which are very reactive towards SO_2. These "lime/fly ash" solids have potential use as reagent for certain systems which may be used to control the SO_2 emissions from coal-fired power plants. Before discussing the reactions of interest, some background material concerning the combustion of coal and the types of emission control systems will be presented to introduce the reader to the technology of flue gas desulfurization using lime/fly ash solids.

1.1 Use of Coal to Produce Electricity

Coal is the most common form of fuel for generating electrical power in the United States. The net maximum capacity for coal-fired power plants in the USA is approximately 308,000 MW of electricity while the capacities of the nuclear, oil, and natural gas power plants are only 87,000, 85,000, and 128,000 MW respectively (Melia et al., 1986). One of the major reasons for the widespread use of coal in the USA is the large deposits found in this country. By some estimates, the United States has enough coal to provide all the electricity needed in this country for the next 600 years (Edgar, 1983).

Due to the large base of installed electrical generating capacity and to the large coal reserves in this country, coal is likely to remain the dominant fuel for electrical power generation well into the next century. However, hazardous

materials are produced when coal is burned and the emissions of these materials must be controlled to minimize their impact on the environment.

When coal is burned, the organic material present in the coal oxidizes to produce mainly carbon dioxide and water. The reactions which occur are very exothermic and produce heat which can be converted to electrical energy. The other constituents of the coal either oxidize to form gaseous species (such as sulfur oxidizing to gaseous SO_2) or fuse together to form small molten particles (this is the case for most of the inorganic species in the coal). These small molten particles become entrained in the exhaust gases and eventually cool to form particulate matter which is called "fly ash". The reactivity of this fly ash material is the main subject of this dissertation.

1.2 The Need for Flue Gas Desulfurization

The combustion of coal in utility boilers results in the release of approximately 18.3 million tons of sulfur dioxide to the atmosphere each year along with significant amounts of other gases (e.g. NO_2 and NO). These acidic gases react with the water vapor present in the atmosphere to form acidic rain. The United States federal government requires all of the newer coal-fired power plants to control their emissions of these gases to some extent, but there are no acid gas emission standards for the older plants in the USA, so these plants do not control their emissions.

Across the United States, only 135 of the 1283 coal-fired utility boilers are equipped with flue gas desulfurization (FGD) systems, which are used to control the emission of sulfur dioxide (Melia et al., 1986). The older, uncontrolled plants, which are located mainly in the eastern part of the country, represent approximately 250,000 MW of generating capacity and commonly burn high sulfur coal (Drummond et al., 1988). The application of FGD systems to these plants may be necessary if pending acid rain legislation is passed by the federal government.

There are many proposed schemes for FGD, but only a few types are actually used in the USA. The processes can be broken down into "regenerable" systems, where the SO_2 in the flue gas is removed and converted to a salable byproduct, and into "throw-away" processes where the waste products are disposed of either in landfills or waste-ponds. The majority (120 out of 135) of the FGD systems currently used in the United States are "throw-away" processes and these will be discussed in the following sections since this dissertation concerns the reactions that occur in one type of these "throw-away" systems.

1.2.1 Limestone Slurry Scrubbing

The state-of-the-art for flue gas desulfurization is wet slurry scrubbing using limestone as the reagent material, and most of the FGD systems installed on power plants in the USA are of this type (99 out of 135 systems). In this process, the flue gas enters a large packed-tower or spray-tower absorber where it is contacted with a slurry of limestone in water. The SO_2 present in the flue gas dissolves into the water and reacts with the liquid phase alkalinity caused by the dissolution of the limestone in the water. The waste product from this process is a sludge which consists mainly of gypsum ($CaSO_4 \cdot 2H_2O$) and/or calcium sulfite hemihydrate ($CaSO_3 \cdot 0.5H_2O$), depending upon the operating conditions of the scrubber system. An excellent review of this and other FGD processes is given by Edgar (1983).

When operated efficiently, the limestone slurry scrubbing process can remove greater than 95% of the SO_2 present in the flue gas while obtaining nearly 100% utilization of the reagent limestone. The advantages of the limestone slurry scrubbing process include high SO_2 removal, high reagent utilization, and reliable operation. Because of the widespread use of these systems, the limestone slurry scrubbing process is also the most well understood process for FGD. The disadvantages to this process include high capital cost, high operating costs associated with the pumping of slurries, high maintenance costs, the production of large amounts of sludge waste, and a large space requirement. This latter

disadvantage is important because many of the older power plants are placed on small tracts of land and do not have room to install a large desulfurization system. These disadvantages make the wet limestone slurry scrubbing process a less likely choice for retrofit FGD.

1.2.2 Spray-Dry Scrubbing

The other dominant commercial FGD process is called spray-dry or wet-dry scrubbing and has been applied to full scale plants both in the USA and in Europe. Spray-dry scrubbing systems are presently installed on 12 coal-fired full-scale utility boilers in the USA. In the spray drying process (Figure 1.1), a slurry of slaked or hydrated lime (that is, $Ca(OH)_2$ in water) is atomized in a vessel where the atomized droplets are contacted with SO_2 laden flue gas. The heat from the flue gas evaporates the water present in the droplets to produce a dry waste product. This drying process also cools and humidifies the flue gas to a temperature near the adiabatic saturation temperature of the flue gas.

During the drying process, the SO_2 present in the flue gas dissolves into the slurry droplets and reacts with the $Ca(OH)_2$ to form calcium sulfite hemihydrate solids ($CaSO_3 \cdot 0.5\ H_2O$). Some of the dry waste solids fall out of the flue gas and are collected in a hopper at the bottom of the spray dryer, but most of the solids are entrained in the flue gas and are later removed in a downstream particulate control device (most commonly a baghouse). Since the waste solids contain residual moisture, additional SO_2 removal occurs in the baghouse. The removal in the baghouse can be as high as 50% of the inlet SO_2 to the baghouse, but since the spray dryer removes 75 - 85% of the original SO_2 , the baghouse removal typically only accounts for 5 -15% of the total SO_2 removal for the system (Babu et al., 1988, Wilkinson and Tonn, 1981).

The SO_2 removal efficiency of the spray drying process is significantly lower that for the limestone slurry scrubbing process and is quite variable depending upon the operating conditions. A reasonable design for a spray dryer system should give a SO_2 removal of approximately 85 percent while obtaining 70

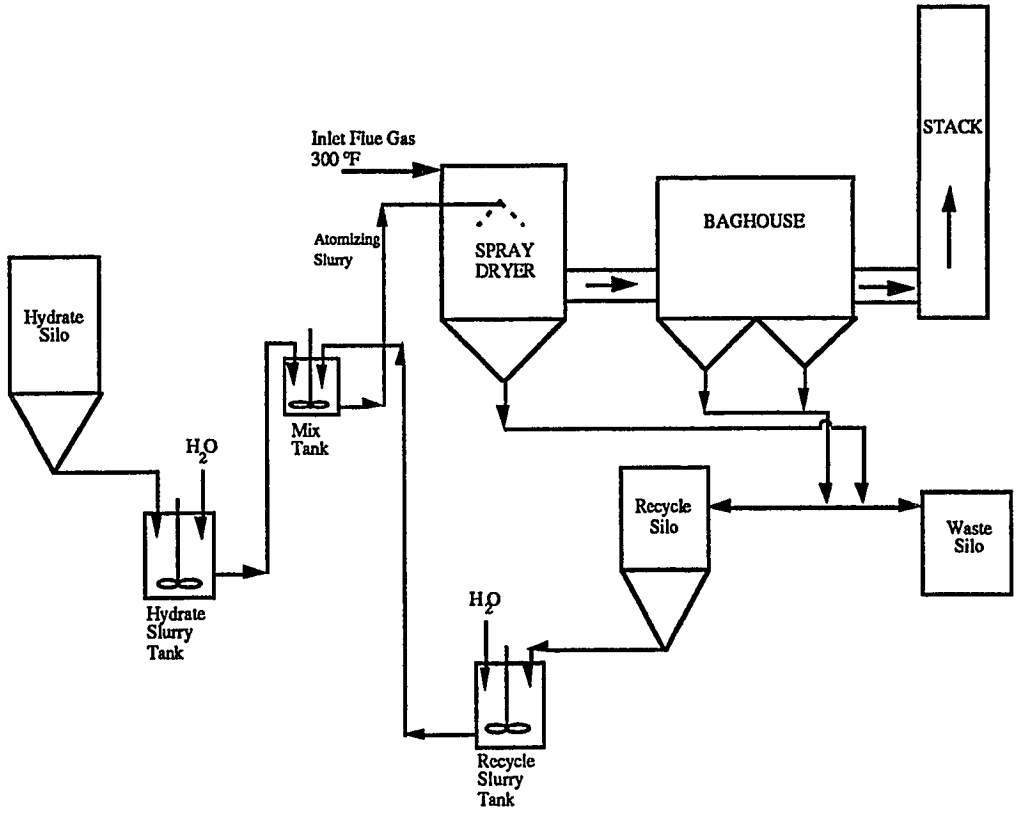

Figure 1.1 Schematic of spray drying process for flue gas desulfurization.

percent utilization of the slaked lime fed to the system. This low level of reagent utilization is important because the cost of the reagent for the spray drying process (i.e. lime) is three to ten times as expensive as the cost of the limestone used in the slurry scrubbing process.

The spray drying process has significant advantages over the limestone slurry scrubbing process. The spray drying process produces a dry waste product so there is no need for the sludge handling systems used in limestone slurry scrubbing. The spray drying process also has lower pumping requirements (Burnett et al., 1981) and consumes less water than the slurry scrubbing process. Also, since the walls of the spray dryer never come in contact with water, the vessel can be constructed out of relatively inexpensive carbon steel instead of using expensive corrosion resistant alloys as is the case for the construction of vessels for the limestone scrubbing process. Economic studies have indicated that spray-dry scrubbing is economically competitive for low and medium sulfur coals (Burnett et al., 1981, Drabkin and Robison, 1981, Ireland et al., 1988). Some recent reports have considered using spray dry scrubbing systems for high sulfur coals, but there are several practical operating limitations which will have to be overcome for the spray drying process to be economically competitive with other forms of FGD (Jankura et al., 1984, Robards et al., 1985).

The main drawbacks to the wet-dry process are relatively low reagent utilization, high sorbent costs, and large space requirements. The process also requires suitable particulate control equipment and may not work well in existing plants without installing a new bag filter or greatly enhancing the existing electrostatic precipitator. The possible particulate control problems and the large space requirement make this technology less suitable for a retrofit FGD system.

1.2.3 Dry FGD Alternatives

The technologies that will be employed by the older, coal-fired power plants to control their SO_2 emissions are likely to be low-capital-cost, high-operating-cost processes that have minimal space requirements. These processes will be chosen because the older plants do not have enough life expectancy to warrant a high capital cost, state-of-the-art FGD system.

A number of low-capital-cost FGD processes have been proposed and tested at the pilot-plant and small commercial-scale levels. These can be divided into two general groups : lime injection into the boiler and sorbent injection into the downstream ductwork. At first glance, these processes seem quite similar as both involve injecting a calcium-based sorbent into the flue gas to react with the SO_2 present. However, the operational conditions for the two processes are not similar and, as a result, neither are the chemical reactions which take place.

1.2.3.1 Boiler Injection Processes

The boiler injection processes are the simplest of all the FGD processes. In these systems, hydrated lime or limestone is injected into the boiler or just downstream of the boiler. The high temperatures in the boiler cause the reagent to "calcine", that is, to lose H_2O or CO_2, depending on the type of sorbent injected. As a result, a high surface area lime (CaO) is created. This lime reacts with the SO_2 and the oxygen present in the flue gas to form $CaSO_4$. Simultaneously, the high surface area lime sinters to form a low surface area CaO, which is relatively unreactive towards SO_2. This sintering process occurs very quickly and limits the utilization of the reagent material to about 25%. Therefore, significant amounts of reagent must be injected into the boiler to attain high levels of SO_2 removal. Most boilers were not designed to handle the increased solids loading from the operation of the boiler injection process, and problems such as slagging and boiler tube fouling occur.

Since the waste solids from the boiler injection process contain a substantial amount of unreacted CaO, several studies have investigated the "reactivation" of the waste solids. That is, the waste solids are contacted with water to re-hydrate some of the unreacted CaO, which is then re-injected into the flue gas. Since the waste solids contain fly ash and re-hydrated CaO, the reactions that occur during the "reactivation" process are essentially the same reactions that occur during the formation of the lime/fly ash solids. Studies of these "reactivation" processes will be discussed in the next chapter.

1.2.3.2 Duct Injection Processes

In the duct-injection processes, a calcium based sorbent, usually $Ca(OH)_2$, is injected either as a slurry or as a dry powder with humidification into the existing flue gas ductwork downstream of the air preheater, and the resulting solids are collected in the existing particulate collection device (Figures 1.2 and 1.3). The injected sorbent reacts with the SO_2 present in the flue gas to produce a dry waste product for disposal.

Since minimal new equipment is required, this process has a lower capital cost, simpler operation, and smaller space requirement than the commercial technologies of wet-limestone slurry scrubbing and spray dry scrubbing with lime reagent. Compared with limestone injection into the boiler, the duct-injection process is advantageous because the duct-injection process does not affect the operation of the boiler and the waste solids do not contain reactive material (i.e. CaO). The use of calcium-based sorbents for duct-injection is preferred to the use of more reactive, sodium-based compounds because of the easier disposal of the insoluble calcium-based waste products and the lower cost of the calcium-based sorbents.

Pilot tests of the duct-injection processes have shown that the maximum expected SO_2 removal is approximately 50%, regardless of the type of injection method, when the systems were operated at reasonable conditions (Peterson et al., 1989, Gooch et al., 1989). This low SO_2 removal dictates that process improvements be made before duct-injection will be an acceptable alternative to other FGD processes.

Most of the work aimed at improving the duct injection process has focused on improving the reactivity of the calcium-based sorbents. These investigations have looked at the use of high surface area hydrated limes, pressure hydrated dolomitic limes, and the use of hydrated limes with additives such as NaOH and NaCl. Bench-scale studies indicated that many of these improved sorbents were

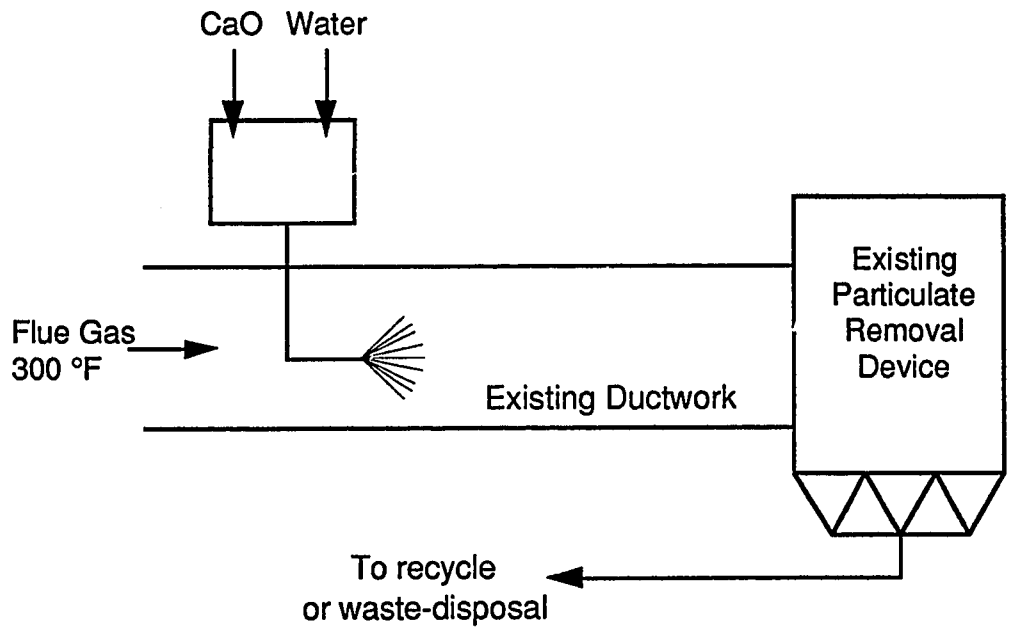

Figure 1.2 Schematic of duct-injection system : slurry injection.

very reactive towards SO_2, but when tested at the pilot plant level, these materials were no more effective at removing SO_2 than was normal hydrated lime. The most likely explanation for this difference in reactivity relates to the different experimental conditions experienced at the bench and pilot scale levels (Peterson et al., 1989).

One type of improved sorbent was found to be very reactive at both the bench-scale and the pilot-scale levels. The sorbent is called "lime/fly ash" material and is formed by the reaction of fly ash with hydrated lime in water. This reaction produces high surface area, highly hydrated materials and is the subject of this

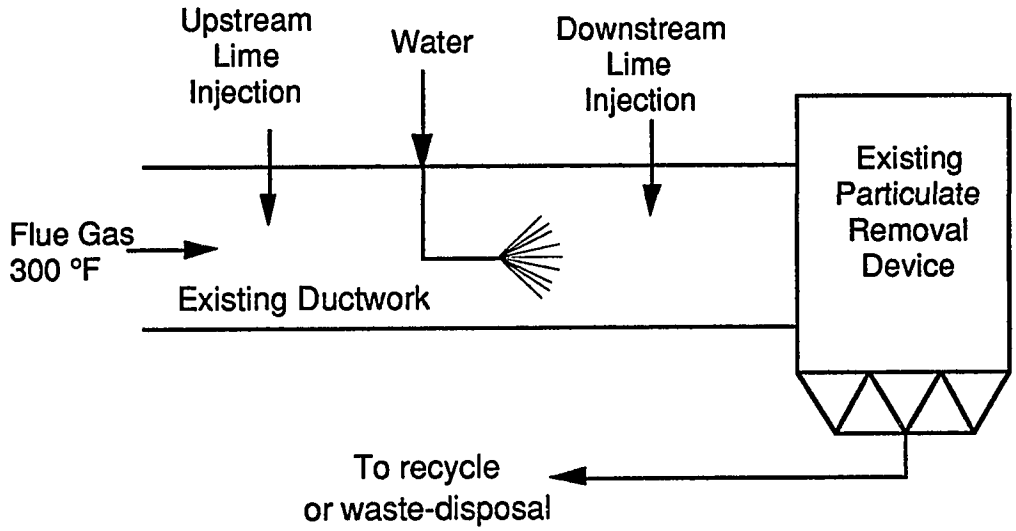

Figure 1.3 Schematic of duct-injection system : dry solids injection with separate humidification.

dissertation. A review of the literature describing the reactivity of this material towards SO_2 is given in the next chapter.

1.3 Objectives and Scope of this Work

The scope of this work was to determine the effects of the important operational parameters on the reaction of hydrated lime with fly ash. To determine these effects, several types of experiments were performed including : fly ash dissolution experiments, where the reactivity of the fly ash was determined in absence of the reaction with $Ca(OH)_2$; solids preparation experiments, where the various fly ashes were reacted with $Ca(OH)_2$ in water; and various types of solids

analyses that characterized the solids produced by the reaction of $Ca(OH)_2$ with fly ash. The parameters investigated were the type and source of the fly ash, the particle size of the fly ash, and the presence of recycle materials in the slurry. A large block of experiments was also conducted using reagent chemicals to simulate the major components of the fly ash. These experiments were performed to determine which components of the fly ash react with $Ca(OH)_2$ to produce solids that are reactive towards SO_2.

Chapter II

Lime/Fly Ash Solids for FGD : Literature Review

As was stated in Chapter I, this dissertation concerns the reactions which take place when hydrated lime is mixed with fly ash in water. There has been a fair amount of previous research related to this topic, but this work focused more on the effects of process variables on the reactivity of the lime/fly ash solids towards SO_2 and less on the reactions which occur when lime is mixed with fly ash. However, the results from those studies are useful for understanding some of the chemistry of the lime/fly ash reaction. This chapter will summarize the results from the bench-scale and pilot-plant studies in order to show which operating conditions are most favorable for SO_2 removal and to illustrate the high reactivity of the lime/fly ash solids towards SO_2.

2.1 Bench-Scale Data

Most of the investigations of the lime/fly ash materials were conducted at the bench-scale level using a test apparatus which is usually referred to as a "sand-bed reactor". In this packed-bed reactor, the lime/fly ash solids were dispersed in silica sand and exposed to a synthetic flue gas stream. The reactivity of the solids was determined by measuring the amount of SO_2 removed from the gas stream, usually determined by gas-phase analyses. Further details on the operation of these sand-bed reactors is furnished in Chapter V of this dissertation.

The reactivity of the lime/fly ash materials in the bench-scale studies was usually related to the conditions present during the formation of the lime/fly ash solids. That is, conditions such as the slurry temperature, the fly ash:$Ca(OH)_2$ ratio

originally present in the slurry, the fly ash type, the fly ash particle size, and the presence of additives in the slurry. The effects of these conditions on the reactivity of the lime/fly ash materials are important and they will be reviewed in the following sections.

2.1.1 Effect of slurry temperature

Jozewicz and Rochelle (1986A, 1986B) investigated the effect of slurry temperature on the lime/fly ash solids' reactivity towards SO_2 for slurry temperatures from 25 to 92 °C. They slurried fly ash with $Ca(OH)_2$ in water, dried the slurry, and then tested the solids for reactivity towards SO_2 in a sand-bed reactor. For solids produced in slurries where the fly ash : $Ca(OH)_2$ ratio was 16:1, they found that the solids' reactivity increased with increasing slurry temperature (Figure 2.1). Note that the data show a discontinuity in the solids' reactivity towards SO_2 for long slurry times. The ultimate reactivity of the solids from the 65 °C slurry was equal to that of the solids from the 92 °C slurry, but significantly greater than that for the solids from the 55 °C slurry. While this discontinuity has not been fully explored, Jozewicz and Rochelle used differential thermal analyses to show that a different phase was formed for slurry temperatures greater than 65 °C.

Jozewicz and Rochelle postulated that the limiting step of the lime/fly ash reaction was the dissolution of the fly ash and therefore assumed that higher slurry temperatures gave higher fly ash dissolution rates and hence higher reactivity of the lime/fly ash solids.

In a later study using an autoclave to obtain slurry temperatures greater than 100 °C, Jozewicz et al. (1988A) showed that there was an optimum slurry temperature of approximately 150 °C for all slurry times if the fly ash:$Ca(OH)_2$ ratio in the slurry was 2.3:1. They related this result to literature data (Taylor, 1964) which indicates that calcium silicates with significantly less molecular water are formed in the 150 to 230 °C temperature range. Jozewicz et al. also suggested that two factors are necessary for a sorbent to be reactive towards SO_2 : the sorbent

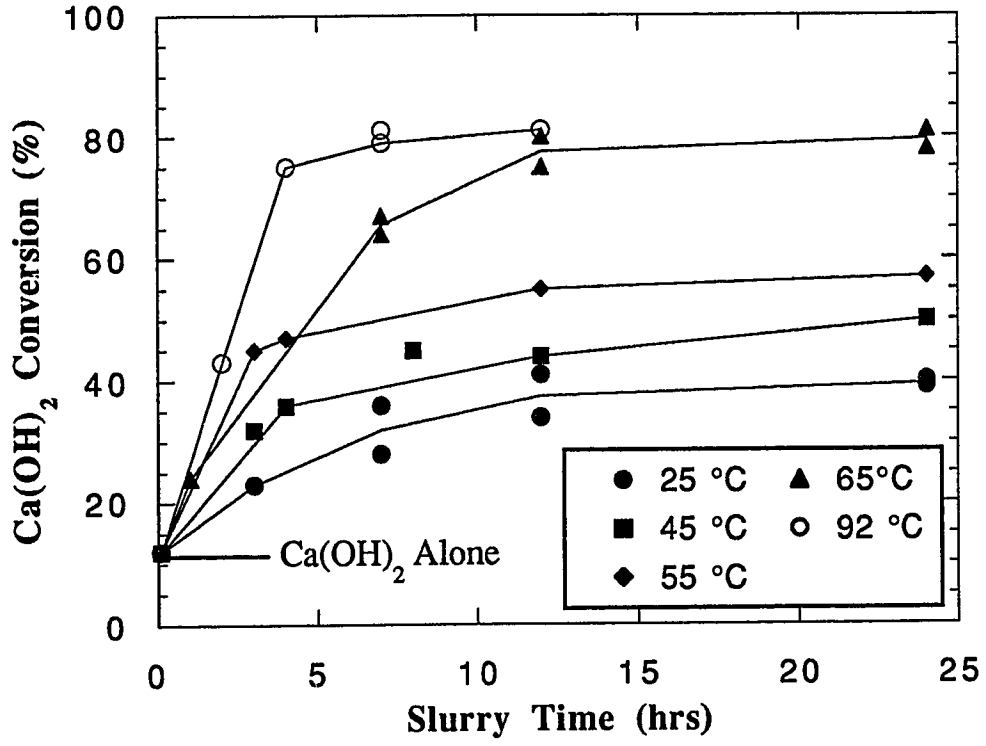

Figure 2.1 Effect of slurry temperature on reactivity of lime/fly ash solids towards SO_2. Data of Jozewicz and Rochelle, 1986A.

must have a large surface area and an amorphous surface structure. They proposed that as the slurry temperature was increased above 150 °C, the product solids became more crystalline and therefore less reactive towards SO_2.

Jozewicz et al. also found that the optimum slurry temperature depended upon the fly ash : $Ca(OH)_2$ ratio originally present in the slurry. If the fly ash:$Ca(OH)_2$ ratio was 1:1, the optimum slurry temperature was lower (near 100 °C). This observation may have related to the relative reactivities of the silica and aluminum present in the fly ash and will be discussed in Chapter VII.

2.1.2 Effect of fly ash:lime ratio

Another important process variable is the fly ash loading or the weight ratio of fly ash:$Ca(OH)_2$ present in the slurry. Jozewicz and Rochelle (1986A) showed that the reactivity of the lime/fly ash solids towards SO_2 increased from 0.17 to 0.78 (mols SO_2 removed/mol $Ca(OH)_2$) as the fly ash loading increased from 0.5 to 20 g fly ash/g $Ca(OH)_2$. These experiments were conducted at 65 °C using a high calcium fly ash. Jozewicz et al. (1986A) found similar results using a low-calcium fly ash and a slurry temperature of 90 °C.

The above results can be interpreted in a simple manner if one assumes that the rate limiting step of the reaction of lime with fly ash is the dissolution of the fly ash. If this is the case, a higher fly ash-to-lime ratio in the slurry simply translates into a faster total rate of fly ash dissolution and therefore a faster production rate of the lime/fly ash solids.

At first glance, it would seem that it would be advantageous to create the lime/fly ash solids using a very high fly ash loading. However, high fly ash loadings translate into more material injected into the ductwork for a given reagent ratio (mols $Ca(OH)_2$ injected/mols SO_2 present in the flue gas). Since the lime/fly ash solids must eventually be collected in a particulate control device, the fly ash loading must be kept as low as possible to avoid overloading the particulate control device. Also, higher fly ash loadings dictate that more material must be slurried with the $Ca(OH)_2$. This increases mixing costs and solids handling costs. These practical limits dictate that the fly ash loading should be as low as possible to avoid particulate control problems.

2.1.3 Effect of fly ash type

The chemical content and the mineralogy of fly ash varies greatly depending upon the coal source and, to a lesser extent, on the power plant operation. Therefore, one would expect that the effect of fly ash type would be one of the primary variables affecting the reactivity of the lime/fly ash solids. However, a review of the previous work shows inconclusive effects of the fly ash type on the reactivity of the lime/fly ash solids towards SO_2.

Jozewicz and Rochelle (1986A) used four different fly ash sources - three from bituminous coals and one from a lignite coal. At low fly ash loadings (4 g fly ash:1 g $Ca(OH)_2$), the reactivity of the lime/fly ash solids increased with the calcium content of the fly ash. The solids produced using the highest calcium fly ash (34% Ca) were 44% more reactive than the solids produced using the lowest calcium fly ash (5% Ca). However, at high fly ash loadings (16:1) there was no correlation between the chemical content of the fly ash and the reactivity of the lime/fly ash solids towards SO_2. It should be noted that Jozewicz and Rochelle reported the reactivity as the number of mols of SO_2 removed per mole of $Ca(OH)_2$ mixed with the fly ash, that is, they did not account for any reactivity of the calcium present in the fly ash. If this calcium was reactive it would artificially increase the reported reactivity of the lime/fly ash solids. Therefore, it is surprising that the high-calcium fly ash (34% Ca) was better at low fly ash loadings and not at high fly ash loadings (where there would be a lot of calcium present from the fly ash). Another questionable observation is the reported composition of their high-calcium fly ash. This ash was reported to contain 34 % calcium which is unbelievably high for an ash from a bituminous coal (see Chapter III).

Jozewicz et al. (1988B) used one bituminous coal ash (4% Ca) and one lignite coal ash (13% Ca) to show that there was no effect of fly ash type on the reactivity of the lime/fly ash solids. However, Peterson and Rochelle (1988A) showed that the reactivity of the lime/fly ash solids increased with the calcium content of the fly ash if one did not consider the calcium present in the fly ash to be

reactive. They found the reactivity of the lime/fly ash solids to be approximately 20% greater when a high-calcium fly ash (30% Ca as CaO) was used instead of a low-calcium fly ash (4% Ca as CaO). However, if one considers the calcium present in the fly ash to be totally reactive, the lime/fly ash solids from the high-calcium fly ashes were determined to be even less reactive than those from the low-calcium fly ashes.

In summary, the previous works do not show a conclusive effect of the fly ash type on the reactivity of the lime/fly ash solids. However, these studies were conducted on a relatively small suite of fly ash types (only 7 different types total for all of the studies combined) which may not be large enough to detect the effects of fly ash type. From studies of the use of fly ash in concrete, it is well known that different fly ashes give markedly different performance, so one would expect to see a more dramatic effect of the fly ash type on the reactivity of the lime/fly ash solids towards SO_2. One of the goals of the current research is to examine the effect of the fly ash type on the reactivity of the fly ash.

2.1.4 Effect of recycle materials

The results from the pilot-scale tests using lime/fly ash solids as reagent for duct-injection systems (see section 2.2) show that the utilization of the $Ca(OH)_2$ present in the lime/fly ash solids was approximately 50% for a single pass. This suggests that a commercial FGD system using the lime/fly ash solids would probably recycle the solids collected in the particulate control device to achieve higher sorbent utilizations (Figure 2.2). These recycle solids would contain mainly $CaSO_3 \cdot 0.5H_2O$ with smaller amounts of $CaSO_4 \cdot 2H_2O$. These compounds may influence the reaction of hydrated lime with fly ash.

The effects of these recycle compounds relate to the reaction of the sulfur species with the aluminum content of the fly ash, a reaction which is well documented by studies pertaining to cement and concrete (Taylor, 1964). It is not known if these calcium-alumino-sulfate materials form at the high temperatures of

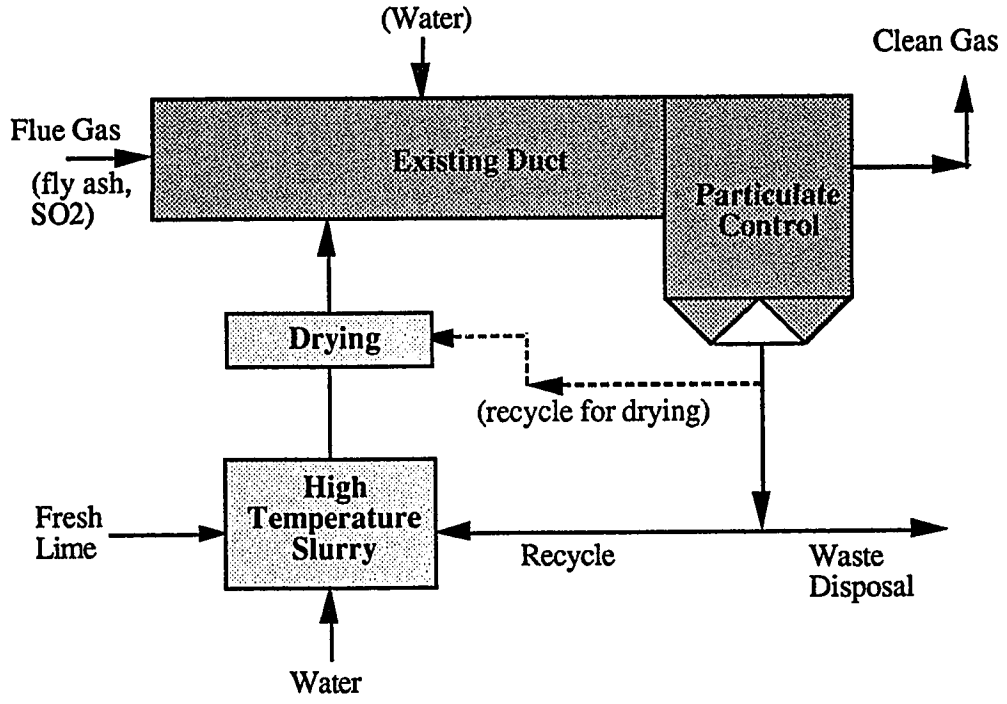

Figure 2.2 Process concept for flue gas desulfurization using lime/fly ash solids.

the lime/fly ash system, nor is it known how the formation of these materials affects the reactivity of the lime/fly ash material towards SO_2.

Jozewicz and Rochelle (1986B) performed several experiments to determine the effects of recycle materials on the reaction of lime with fly ash, but were unable to make any definite conclusions on the effects of these materials. When present at high concentrations in the slurry, $CaSO_3 \cdot 0.5H_2O$ increased the reactivity of the

product solids. At lower concentrations, it had a negative effect. Similar results were found for the effect of gypsum, but the effect was more dependent on the slurry temperature. At low slurry temperatures (25 °C) the presence of gypsum increased the reactivity of the lime/fly ash solids, but at higher temperatures (65 °C) it decreased the reactivity of these solids. The fly ash used in these experiments had a high silica content (67%) and a relatively low aluminum content (16%), so it was probably not the ideal choice for investigating the effect of the sulfur species on the reaction of fly ash with $Ca(OH)_2$, since the reactions of interest involve the aluminum content of the fly ash.

Chu and Rochelle (1986A, 1986B) used a fly ash with a high silica (57%), moderate alumina (24%) content and determined that the presence of $CaSO_3 \cdot 0.5H_2O$ in the slurry had no effect on the reactivity of the solids towards SO_2, but found a strong beneficial effect on the solids' reactivity towards NO_x. Peterson and Rochelle (1988A) (using the same fly ash) found that the presence of $CaSO_3 \cdot 0.5H_2O$ had only a slight beneficial effect on the solids' reactivity towards SO_2 when no NaOH was present in the slurry, but the $CaSO_3 \cdot 0.5H_2O$ had a large, beneficial effect on the solids' reactivity when NaOH was present in the slurry. In a separate experimental study using the same fly ash, Peterson and Rochelle (1988B) found that the presence of $CaSO_3 \cdot 0.5H_2O$ in the slurry had a slight beneficial effect on the reactivity of the lime/fly ash solids towards SO_2 for the solids which were slurried for long times, but had no effect for the shorter slurry times.

The previous investigations into the effect of recycle materials on the production of lime/fly ash solids have focused on the reactivity of the solids produced in the recycle-containing slurries. The data indicate that $CaSO_3 \cdot 0.5\ H_2O$ has no strong effect and that the effect of $CaSO_4 \cdot 2\ H_2O$ is inconclusive. One of the objectives of the current project is to determine the effect of the recycle materials on the reaction of fly ash with $Ca(OH)_2$. This work will focus more on the chemistry taking place when these recycle materials are present, and relate these observations to the reactivity of the solids towards SO_2.

2.1.5 Effect of fly ash particle size

Fly ash does not have a set particle size. The fly ash particles vary in size from less than 1 micron to greater than 100 microns. If the dissolution rate of the fly ash controls the reaction rate between fly ash and $Ca(OH)_2$, it is likely that the smaller particles would react faster than the larger particles due to the higher specific surface area of the small particles. Two studies have investigated the effect of fly ash particle size on the reaction of fly ash with $Ca(OH)_2$ to produce solids for FGD.

Jozewicz and Rochelle (1986B) wet-sieved one sample of low-calcium fly ash into five different sizes and then reacted each of these samples with $Ca(OH)_2$ in water at a slurry temperature of 65 °C for 16 hours. The solids produced in these slurries were dried and tested for reactivity towards SO_2 in a sand-bed reactor system. The results showed that the solids produced from the smallest particles were the most reactive towards SO_2. The solids made from the fly ash which passed through the 20 micron sieve were 220 percent more reactive than the solids prepared from the ash retained on the 125 micron sieve.

Petersen et al. (1988) used a pebble mill to wet-grind two samples of fly ash in order to change the fly ash particle size. When they ground a low-calcium fly ash, the mean particle size decreased from 12.1 to 1.2 microns. This ground fly ash was then slurried with $Ca(OH)_2$ at a weight ratio of 3:1 and a slurry temperature of 85 °C. The surface areas of the solids produced using this ground fly ash were up to 3 times greater than for those produced using the unground fly ash. When tested for reactivity towards SO_2 in a bench-scale duct-injection apparatus, the ground fly ash solids were approximately twice as reactive as the unground fly ash solids and three times as reactive as $Ca(OH)_2$ alone.

Another interesting result of this study was that the grinding of a high-calcium fly ash produced a very high surface area product which was very reactive towards SO_2. Apparently, the wet-grinding process hydrated some of the CaO present in the high calcium fly ash and caused the slurry to become very hot. This

combination of heat and mixing in the grinder gave rise to the formation of reactive lime-fly ash solids without the need for the additional high temperature slurrying process.

These two works clearly indicate that the reaction of lime with fly ash is enhanced if the fly ash particles are small. This enhancement presumably results from the higher dissolution rate of the smaller fly ash particles which leads to an increased rate of production of lime/fly ash solids.

One objective of the current study was to further determine the effect of fly ash particle size on the reactivity of the lime/fly ash solids towards SO_2. This was accomplished by using both wet- and dry-ground fly ash samples.

2.1.6 Effect of additives for fly ash dissolution

Since the reaction rate of fly ash with $Ca(OH)_2$ is thought to be limited by the dissolution rate of the fly ash, an obvious way to increase the overall reaction rate is to add materials to the lime/fly ash slurry which increase the fly ash dissolution rate. Since fly ash is a glassy-siliceous substance, most of the additives which have been tested are those which are known to dissolve glass.

Chu and Rochelle (1986A, 1986B) added NaOH to slurries of $Ca(OH)_2$ and a low-calcium fly ash. They dried the slurries and tested the product solids for reactivity towards SO_2 in a sand-bed reactor. They found that increasing the sodium hydroxide concentration in the slurry increased the product solids reactivity towards SO_2 and NO_x. At high relative humidity (55%), the addition of 0.08 M NaOH to the slurry increased the solids reactivity towards SO_2 from 18 to 70 moles SO_2 removed/100 mole $Ca(OH)_2$. At low relative humidity (17%), the addition of 0.08 M NaOH increased the solids reactivity towards NO_x from 1 to 3 moles NO_x removed/100 mole $Ca(OH)_2$.

Peterson and Rochelle (1988A, 1988B) also used NaOH as and additive to the lime/fly ash slurries. The results showed there to be an optimum concentration of NaOH in the slurry. The solids produced in slurries containing 0.10 M NaOH

were up to 30% more reactive towards SO_2 than the solids produced in slurries containing no NaOH and 50% more reactive than those produced in slurries containing 0.25 M NaOH. The authors rationalized the data by assuming that at very high concentrations of NaOH the solids that were produced had a very high silica content which made them unreactive towards SO_2.

Jozewicz et al. (1988B) showed that the addition of small amounts of phosphate to the lime/fly ash slurries increased the reactivities of the resulting lime/fly ash solids. They state that the phosphate functions in a similar manner to that of NaOH - it dissolves the glassy portion of the fly ash to increase the lime/fly ash reaction rate. They found that the optimum amount of phosphate was approximately 8 moles of phosphate/100 moles of $Ca(OH)_2$ if the phosphate was added as either sodium or ammonium phosphate. Slightly higher levels were required if the phosphate was added as phosphoric acid. The addition of these levels of phosphate to the slurry increased the lime/fly ash solids' reactivity towards SO_2 by nearly 70 percent.

2.1.7 Investigations with other materials

Fly ash is not the only material that has been considered for the production of reactive solids for FGD. Several studies have looked at the use of diatomaceous earth which is a natural source of amorphous silica having a surface area of 40 to 90 m^2/g. It is composed of the microscopically minute remains of marine or fresh water diatom plants (Cummins and Miller, 1934). The most important commercial deposits of diatomaceous earth are found in California, Nevada, Oregon, and Washington.

Jozewicz et. al. (1986A) slurried a number of natural and calcined diatomaceous earths with $Ca(OH)_2$ to produce solids which were tested in a sand-bed reactor. The data showed that all of the earths generated solids which were more reactive than was $Ca(OH)_2$ alone, but the best performance was achieved with the natural earths, which had much higher initial surface areas than did the calcined diatomaceous earths. Jozewicz et al. also showed that the natural diatomaceous

earth/lime solids were 5 to 7 times as reactive towards SO_2 as the lime/fly ash materials formed under the same experimental conditions.

The higher reactivity of the lime/diatomaceous earth solids compared to the lime/fly ash materials is due to the high surface area and amorphous structure of the diatomaceous earth. Both of these facilitate the dissolution of silica from the earth, and therefore encourage the formation of high surface area calcium silicate materials which are very reactive towards SO_2.

There are two major disadvantages for using diatomaceous earth as a silica source. The first is cost. Fly ash is produced in massive amounts by every coal-fired power plant, so its cost is essentially zero. This compares to approximately $100 per ton for diatomaceous earth. The second disadvantage is that the availability of diatomaceous earth limits its use to only the Western part of the United States.

2.1.8 Reactivation of boiler injection solids

As was mentioned in chapter I, one proposed retrofit FGD process involves injecting calcium-based reagent into the boiler. The injected material quickly calcines to form a high surface area CaO which reacts with SO_2 and O_2 to form $CaSO_4$. Simultaneously, the high surface area lime sinters to form a low surface area CaO, which is relatively unreactive towards SO_2. This sintering process occurs very quickly and limits the utilization of the reagent material to about 25%. Therefore, significant amounts of reagent are required to attain high levels of SO_2 removal.

Since the waste solids from the boiler injection process contain a substantial amount of unreacted CaO, several studies have investigated the "reactivation" of the waste solids. The studies propose to take this reactivated material and inject it into the existing flue gas duct upstream of the particulate control device. The method for the reactivation step is to slurry the waste solids in water, usually at high temperature. Since the waste solids contain fly ash and CaO (which is hydrated to

$Ca(OH)_2$ during the reactivation step), the reactions which occur during the reactivation step are very similar to those occurring during the "normal" production of lime/fly ash solids. The principle difference is that the waste solids contain a large amount of calcium sulfate materials which may influence the reactions occurring in the lime/fly ash system.

Jozewicz et al. (1986B, 1987) reactivated six different post furnace injection solids by slurrying the solids in water at slurry temperatures from 25 to 90 °C. They dried the slurries and tested the solids for reactivity towards SO_2 in a sand-bed reactor. The data showed that the solids as received were totally unreactive towards SO_2, but the reactivated solids were very reactive towards SO_2. The reactivity increased with slurry time and slurry temperature. Jozewicz et al. analyzed the solids and determined that the increase in reactivity towards SO_2 was due to the formation of various calcium silicates and calcium-sulfo-aluminates. These compounds increased the surface area of the product solids and therefore increased their reactivity towards SO_2.

2.2 Pilot-Scale Data

Several studies have also demonstrated the use of the lime/fly ash materials at the pilot plant scale. The testing conditions of these pilot plants were designed to simulate those present for the duct injection process (i.e. low temperature, high relative humidity, and a short residence time).

It should be noted that the lime/fly ash solids have less potential use as reagent for FGD spray dryer systems because they do not spray dry easily. Jozewicz et al. (1986A) attempted to spray dry the lime/fly ash solids in a pilot unit, but were only able to operate the unit when the spray dryer outlet temperature was 75 °C above the adiabatic saturation temperature for the flue gas. This high outlet temperature reduces the ability of the solids to remove SO_2 and therefore precludes the use of the lime/fly ash solids as reagent for spray dryer systems.

2.2.1 Effect of process variables

In pilot plant experiments with a 100m^3/h (58 cfm) duct injection system using a fabric filter for particulate control, Jozewicz et al. (1986A) showed that the lime/fly ash solids were more reactive than $Ca(OH)_2$. Using the lime/fly ash solids (fly ash:$Ca(OH)_2$ loading of 3:1, slurried at 85 °C) at a reagent ratio of 1.8 and a 20 °F approach to saturation, 80% of the SO_2 fed to the system was removed. Using $Ca(OH)_2$ at a reagent ratio of 3 and a 20°F approach to saturation, only 30 - 40 % of the SO_2 fed to the system was removed. More significant is the difference in $Ca(OH)_2$ utilization (moles of SO_2 removed/moles of $Ca(OH)_2$ fed to the system); using $Ca(OH)_2$ the utilization was only 10 - 16% versus 40 - 50% for the lime/fly ash solids.

Also in pilot plant experiments (2000 - 4000 acfm), Blythe et al. (1986) showed that the lime/fly ash solids (loading of 3:1, slurry temperature of 95 °C) were much more reactive than hydrated lime under identical testing conditions. Using an ESP for particulate control, a reagent ratio of 2, and a 20 °F approach to saturation, the lime/fly ash solids removed 55% of the SO_2 compared with 35 - 40% removal when hydrated lime was used. When a baghouse was used for particulate control and steam was co-injected with the sorbent, the lime/fly ash solids removed more than 90 % of the SO_2 compared with 65 - 70% removal when the hydrated lime was used.

2.2.2 Effect of solids water content

The lime/fly ash solids which were used in the above studies were dried almost to completion before injecting them into the ductwork containing humid flue gas at a temperature very close to the adiabatic saturation temperature. Recently, it has been discovered that the lime/fly ash solids have a very unique property : they can retain a large amount of free water without becoming difficult to handle. Several studies have exploited this property to humidify the flue gas and increase the SO_2 removal for the process.

Chang and Sedman (1988) tested lime/fly ash solids in a pilot plant duct injection system which used a baghouse for the particulate control. The injected solids contained up to 25 percent moisture which evaporated to 5 percent when the solids were injected into the ductwork. The data showed that the utilization of the injected solids increased from 22 to 50 % as the initial moisture content increased from 2 to 15% and that up to 94 % SO_2 removal was observed for a reagent ratio of 1.8 and a 20 °F approach to adiabatic saturation temperature.

The great increase in reactivity for the damp solids occurs because the mechanism of SO_2 removal is similar to that for the wet-dry FGD process. That is, the SO_2 must dissolve into water before it can react with the sorbent. Pre-wetting the lime/fly ash solids causes the solids to contain a lot of water in their pores. This water is available for SO_2 dissolution and therefore greatly increases the reaction rate between lime/fly ash and SO_2.

2.3 Summary of Lime/Fly Ash for FGD

All of the previous studies mentioned above have shown that the lime/fly ash solids are very reactive towards SO_2 under the low temperature, high relative humidity conditions experienced in the duct-injection processes. However, since the lime/fly ash technology is only about five years old, there are a number of important, unresolved questions concerning the formation of the lime fly ash solids.

For example, due to the small number of fly ashes tested to date, the effect of the fly ash type on the reactivity of the lime/fly ash solids is not understood. All of the studies showed that, regardless of the fly ash type, the lime/fly ash solids were more reactive than was $Ca(OH)_2$ and that the high-calcium fly ashes seemed to be beneficial because SO_2 could react with some of the calcium present in these fly ashes. However, no data have been presented which show the effect of fly ash type on the availability of silica and alumina from the fly ash. It is this availability which ultimately controls the reactivity of the lime/fly ash solids.

Another significant area of inconclusive research is the effect of recycle materials on the reaction of lime with fly ash. The previous work is fairly inconclusive on the effects of the recycle materials, but it does show that the reactivity of the lime/fly ash solids is not significantly degraded by the presence of recycle materials in the slurry. However, since it is highly probable that recycle would be used for a commercial lime/fly ash FGD system, the previous work should be expanded before the lime/fly ash technology is employed at a commercial level.

The effect of fly ash grinding is also a very interesting research area since the reactivity of the solids produced using ground fly ash is much greater than for the solids produced using the unground fly ash. However, the previous research is lacking in that the extent of fly ash grinding required for the increase in reactivity is not quantified.

The present research will aim to provide answers to some of these unresolved questions by performing a variety of experiments on fly ash and the lime/fly ash solids. Chapter V of this dissertation describes these experiments in detail.

Chapter III

Chemistry and Mineralogy of Pozzolans

3.1 Introduction to Pozzolanic Materials

A pozzolanic material is defined by ASTM (1980) as : "... a siliceous or siliceous and aluminous material which itself possesses little or no cementitious value but which will, in finely divided form and in the presence of moisture, chemically react with calcium hydroxide at ordinary temperature to form compounds possessing cementitious properties".

From this definition and previous research, it is clear that fly ash can be defined as a pozzolanic material. Indeed, it is the "pozzolanic reaction" which produces the reactive lime/fly ash materials that are the subject of this study.

There are also other types of pozzolanic materials which may be of interest for the production of solids for FGD. Some of these materials have already been tested with good results (e.g. diatomaceous earth). Because the chemical reactions which occur during the "pozzolanic reaction" are quite similar for all of the pozzolanic materials, the literature discussed in this chapter will only concern fly ash. Fly ash is probably the only likely candidate for the production of reactive solids because its cost to the power plants is essentially free, whereas the other pozzolanic materials would have a much higher cost.

3.2 Chemistry and Mineralogy of Fly Ash

Fly ash is a waste product from all coal-fired power plants and is currently produced at the rate of 60 million tons/year in the USA alone (McCarthy et al., 1986). Of this massive amount, only about 20 % is utilized each year, while the rest is most commonly land-filled.

3.2.1 Origin of fly ash

Fly ash is created from the inorganic constituents which are present in the coal that is burned in the boiler. The organic portion of the coal reacts with oxygen in the boiler to produce the heat which is converted to electrical energy at the power plant. Most of the inorganic constituents present in the coal melt in the high temperature zone of the boiler. Reactions can occur in this melt, which quickly forms small spherical droplets to minimize its surface energy. These droplets become entrained in the exhaust gas from the boiler (i.e. the "flue gas") and subsequently "fly" out of the boiler. Hence the name "fly ash".

The melted fly ash is rapidly cooled when the flue gas exits the boiler. This rapid cooling causes the fly ash to consist of small, mostly spherical, glassy particles. These particles range in size from less than 0.1 μm to more than 200 μm, although most are less than 50 μm with an average particle size of 10-30 μm.

Many researchers have used scanning electron microscopy to show that although most of the fly ash particles are spherical, a variety of sphere types are present in most fly ashes. Some particles are hollow, but empty, spheres (cenospheres), others are hollow but contain smaller spheres inside (plerosperes), and still others are solid spheres. The variety of sphere types relates to the chemical compositions of the fly ash particles and will be discussed later.

3.2.2 Chemical composition of fly ash

The chemical composition of the bulk fly ash depends strongly on the parent coal. Bituminous coals yield fly ashes which contain more silica and alumina and less calcium than the ashes from lignite and subbituminous coals (Table 3.1).

The calcium content of fly ash comes from the calcium present in the coal and the calcite and gypsum which are mined along with the coal. The silica and aluminum are derived from the clay minerals which are mined along with the coal. The most important clay minerals in coal, their nominal chemical compositions, and the Al_2O_3/SiO_2 weight ratios for these compositions are :

Smectite	$Na_{0.33}(Al_{1.67}Mg_{0.33})Si_4O_{10}(OH)_2 \cdot nH_2O$	0.35
Illite	$K_{0.5}Al_2(Al_{0.5}Si_{3.5}O_{10})(OH)_2$	0.61
Kaolinite	$Al_4Si_4O_{10}(OH)_8$	0.85

McCarthy et al. (1987) state that lignite coal contains the greatest proportion of smectite, the clay mineral with the lowest ratio of Al_2O_3 to SiO_2, and bituminous coal contains no smectite but some illite and kaolinite, minerals with higher ratios of Al_2O_3 to SiO_2. These ratios, combined with the dilution of both Al_2O_3 and SiO_2 by CaO in high-calcium fly ashes, results in the observed lower Al_2O_3 contents for the lignite and subbituminous fly ashes.

Although the chemical composition of the bulk fly ash depends upon the parent coal, the compositions of the individual fly ash particles are quite variable, regardless of the coal type. Stevenson and Huber (1987) used analytical electron microscopy to show that the chemical composition of fly ash particles can differ widely from particle to particle and even within single fly ash particles. Figures 3.1 through 3.3 show their results for fly ashes obtained from a bituminous, a lignite, and a subbituminous coal, respectively. Figure 3.1 shows that the fly ash from the bituminous coal is fairly uniform in chemical composition. However, several particles were observed to contain very high amounts of calcium even though the calcium content of the bulk fly ash was very low.

TABLE 3.1 EFFECT OF COAL TYPE ON THE CHEMICAL COMPOSITIONS OF FLY ASH.

Percent Element as:	COAL TYPE		
	Bituminous	Lignite	Subbituminous
CaO	0-10	5-20	15-35
SiO_2	45-65	25-55	20-50
Al_2O_3	20-30	<16	15-20
Fe_2O_3	4-20	5-10	5-10
MgO	1-2	3-5	3-5
alkalis	<3	<5	<5
LOI	<5	<5	<1

Figures 3.2 and 3.3 show that the situation was quite different for the ashes created from the lignite and subbituminous coals. These fly ashes were seen to contain high concentrations of several types of particles. Some of these particles approximated the composition of the bituminous fly ash particles, while others were markedly different. Based on these inter-particle differences in chemical composition, it is likely that these fly ashes do not exhibit a single type of reactivity towards $Ca(OH)_2$.

3.2.3 Crystalline species in fly ash

The crystalline material present in fly ash accounts for only 10 to 40 % of the fly ash matrix. The major crystalline species present in low-calcium fly ashes are mullite ($3Al_2O_3 \cdot 2SiO_2$), quartz, and magnetite or ferrite spinel. These crystalline species are deemed unreactive towards $Ca(OH)_2$ (Mehta, 1983). High-calcium fly ashes contain quartz, tri-calcium aluminate, $Ca_4Al_2SO_{11}$, calcium sulfate, and alkali sulfates. The calcium compounds and the alkali sulfates present in the high-calcium fly ashes are reactive towards water.

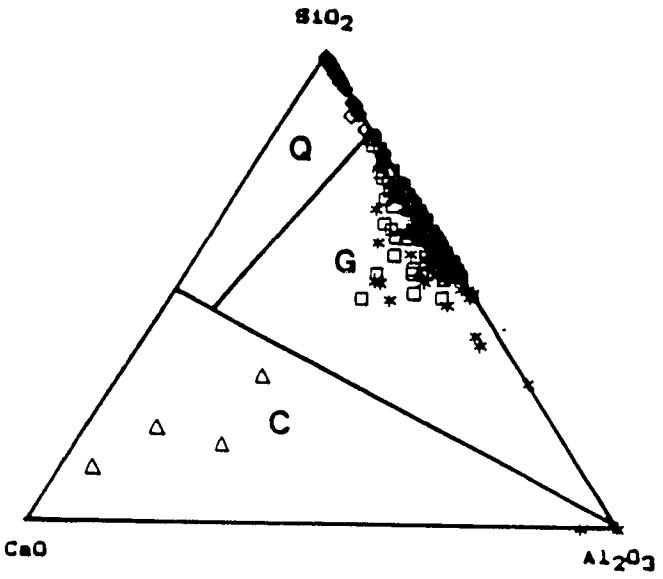

Figure 3.1 Electron microprobe chemical analyses for a low-calcium fly ash obtained from a bituminous coal.

Bulk chemical analysis : SiO_2: 51.5; Al_2O_3 : 24.4; Fe_2O_3 : 13.3; CaO : 3.0 (values in percent)

Data of Stevenson and Huber (1987).

The quartz that is found in almost all fly ashes is derived from the quartz that was present in the original coal (Manz and McCarthy, 1986). The alumino-silicates form from the melted clay material present in the coal as the fly ash is cooled upon exiting the boiler. The calcium- and alkali sulfates are thought to form in the boiler as reactions occur between the gaseous SO_2 and the calcium and alkali material present in the coal.

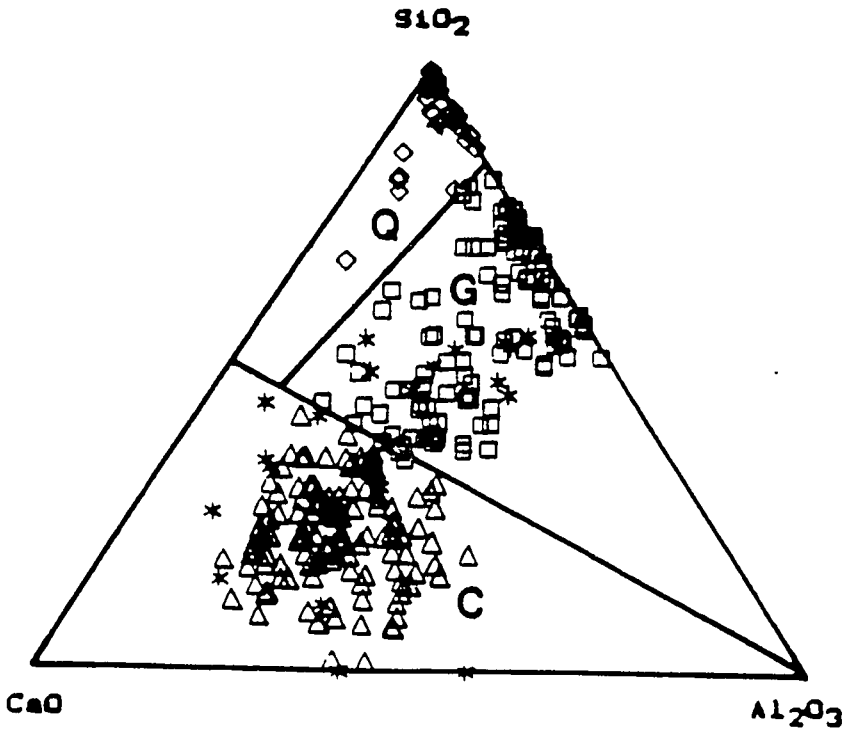

Figure 3.2 Electron microprobe chemical analyses for a high-calcium fly ash obtained from a lignite coal.

Bulk chemical analysis : SiO_2: 28.9; Al_2O_3 : 11.1; Fe_2O_3 : 11.1; CaO : 18.9 (values in percent)

Data of Stevenson and Huber (1987).

3.3 Chemistry and Structure of the Glassy Fraction of the Fly Ash

The glass present in fly ash generally makes up the majority of the fly ash matrix and the nature of this glass is believed to control the reactivity of the fly ash

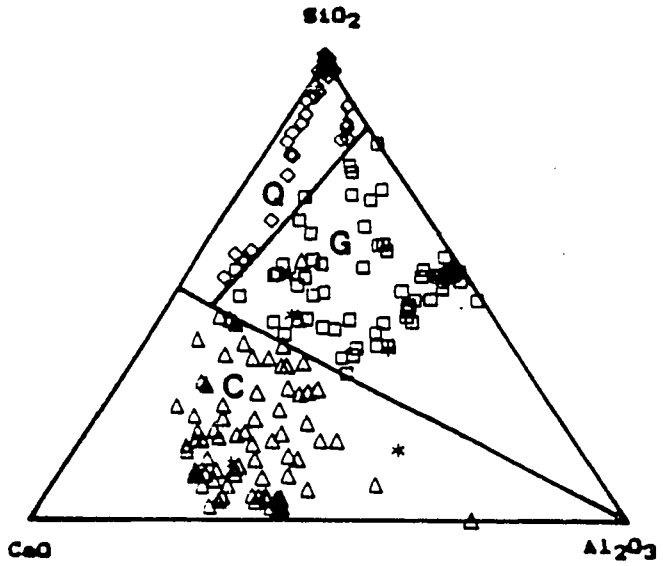

Figure 3.3 Electron microprobe chemical analyses for a high-calcium fly ash obtained from a subbituminous coal.

Bulk chemical analysis : SiO_2: 34.1; Al_2O_3 : 18.3; Fe_2O_3 : 5.9; CaO : 26.0 (values in percent)

Data of Stevenson and Huber (1987).

towards $Ca(OH)_2$. Therefore, understanding the composition and reactivity of the glass in the fly ash is key to understanding the reactivity of the fly ash.

Hemmings and Berry (1989) have proposed that the structure of the glass present in the fly ash is similar to the structure of amorphous silica. Figure 3.4 shows the structure of amorphous silica compared to crystalline silica. In crystalline silica, each silicon is associated with four oxygen atoms in a SiO_4

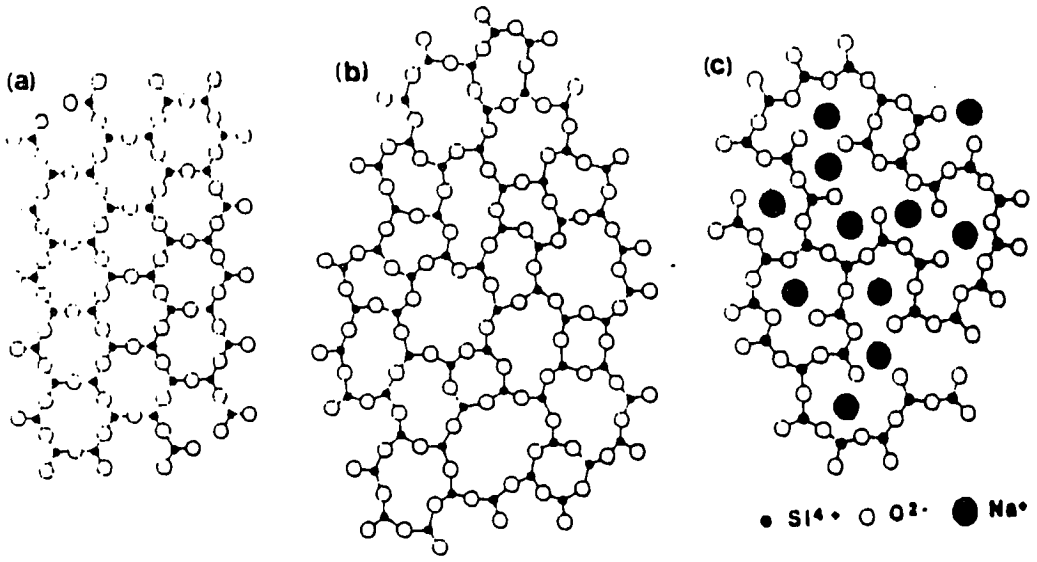

Figure 3.4 Schematic representation in two dimensions of the structure of (a) crystalline silica, (b) glassy silica, and (c) a binary silicate glass.

From Hemmings and Berry (1989).

tetrahedra and there are regular repeating unit cells. Notice that while there is no long-range order present in amorphous silica, short range order is retained with similar Si - O relationships. However, local perturbation of the SiO_4 tetrahedra can be presumed.

The polymeric nature of the amorphous silica present in fly ash is altered by the actions of two types of atoms : "network formers" and "network modifiers".

Network formers are elements with coordination numbers of 3 or 4, such as Al or Fe, which are capable of replacing silica in the polymeric network. Other materials, with coordination numbers ≥ 6, induce depolymerization of the network and are deemed "network modifiers". Examples of these modifiers include the alkalis and the alkaline earth elements. To preserve electroneutrality, Si-O-Si bonds break and two sorts of oxygens then co-exist : bridging and non-bridging oxygens (NBOs), the latter having essentially a dipolar interaction with the modifier metal (Figure 3.4c).

Since aluminum has a lower valency than silicon, when aluminum replaces silicon, the continuous polymeric nature of the network is broken and an excess negative charge must be neutralized by the inclusion of a cation as shown in Figure 3.5a. Note that the substitution of aluminum into the network depolymerizes the network and requires the presence of cations, but the presence of cations alone is sufficient to depolymerize the network (Figure 3.5b). In fact, Hemmings and Berry (1989) state that there are two types of glass present in fly ash. They call these glasses : "Glass I" and "Glass II" and distinguish them by the content of cation modifiers present in the fly ash. They have shown that glasses of type I have minimal levels of cation modifiers (they calculate that the level is the amount needed to handle the substitution of aluminum into the network). The glasses of type II are shown to have higher levels of cation modifiers and, as a result, the glass is less polymerized and more reactive than the glass of type I.

The degree of polymerization of the glass present in the fly ash has been inferred by x-ray diffraction, infrared absorption, Raman scattering, and other measurements on fly ash. Perhaps the most widely used technique is x-ray diffraction, which is normally used to identify the crystalline species present in a material.

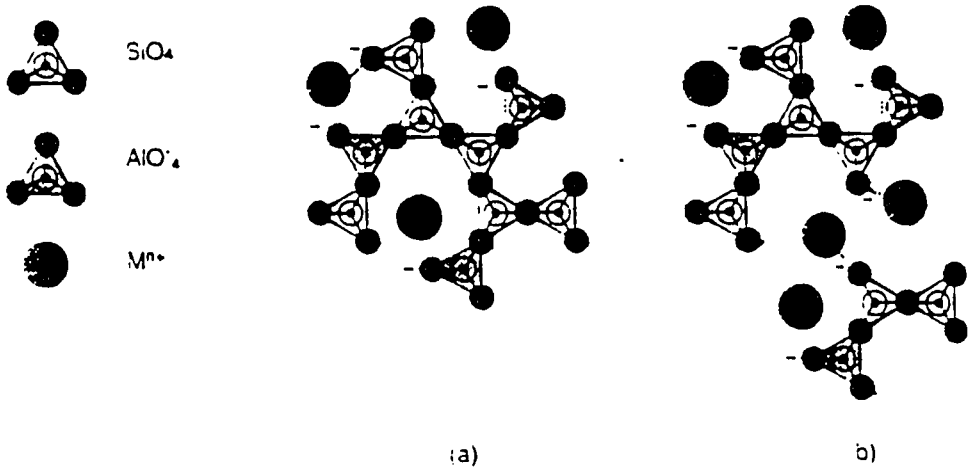

Figure 3.5 Proposed structural differences between fly ash glass types.

Proposed by Hemmings and Berry (1989).
(a) = Type I glass. (b) = Type II glass.

The highly amorphous nature of the fly ash produces an "amorphous hump" in the x-ray diffraction pattern (Figure 3.6). Hemmings and Berry (1989) state that the location of this hump on the x-ray diffraction pattern indicates the degree of polymerization of the fly ash. They cite data from experiments using a sodium silicate model glass in which the Na_2O content was varied from 0 to 50%. This

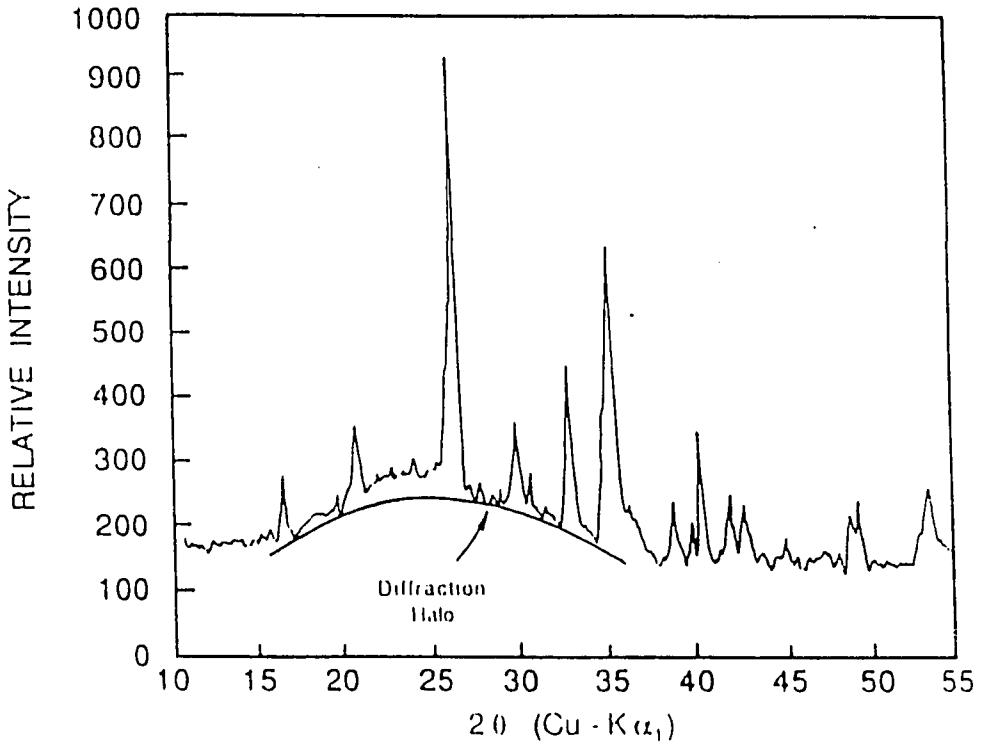

Figure 3.6 Use of x-ray diffraction for the detection of the "amorphous hump" present in fly ash.

From Tikalsky (1989).

increased the ratio of non-bridging oxygens:silicon from 0 to 2. That is, the glass became successively depolymerized as the sodium content increased (i.e. 3D ⇒ sheets ⇒ chains ⇒ monomer). Figure 3.7 shows that the position of the amorphous hump (i.e. $2\theta_{max}$) increased from 21.3 ° 2θ for the totally polymerized glass to 34 ° for the totally de-polymerized glass (Copper K^{α} radiation). However,

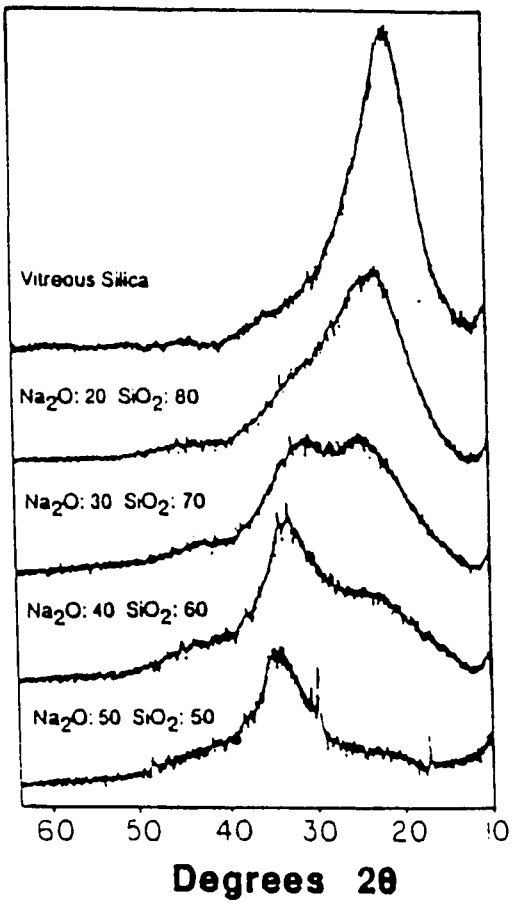

Figure 3.7 X-ray diffraction patterns for Na_2O-SiO_2 model glasses.

From Hemmings and Berry (1989). Copper K^{α} radiation.

the authors also noted the presence at least two maxima of varying intensity : a low angle feature at 22-24° $2\theta_{max}$, and a high angle feature at 30-34° $2\theta_{max}$. Thus,

even for this simple system, different glass types co-exist over a range of compositions. The $2\theta_{max}$ values correlated with the Na_2O content of the glass (Figure 3.8). The low angle maximum was invariant and most likely represents a highly polymerized SiO_2 network (possibly sheets), while the high angle maximum showed a strong correlation with the Na_2O content and represents decreasing polymerization of the silicate network.

In an earlier study, Hemmings and Berry (1986) fractionated a subbituminous fly ash by particle size and by particle density into six different size or density fractions. They found no correlation between the fly ash particle size and the chemical composition or the mineralogy of the particles. However, the separation of the fly ash by particle density produced a very strong correlation with chemical composition and mineralogy. The most dense particles had higher calcium and iron contents than the less dense particles, which were richer in silica and aluminum. The dense particles also had much higher values of $2\theta_{max}$ than the less dense particles which indicates the high degree of depolymerization of the dense particles. This data also emphasizes the degree of inhomogeneity present in fly ash. Both the chemical and the mineralogical compositions of the fly ash can vary greatly from particle-to-particle as well as from ash-to-ash. In fact, several studies have used transmission electron microscopy to show that there are many instances of intra-particle chemical and mineralogical differences present in fly ash (Quian and Glasser, 1988; Quian et al., 1989).

The strong correlation of particle density with chemical composition results from the effects of chemical composition on the viscosity of the fly ash melt. The presence of calcium and alkali metals in the melt lowers the viscosity of the fly ash melt. Hemmings and Berry (1989) estimate that, at 1500 °C, the viscosity of Glass I falls in the range of 400-1200 poise, while the viscosity of Glass II is only 5-12 poise. When the melted fly ash spheres expand during formation (due to the expansion of gases released inside the spheres), the spheres with low viscosity

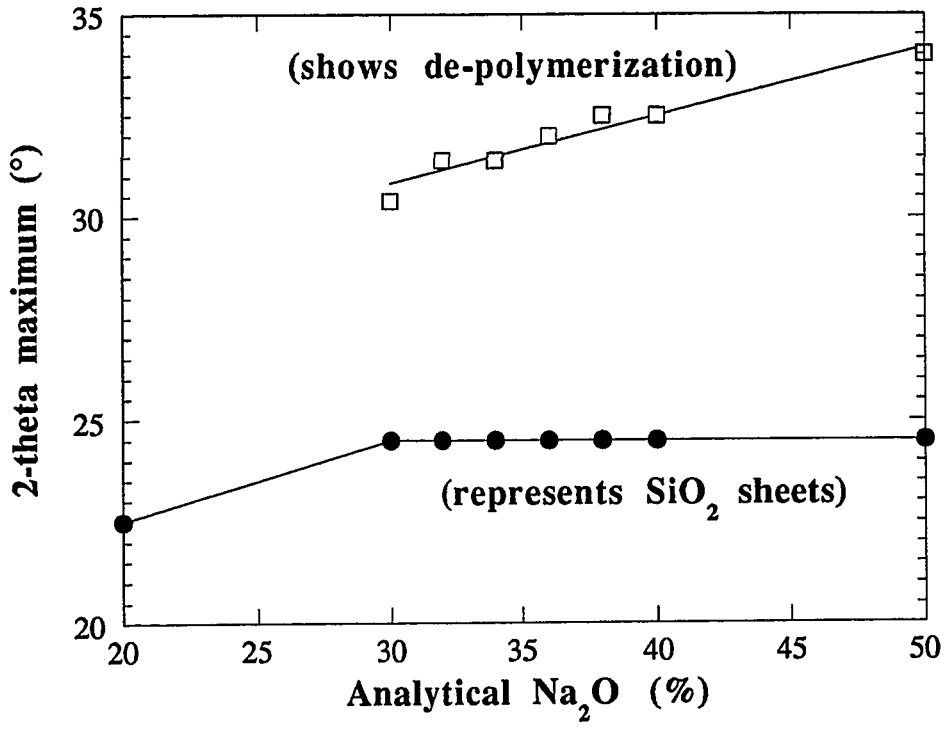

Figure 3.8 Effect of modifier content on $2\theta_{max}$ for Na_2O-SiO_2 model glasses. Data from Hemmings and Berry (1989).

burst to form smaller, solid particles. The spheres with moderate viscosity get "frozen" into hollow spheres when they are rapidly cooled upon exiting the boiler. Note that these spheres are larger, cool slower, and are more crystalline than the "bursted" spheres.

3.4 Summary

A review of the literature has shown that fly ash is a very diverse material. Its chemical and mineralogical composition varies from ash-to-ash, particle-to-particle, and even within particles. This makes the study of the reaction of fly ash with $Ca(OH)_2$ a more difficult task. Because of this diversity, it is probably a misnomer to speak of the "lime/fly ash" reaction since a number of different reactions are possible in the lime/fly ash system.

The next chapter will describe the reactions which can take place in the lime/fly ash system. This material will be presented to facilitate the analysis of the data from the current study.

Chapter IV

Chemical Reactions in the $Ca(OH)_2$-Pozzolan System

4.1 Introduction

The literature reviewed in the previous chapter showed that fly ash consisted of small, glassy particles which contain a large fraction of silicon and aluminum. These metals enable the fly ash to react with $Ca(OH)_2$. The reactions that occur are usually lumped under the general term "pozzolanic reaction", but are actually quite diverse and should be discussed separately. This chapter reviews the literature pertaining to these reactions in order to give a base of understanding for interpreting the lime/fly ash reaction.

Most of the published work that concerns the reactivities of silica and alumina under alkaline conditions has application to the chemistry of cement and concrete. Therefore, the experimental conditions for most of these studies involved low temperature (usually 25 °C), long reaction times (days to years), and stagnant solutions (i.e. no mixing). However, some relevant data are available and will be discussed in this section.

4.2 Reactivities of silica and alumina

Silica dissolves in water according to the following equation (Iler, 1979) :

$$(SiO_2)_x + 2H_2O \Rightarrow (SiO_2)_{x-1} + Si(OH)_4 \qquad (A)$$

Since this reaction is catalyzed by the hydroxide ion, Iler has proposed that the dissolution of amorphous silica proceeds according to the mechanism presented in Figure 4.1.

The solubility of amorphous silica increases with the temperature and pH of the solution (Figure 4.2). The increase in the solubility with the solution pH occurs because the monosilicic acid formed by the dissolution of silica is converted to an ionic species by reaction with hydroxide :

$$Si(OH)_4 + OH^- \Rightarrow H_3SiO^-_4 + H_2O \qquad (B)$$

The consumption of monosilicic acid causes reaction (A) to proceed to the right. The pK_a 's for monosilicic acid are reported to be 9.7 and 11.7 at 30 °C for the first and second dissociation constants, respectively (Greenberg and Chang, 1965).

The hydroxide ion also has a strong effect on the rate of silica dissolution. Iler (1979) reports that the dissolution rate of amorphous silica is approximately first order in the hydroxide concentration when the solution pH is between 6 and 9 (Figure 4.3). At higher pH, the effect of the hydroxide concentration on the dissolution rate was not as great, but, at very high pH, Iler indicates that the dissolution rate might have been iimited by diffusion of silica away from the surface of the silica particles. Note that the dissolution mechanism proposed by Iler (Figure 4.1) suggests a first order dependence on the hydroxide concentration.

Greenberg (1957) found that the dissolution rate of silica in alkali solution was highly dependent upon the surface area of the silica. He also determined that the activation energy for silica dissolution was 21.5 kcal/mol. In a later study using a different amorphous silica, O'Conner and Greenberg (1958) found the activation energy to be 18 kcal/mol.

The dissolution rate and solubility of pure silica is also highly dependent upon the presence of other metals in the system. For example, Iler (1973) showed that the presence of small amounts of dissolved aluminum (less than 100 ppm)

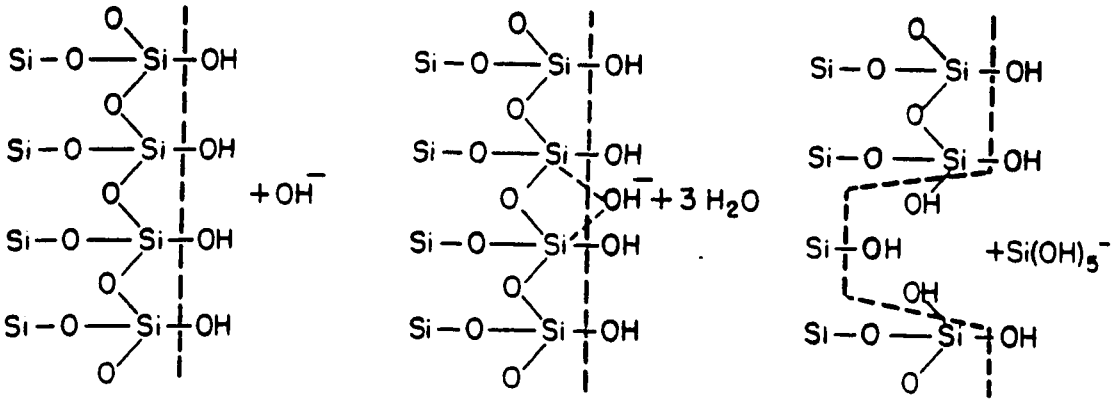

Figure 4.1 Mechanism for the dissolution of silica in the presence of the hydroxide ion. From Iler (1979).

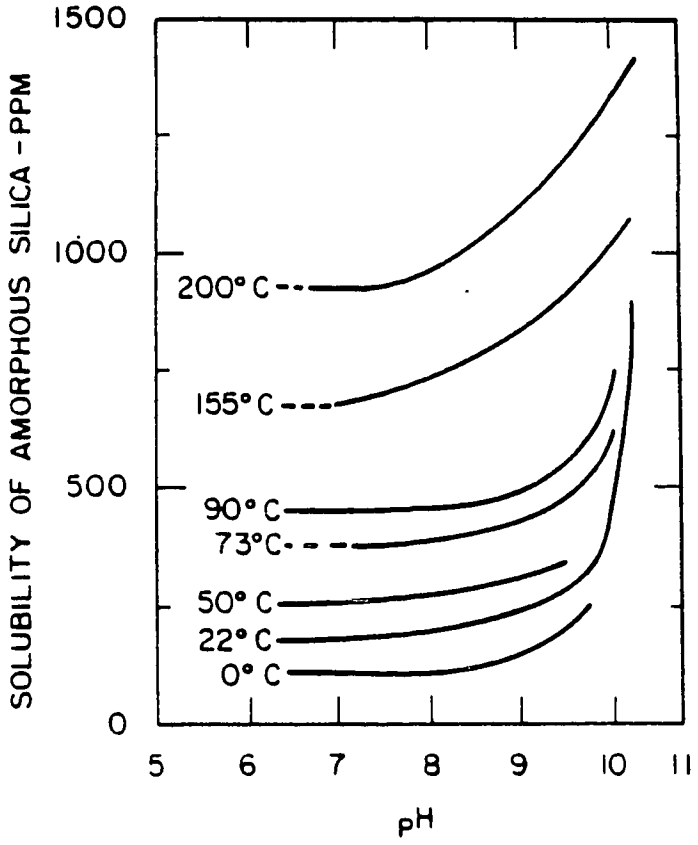

Figure 4.2 Effect of solution pH and temperature on the solubility of amorphous silica in water. From Iler (1979).

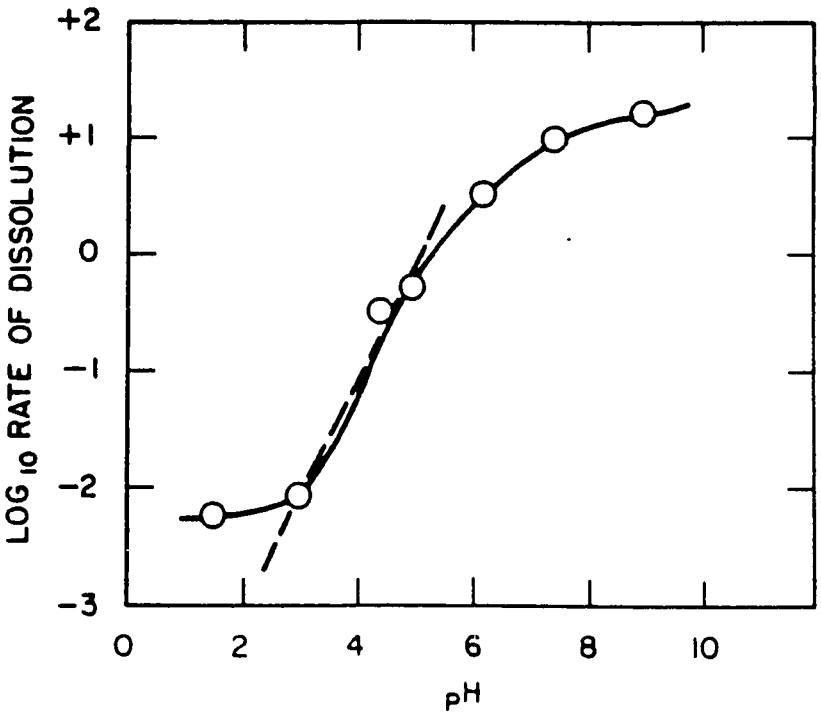

Figure 4.3 Effect of solution pH on the dissolution rate of amorphous silica. From Iler (1979).

dramatically decreased the dissolution rate and the solubility of amorphous silica. Iler states that the aluminum adsorbs onto the surface of the silica and forms a layer which is impenetrable to hydroxide, so no dissolution of the silica occurs. This study was conducted at a pH of 8, where the effect of aluminum is the strongest. No data were found for solutions in the pH range of interest for the production of lime/fly ash solids.

Aluminum is one of the major constituents of fly ash and is able to react with calcium hydroxide to form calcium-aluminate compounds. Much less work has been published concerning the reactivity of aluminum in aqueous, alkaline solutions. However, it is well known that aluminum is readily soluble at very high pH (where it exists as $Al(OH)^-_4$), as well as at very low pH (where it exists as Al^{3+}).

4.3 The CaO-SiO2-H2O system

The reactions occurring in the $CaO\text{-}SiO_2\text{-}H_2O$ system have been studied extensively because they are the major reactions occurring during the hydration of Portland cement. When cement is mixed with water, the tricalcium silicate and dicalcium silicate materials react with water to produce $Ca(OH)_2$ and calcium-silicate-hydrate gel. The reaction for tricalcium silicate can be written as :

$$2\,(3CaO.SiO_2) + 6H_2O \Rightarrow 3CaO.2SiO_2{\bullet}3H_2O + 3Ca(OH)_2 \qquad (C)$$

but this simple equation does not represent the complexities of the reaction. For example, the composition of the gels produced during the hydration changes during the period of reaction and also varies with the water:solids ratio of the cement paste.

Two types of calcium-silicate-hydrate gels form and are distinguished by the ratio of calcium-to-silica present in the gel. Those gels with a calcium-to-silica ratio from 0.8 to 1.5 usually have the morphology of "crumpled foils" and are denoted as Type I hydrates (or C-S-H (I)). The Type II hydrates, or C-S-H (II), have a fibrous morphology and a calcium-to-silica ratio of 1.5 to 2. Both types are very

poorly crystallized and exhibit only a few diffraction lines. Both types also have a high specific surface area and readily absorb water, although the actual combined water present in the hydrates is less than or equal to 2.5 mols of water/mol of silica.

Even though most of the literature concerning the C-S-H gels pertains to cement and concrete, there is ample evidence that these gels are the only materials formed for temperatures less than 100 °C, regardless of the preparation method. There are a variety of well-crystallized calcium-silicate-hydrates, but all of these are formed under pressure-hydration conditions (i.e. $T > 100$ °C, $P > 1$ atm), so these materials will not be discussed here. For a complete review of these materials, see Lea (1971) or Taylor (1964).

Numerous investigations have been made on the gelatinous products of the reactions occurring in the CaO-SiO_2-H_2O system. The data from these studies is usually represented by plotting the calcium-to-silica ratio in the solid phase versus the calcium concentration in the solution (Figure 4.4). When the data is plotted this way, it is evident that C-S-H (I) is only in equilibrium with undersaturated solutions of $Ca(OH)_2$, and that C-S-H (II) is the equilibrium product for saturated solutions. However, Lea (1971) reports that both products may form simultaneously and that no clear-cut dividing line is present to distinguish the two.

Taylor (1950) found no significant change in the x-ray diffraction pattern as the calcium-to-silica ratio varied from 1.0 to 1.5, which indicates that the basic structure of C-S-H (I) does not change with the incorporation of calcium into the gel. Taylor also examined C-S-H (II) with a calcium-to-silica ratio of about 2 and found that $Ca(OH)_2$ was not present, but that the x-ray diffraction pattern was significantly different from the Type I hydrate.

The reasons for the changing ratio of calcium-to-silica in the solid are not clear. Lea (1971) suggests that it may be due to the incorporation of extra calcium ions into the lattice, to the replacement of silicate by hydroxide, or to the condensation of silica monomers to form oligomers or polymers in the calcium-

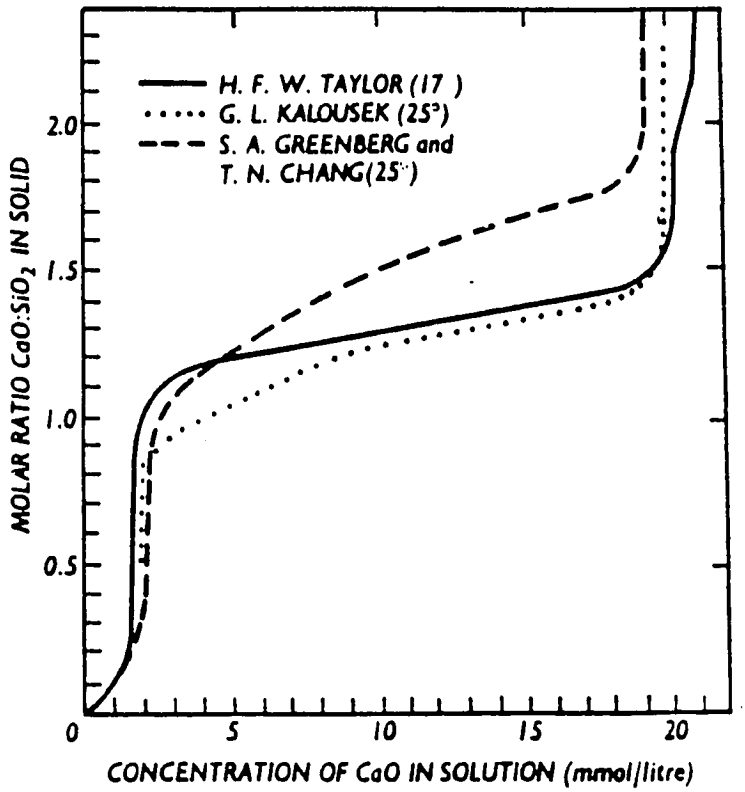

Figure 4.4 Equilibria between hydrous calcium silicates and solutions.

From Iler (1979).

silicate-hydrate gel. Alternatively, since the C-S-H gel has a layered structure that is poorly crystallized, the variable ratio may be due to a mixed layer structure.

Greenberg and Chang (1965) have concluded that for calcium-to-silica ratios from 0.14 to 1.0, the solids consisted of mixtures of CaH_2SiO_4 and silica gel. For ratios of 1.0 to 1.75, the solid was regarded as a solid solution of $CaH_2SiO_4 \cdot nCa(OH)_2$. They were able to derive a solubility product for CaH_2SiO_4 ($K_{sp} = a_{Ca}{}^* a_{H2SiO4} = 10^{-7.2}$) which applied for solids having calcium-to-silica ratios of 0.2 to 1.8.

4.4 The CaO-Al2O3-H2O system

The $CaO\text{-}Al_2O_3\text{-}H_2O$ system has also been studied extensively by cement and concrete chemists, since Portland cement contains a significant fraction of tricalcium aluminate which reacts with water in a similar manner to tricalcium silicate.

Fortunately, however, the $CaO\text{-}Al_2O_3\text{-}H_2O$ system is not as complicated as the $CaO\text{-}SiO_2\text{-}H_2O$ system. The hydrated calcium aluminates generally crystallize more readily than do the hydrated calcium silicates. Lea (1971) indicates that $3CaO.Al_2O_3.6H_2O$ (abbreviated as C_3AH_6) is probably the only stable reaction product for temperatures from 20 to 225 °C. Other metastable products may form, but these transform fairly rapidly into C_3AH_6, especially at temperatures of greater than 50 °C.

One major area of research pertaining to the hydration of tricalcium aluminate in cement is the interaction of sulfate with the hydration products. The sulfate is usually present as gypsum, which is added to all cements to control the rate of hydration (i.e. the set time). The sulfate can interact with the calcium-silicate-hydrate gels by substitution into the gels, but the effect is minor compared to the effect on the tricalcium aluminate hydration.

Gypsum reacts with the initial hydration products of tricalcium aluminate to form ettringite or calcium-monosulfate-aluminate materials on the surface of the tricalcium aluminate particles. These materials form a barrier to the further hydration of the tricalcium aluminate. This barrier holds for a while, but then fissures develop and the hydration of tricalcium aluminate continues, albeit at a slower rate (Brown and La Croix, 1989).

4.5 Other considerations

Although the reactions occurring in the above systems are fairly well-understood, such is not the case for more complicated systems, where interactions of calcium, aluminum, and silica can take place with each other and with other materials such as iron or sulfate.

Lea (1971) writes that Al^{3+}, Fe^{3+}, and sulfate can all enter into the structure of the calcium-silicate-hydrate gel. The maximum amount of aluminum is about 1 atom of Al per 6 atoms of Si. The aluminum can enter the gel in two ways :

- Al^{3+} and H^{+} can replace Si^{4+}
- 2 Al^{3+} can replace 3 Ca^{2+}

Similarly 2 Fe^{3+} can replace Ca^{2+} and Si^{4+} with a maximum of 1 atom of Fe per six atoms of Si.

While these values indicate the maximum substitution possible, Lea states that there is some evidence that the C-S-H phase finally formed in set cement contains considerable alumina, but little ferric oxide or sulfate, though the latter is taken up slightly.

The only well-established hydrated calcium silicoaluminate is the compound $2CaO.Al_2O_3.SiO_2.8H_2O$ which is sometimes called 'gehlenite hydrate'. This material is difficult to prepare in a pure form and dissolves incongruently in water.

It is unstable in saturated lime solutions at room temperature or in weaker lime solutions at 50 °C (Lea, 1971).

4.6 Summary of pozzolanic reactions

From a review of the literature concerning the reactions of aluminum and silica in cement and concrete, it is clear that the $Ca(OH)_2$-Pozzolan-H_2O system is very complicated and not entirely understood. Since fly ash contains both reactive silica and reactive alumina, it is expected that several reactions will occur in the "lime/fly ash" reaction.

Calcium-silicate-hydrate gels should form in the lime/fly ash system. In fact, based on the work of Jozewicz and Rochelle (1986A, 1986B), it is likely that these gels are what give the lime/fly ash materials their high surface area and high reactivity towards SO_2.

However, since the lime/fly ash system includes reactive aluminum, we should expect at least some substitution of the aluminum into the the calcium-silicate-hydrate gels. It is not known how much of the gel will be substituted with aluminum, although it should be less than 15 percent of the total silica. It is also not known how this substitution will affect the reactivity of the solids towards SO_2. Pure hydrated calcium aluminates might also form in the lime/fly ash system, but these are quite crystalline and are not expected to be reactive towards SO_2.

Chapter V

Experimental Apparatus and Procedure

As was stated in Chapter I, the overall goal of this research is to determine the important elements involved in the production of lime/fly ash materials for flue gas desulfurization. To accomplish this broad-based task, a number of different types of experiments were performed. These experiments varied from well established analytical tests (such as BET surface area measurements) to unconventional procedures (such as the fly ash dissolution experiments). The unconventional procedures are described in the following sections, while the more established techniques are documented in Appendix A.

5.1 Fly ash dissolution experiments

The overall reaction rate between fly ash and $Ca(OH)_2$ is believed to be limited by the dissolution rate of silica from the fly ash (Jozewicz and Rochelle, 1986A, 1986B). Thus, the overall reaction can be assumed to occur by the following simplified mechanism :

$Ca(OH)_2$ (s) $\Leftrightarrow$ Ca^{2+} + 2 OH^- (fast)

Fly Ash (s) $\Leftrightarrow$ silica (aq) (slow)

Ca^{2+} + silica (aq) $\Leftrightarrow$ calcium silicates (fast)

Since this dissertation studies the reaction of lime with fly ash and since fly ash dissolution is the rate limiting step occurring in this reaction, it is logical to

study fly ash dissolution separately from the overall reaction of fly ash with $Ca(OH)_2$.

To set up a fly ash dissolution experiment, the literature was reviewed to determine which existing experimental procedure, if any, would be the most representative test for studying the dissolution rate of silica from fly ash. Most of the literature concerns the use of fly ash as additives to concrete in order to replace part of the Portland cement normally present in the concrete (Chapter III). Since the reaction conditions experienced for the fly ash in concrete (low temperatures, long times) are quite different than those experienced in the production of lime/fly ash solids (high temperatures, short times), the tests proposed for determining the reactivity of fly ash in concrete are probably not adequate to determine fly ash reactivity under the conditions of lime/fly ash reaction. However, these well-known techniques will be discussed for completeness.

The Raask test (Raask and Bhaskar, 1975) determines the availability of the silica by stirring 150 mg of fly ash in 150 ml of 0.1 M HF and then monitoring the conductivity of the solution after 10 minutes. The reactivity of the fly ash is determined by the increase in the solution conductivity. The experiment is performed at 300 K. This test has been criticized due to the assumption that the increase in conductivity is due only to the dissolution of silica from the fly ash. Most fly ashes, especially high-calcium fly ashes, contain materials that will dissolve easily (e.g. Ca, Na, K) and will therefore increase the conductivity of the solution and give artificially high silica dissolution rates.

Another test, proposed by Cabrera et al. (1986) involves repeatedly boiling and cooling a mixture of fly ash and 5 M NaOH and determining the amount of silica and aluminum that dissolve from the fly ash by analyzing the solution with atomic absorption spectroscopy. This test approximates the reaction conditions which occur during the lime/fly ash reaction (i.e. high temperature, high pH). This test has shortcomings, however, since no effort was made to avoid precipitation of calcium silicates on the surface of the fly ash particles. This precipitation would

occur due to the reaction of the calcium with silica, both of which are present in fly ash. This precipitation would lead to a lower rate of silica dissolution from the fly ash due to the removal of silica by the precipitation of calcium silicates and due to the increased mass transfer resistance of the product calcium silicate layer on the surface of the fly ash.

For this study, the dissolution rate of fly ash was studied using NaOH, as in the test described by Cabrera, but in the absence of the precipitation reaction of calcium silicates. This was accomplished by adding EDTA to the solution to complex the calcium that dissolves from the fly ash, so as to avoid the precipitation of calcium silicates.

The fly ash dissolution experiments were performed in a temperature controlled, 500 ml stainless steel autoclave (Figure 5.1). The autoclave was covered to minimize any evaporative loss of H_2O, but the reactor was not gas-tight for these experiments which were performed at ambient pressure. In the fly ash dissolution experiments, 500 mg of fly ash were added to 400 ml of distilled water containing 2.0 g of Na_2EDTA/400 ml H_2O. The NaOH concentration was adjusted with 5 N NaOH before the addition of the fly ash to the solution. The NaOH concentration was varied from 0.0 to 0.5 M and the slurry temperature was varied from 25 to 90 $\pm$ 1.0 °C (the temperature of the solution was attained before the addition of the fly ash). The solutions were stirred at 1000 rpm for up to 24 hours as the fly ash dissolved. Ten types of fly ash, ranging from 2 to 34% CaO (Table 5.1), were used in the experiments.

Solution samples were taken with time and filtered through a 0.45 micron membrane-type filter. The filtrates were cooled to room temperature and then analyzed for calcium, silicon, and aluminum using atomic absorption spectrophotometry (AA). The operating procedures and parameters for the atomic absorption analyses are given in Appendix A. The conversion of the metals in the fly ash was determined by dividing the measured concentration of the metals in

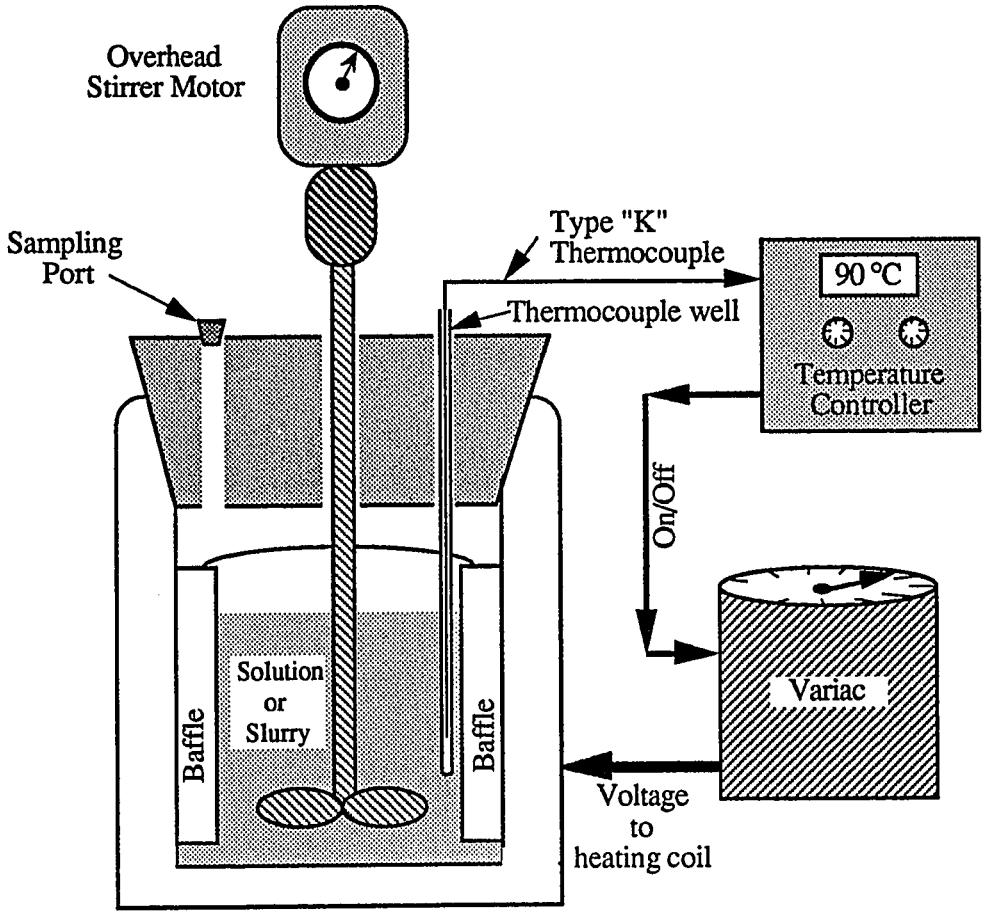

Figure 5.1. Apparatus used for fly ash dissolution experiments and solids preparation experiments.

TABLE 5.1 CHEMICAL COMPOSITIONS OF FLY ASHES.

Fly Ash	Plant Location	Mine Location	Coal Type[a]	Ash Composition as Oxides (%) CaO	SiO_2	Al_2O_3	Fe_2O_3
Big Brown	Texas	Texas	L	10	53	18	9
Clinch River	Virginia	Virginia	B	4	57	27	8
Deseret	Utah	Utah	B	4	46	24	5
Fayette	Texas	Wyoming	S	26	33	24	6
Harrington	Texas	Wyoming	S	30	32	22	5
Huntington	Utah		B	9	51	18	6
Kingston			B	2	50	28	8
Laramie River	Wyoming	Wyoming	S	30	33	18	6
Monticello	Texas	Texas	L	7	56	19	4
Salt River	Utah	Utah	B	8	61	23	5
Welch	Texas	Wyoming	S	34	28	20	5

[a] B = Bituminous; L = Lignite; S = Subbituminous

solution by the calculated concentration for total dissolution of the fly ash (based on the chemical analyses presented in Table 5.1).

The need for the presence of EDTA in the solution is evidenced in Figure 5.2 which compares the dissolution of fly ash with and without EDTA present in the slurry. The data clearly shows that EDTA was necessary to complex the calcium which dissolves from the fly ash so as to prohibit the precipitation of calcium silicates from the solution.

5.2 Solids Preparation

Lime/fly ash solids were prepared by slurrying fly ash with $Ca(OH)_2$ in the same autoclave used for the fly ash dissolution experiments. In the base-case slurry conditions, 35 grams of $Ca(OH)_2$ were slurried with 105 grams of fly ash in 400 ml of distilled water. The reagent $Ca(OH)_2$ was added before the fly ash to completely saturate the solution to $Ca(OH)_2$. After 15 minutes the fly ash was added, normally at a loading of 3 g fly ash/g $Ca(OH)_2$. Nine types of fly ash (Table 5.1) were used in the base-case experiments to determine the effect of fly

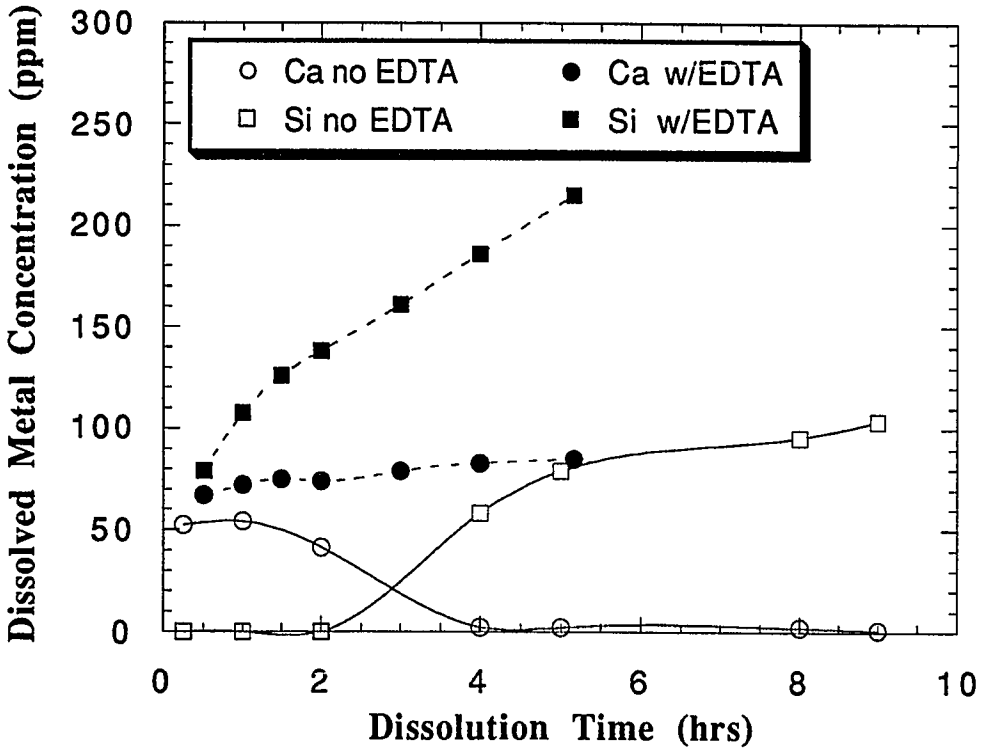

Figure 5.2 Effect of EDTA on the dissolution rate of fly ash.

Dissolution Conditions : 90 °C; 0.10 M NaOH; 1.25 g Clinch River fly ash/liter;1000 rpm; with EDTA : 5.0 g Na_2EDTA/l.

ash type on the reaction of lime with fly ash. The slurry temperature was varied from 25 to 92 °C and the stirring speed was 1000 rpm.

Five slurry samples were taken during each run, usually at slurry times of 0.25, 1.0, 3.0, 5.0, and 8.0 hours. The samples were vacuum filtered and both the solids and the filtrates were recovered. The solids were oven dried for approximately 1 hour at 110 °C in an atmospheric oven. These dried solids were stored in air-tight glass sample bottles until they were used in the solids characterization tests. The filtrates were pressed through a 0.45 micron membrane type filter, stored in air-tight polypropylene sample bottles, and cooled to room temperature. The pH of the filtrates was measured at room temperature and the dissolved metal concentrations were determined using atomic absorption spectroscopy.

In a large block of tests, reagent materials (i.e. silica fume or $Al(OH)_3$) were substituted for the fly ash to determine more information about the reaction of fly ash with $Ca(OH)_2$. These experiments were carried out at the same conditions as the lime/fly ash tests, but the total solids loading in the slurry was different than that for the lime/fly ash tests.

Another large block of tests investigated the presence of recycle materials in the slurry. In these tests, laboratory produced $CaSO_3 \cdot 0.5H_2O$ or reagent-quality gypsum was added to the slurry along with the $Ca(OH)_2$ (i.e. before the addition of the fly ash). The operating procedures and parameters were the same as for the base-case slurry except for the increased solids concentration in the slurry due to the presence of the recycle materials.

5.3 Solids characterization experiments

The lime/fly ash solids that were produced in the above experiments were subjected to various characterization experiments. Some of these experiments are well known and do not need to be extensively documented, but others have been

created expressly for this study or have been adapted for use from other studies. These latter types of experiments are documented below.

5.3.1 Solids reactivity experiments - equipment and procedure

The solids reactivity experiments were performed in a packed bed reactor system which was designed to simulate bag filter conditions downstream of a cool-side dry FGD process (Figure 5.3). In these experiments, the test solids were exposed to a synthetic flue gas to determine their reactivity towards SO_2. The solids were dispersed in fine silica sand to prevent the channelling of gas which would otherwise occur due to $Ca(OH)_2$ agglomeration (Karlsson, 1983). The sand mixture was supported on a glass frit which was positioned just above the outlet of the reactor. The glass frit accounted for most of the 2 psi pressure drop across the reactor and therefore further minimized the channelling of the gas through the reactor.

The synthetic flue gas was created by combining N_2, CO_2, and SO_2 with compressed air. Precisely calibrated Brooks Mass Flow Controllers, Series 5850, powered and controlled by a Brooks Controller, Model 5878, were used to deliver all of the gases to the packed bed reactor. These flow controllers have a reported reproducibility of ±0.20 percent of full scale. Water vapor was added to the system by injecting distilled water into an evaporation chamber via a constant flowrate syringe pump (Harvard Apparatus Model # 980). The total flue gas flowrate to the reactor was 5.8 slpm (wet) and consisted of 8.7% CO_2, 10.4% O_2, 14.1% H_2O, and the balance nitrogen. The inlet SO_2 concentration was normally 1000 ppm (dry).

The pyrex reactor (4 cm diam, 12 cm height) was filled with the lime/fly ash - sand mixture and then placed in a constant temperature water bath where the temperature was controlled at 70 °C ± 0.5 °C. The pressure upstream of the reactor was adjusted before every run to 6 psig, which gives a calculated relative humidity of 64 % for the synthetic flue gas. These experimental conditions correspond to an approach-to-adiabatic saturation temperature of approximately 10 °C.

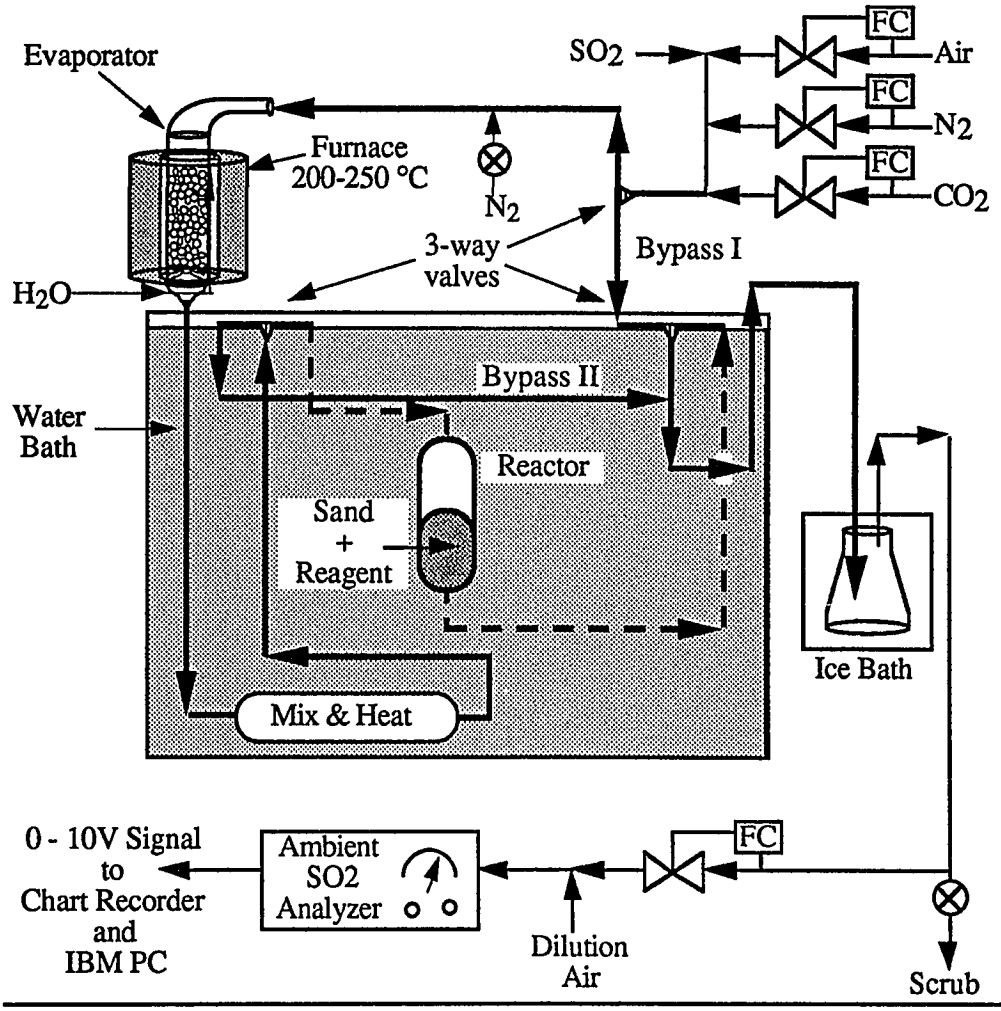

Figure 5.3. Packed Bed Reactor System

Reaction Conditions : 70 °C, 64% Relative Humidity, 5.0 slpm, 1000 ppm SO_2, 12 % O_2, 10% CO_2, 78% N_2 (dry basis).

The reactor was equipped with a bypass to allow for preconditioning of the solids and to allow the gas concentration to stabilize before starting the experiment. After the reactor, the gas was cooled and the water condensed out by an ice water condenser. A small sample of the dry gas (approx. 2.5 sccm) was diluted with air so that the SO_2 concentration was less than 1 ppb (the dilution air was monitored with a rotameter). This diluted gas was then sent to a flame photometric SO_2 analyzer (Columbia Scientific Instruments Model SA285E). The majority of the dry gas, that is, the gas that was not diluted and sent to the analyzer, was sent to a solution of NaOH in water to scrub the SO_2 out of the gas before it was released to the atmosphere. The SO_2 concentration at the outlet of the reactor was continuously recorded and was integrated to determine solids reactivity.

The SO_2 analyzer/dilution system was calibrated at least once a week using a certified span gas of 1000 ppm SO_2 in nitrogen. Note that although the span gas did not contain oxygen or carbon dioxide, this did not cause a bias in the experimental results since the span gas was diluted by the dilution system to a concentration of about 1 ppb before entering the analyzer. The use of this dilution system was advantageous because the carrier gas that was sent to the analyzer was essentially pure air, and changing the flue gas composition caused no bias in the measured SO_2 concentration.

The solids loading in the reactor was typically 0.4 g of $Ca(OH)_2$ with 1.2 g of fly ash. The amount of material placed in the reactor was adjusted so that the $Ca(OH)_2$ loading was always 0.4 grams. Before each experiment the solids were preconditioned at 95% relative humidity for 8 minutes and for 10 more minutes at 64% relative humidity. This humidification procedure was designed to bring the solids to an equilibrium moisture content before they were subjected to reaction with SO_2. After this preconditioning, the solids were exposed to the synthetic flue gas for 1 hour.

5.3.2 Solids reactivity experiments - data analysis

The raw data from the solids reactivity experiment was a curve of SO_2 concentration leaving the reactor versus time (Figure 5.4). The reactivity of the sorbent was calculated using a mass balance and integrating the outlet SO_2 concentration. In most experiments, the integration was performed by an on-line PC equipped with a data acquisition system which received voltage signals from the SO_2 analyzer. The PC was programmed to calculate percent SO_2 removal, the $Ca(OH)_2$ conversion, and the SO_2 capture for the test solids.

The dilution system used in the sandbed reactor system caused a time lag in the analyzed SO_2 concentration. The SO_2 concentration, as determined by the analyzer, did not change until approximately 1 minute after the gas was started through the reactor. In determining the amount of SO_2 removed during the reaction, the initial time (time 0) was taken as that when the SO_2 concentration started to drop at the SO_2 analyzer. The final time (time 60) was taken as 60 minutes after the initial time.

The reactivity of the sorbents towards SO_2 is expressed either as "$Ca(OH)_2$ conversion" or as "SO_2 capture". $Ca(OH)_2$ conversion is defined as the total number of moles of SO_2 removed after 1 hour divided by the initial number of moles of $Ca(OH)_2$ in the sorbent. SO_2 capture is defined as the number of millimoles of SO_2 removed from the gas divided by the weight of the lime/fly ash solids initially placed in the sandbed reactor.

5.3.3 Sugar Dissolution of Fly Ash/Lime Solids

Since fly ash is a waste product, it has no set chemical composition, reactivity, or morphology. This makes the study of the reaction of fly ash with $Ca(OH)_2$ more complicated than simply studying the reaction of two reagent chemicals. In fact, it is very difficult, if not impossible, to determine the reaction

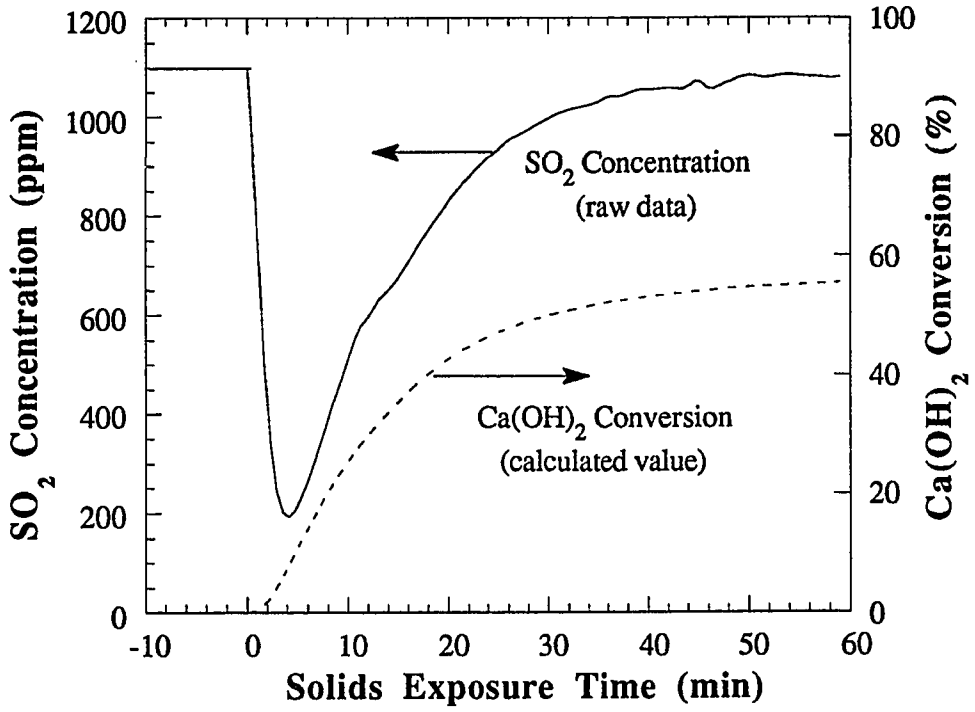

Figure 5.4 Typical data from packed bed reactor experiments.
SO_2 removal : 21.2 %; $Ca(OH)_2$ Conversion : 55.5 %

Reaction Conditions : 70 °C, 64% Relative Humidity, 5.0 slpm,
1000 ppm SO_2, 12 % O_2, 10% CO_2, 78% N_2 (dry basis).

rate of fly ash because fly ash is highly amorphous and there is no way to determine how much unreacted fly ash is left in the slurry. To further complicate matters, the fly ash/lime reaction products are generally non-crystalline, so it impossible to study the rate of their formation using such methods as quantitative x-ray diffraction.

However, there are established methods to determine the amount of $Ca(OH)_2$ in a slurry or in a mixture of cement solids. One of these methods has been adapted to determine the disappearance rate of $Ca(OH)_2$ when it is reacted with fly ash. This method was applied to a number of solids to determine the fraction of $Ca(OH)_2$ which had reacted with the fly ash for various slurry times under various experimental conditions.

The method is called "sugar dissolution" because the $Ca(OH)_2$ present in the lime/fly ash solids is dissolved in a solution of sugar water. The actual mechanism behind this dissolution is complicated, but for our purposes it may be described as an acid-base reaction :

$$Ca(OH)_2\,(s) + 2\ \text{sucrose}^- H^+ \leftrightarrow Ca^{2+} + 2\ \text{sucrose}^- + 2\ H_2O \qquad (a)$$

After the dissolution is complete, the amount of $Ca(OH)_2$ in the solids is determined by titrating the dissolution solution with HCl to quantify the amount of sucrose anion formed from the dissolution of the calcium hydroxide solids :

$$Ca^{2+} + 2\ \text{sucrose}^- + 2\ H^+Cl^- \leftrightarrow 2\ \text{sucrose}^- H^+ + CaCl_2 \qquad (b)$$

The sugar dissolution experiments were performed by adding 100 ml of 15 $\%_{wt}$ sugar solution to a small amount of solids (weighed out on a four-place balance to contain about 250 mg of $Ca(OH)_2$). The mixture was placed in a 250 ml pyrex beaker, covered with parafilm, and stirred with a magnetic stirrer at room temperature for 10 to 15 minutes. The mixture was then vacuum filtered through Whatman #2 filter paper and the solids were washed with distilled water. Several drops of phenolpthalein indicator solution were added to the filtrate which was then

immediately titrated with 0.20 M HCl to the phenolpthalein endpoint (pH≈8.3). The amount of HCl added was recorded to ± 0.03 ml and used to calculate the amount of free $Ca(OH)_2$ present in the solids. The measured amount of free $Ca(OH)_2$ was compared with the total amount of $Ca(OH)_2$ which should be present in the solids (calculated from fly ash:$Ca(OH)_2$ ratio in the slurry) to give the fraction of $Ca(OH)_2$ which had reacted with the fly ash.

Several sugar dissolution experiments were performed with $Ca(OH)_2$ and with laboratory produced fly ash/lime materials to determine the dissolution time needed to completely dissolve the free $Ca(OH)_2$ present in the solids. The results of these experiments show that a dissolution time of 10 minutes is sufficient to dissolve all of the free $Ca(OH)_2$ solids contained in the fly ash/lime materials (Figure 5.5). The sugar dissolution method indicates that the reagent $Ca(OH)_2$ used in the control experiments contains only 98% $Ca(OH)_2$. This discrepancy probably arises because the $Ca(OH)_2$ contains a small amount of calcium carbonate formed by the reaction of $Ca(OH)_2$ with the CO_2 present in the atmosphere. The pH of the sugar solution is not low enough to cause the calcium carbonate to dissolve.

One potential source of error with the sugar dissolution experiments relates to the pH of the dissolution solution. The $Ca(OH)_2$ dissolves to a greater extent in sugar water than in pure water because the sugar keeps the pH relatively low so the $Ca(OH)_2$ can continue to dissolve (the measured pH after the dissolution was complete was 11.8). However, since the calcium silicate solids are also basic, they will dissolve if the pH is sufficiently low. If the calcium silicate solids dissolve in the sugar water solution, this technique is useless for determining the amount of $Ca(OH)_2$ which has been converted in the lime/fly ash solids.

To test whether the calcium silicate solids dissolve in the sugar water, the sugar dissolution technique was applied to solids which were produced by slurrying silica fume with $Ca(OH)_2$ at a 1:1 mole ratio for up to 7 hours at 90 °C. Since silica fume is a high surface area, highly reactive form of silica, it should

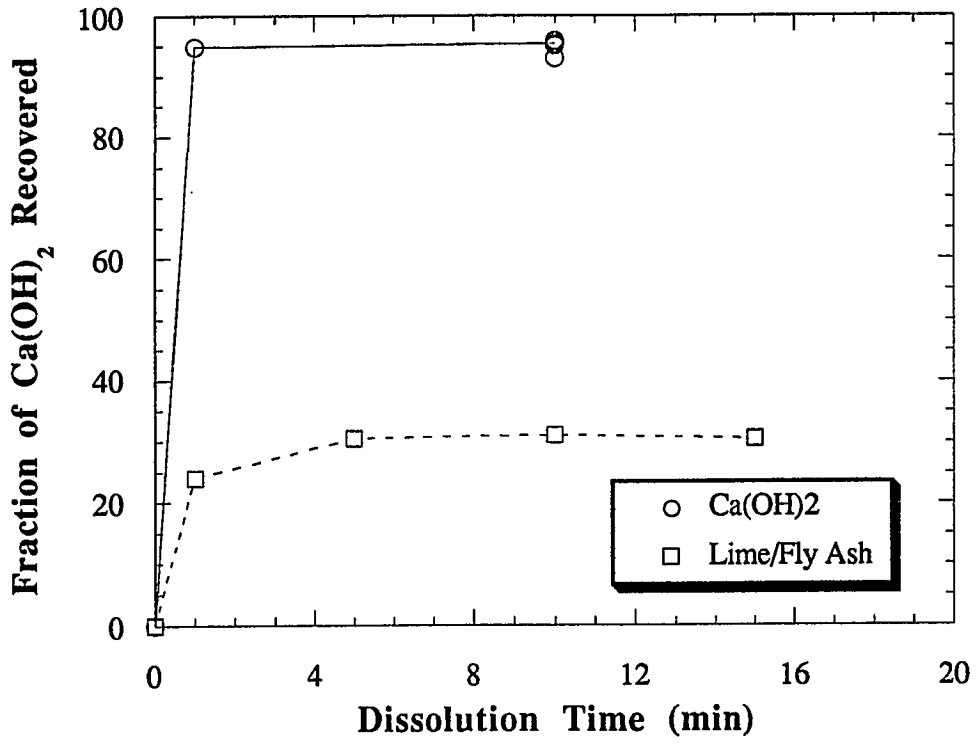

Figure 5.5 Determination of the time required for sugar dissolution tests.

react quickly and completely with the $Ca(OH)_2$, so the solids described above should be almost pure calcium silicate solids (i.e. they should contain only a small amount of free $Ca(OH)_2$). The data from these sugar dissolution tests are shown in Figure 5.6 and illustrate two important points: 1) calcium silicate solids do not dissolve appreciably in sugar water solutions; and 2) the sugar dissolution experiments confirm that the solids described above contain only a small amount of unreacted $Ca(OH)_2$ solids.

Since the calcium silicate solids do not dissolve in the sugar solution, but $Ca(OH)_2$ does dissolve, the sugar dissolution method supplies both quantitative and qualitative data for the study of the reaction of fly ash with $Ca(OH)_2$.

5.3.4 Selective Dissolution Experiments

Although there have been many studies investigating the production of lime/fly ash solids for FGD, little is known about the chemical composition of the product solids which form on the surface of the fly ash particles. These product solids give the lime/fly ash solids their high reactivity towards SO_2 and their unique ability to absorb water and remain free flowing. The present study sought to determine the chemical composition of the product solids by wet chemical techniques.

The chemical composition of the reactive, calcium-silicate-aluminate surface layer on the fly ash-$Ca(OH)_2$ reaction products was determined by selectively dissolving the surface layer while leaving the unreacted fly ash core intact. The data from these experiments were combined with those from the sugar dissolution experiments to estimate the chemical composition of the reactive surface layer.

The selective dissolution experiments were accomplished by adding 200 mg of the solids to 100 ml of 0.1 M HCl. The mixture was agitated with a magnetic stirrer for 5 minutes at room temperature. An aliquot of the mixture was taken and filtered with a 0.45 micron membrane type filter. The filtrate was analyzed for

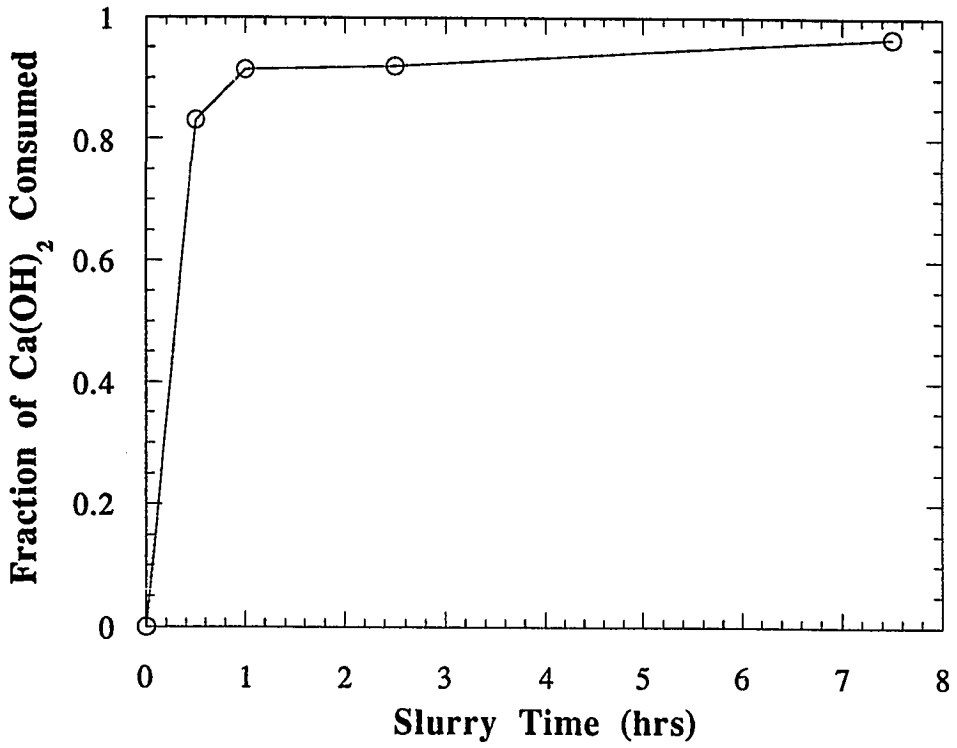

Figure 5.6 Results from sugar dissolution tests on calcium silicate solids. Slurry Composition : 33 g $Ca(OH)_2$ + 33 g Silica Fume + 400 ml H_2O; 90 °C; stir speed = 700 rpm.

aluminum, silicon, and calcium concentrations using atomic absorption spectrophotometry.

The composition of the reactive surface layer was approximated by the molar ratio of calcium to silicon and aluminum in the filtrate solution. The conversion of the metals in the fly ash was determined by dividing the measured concentration of the metals in filtrate solution by the calculated concentration for total dissolution of the fly ash (based on the chemical analyses presented in Table 5.1).

Chapter VI

Fly Ash Dissolution Experiments

As was discussed in Chapter II, the dissolution rate of fly ash is believed to control the rate of reaction of lime with fly ash, thereby indirectly controlling the reactivity of the lime/fly ash solids towards SO_2. For this reason, the dissolution of fly ash was studied extensively in the absence of any precipitation reactions which might inhibit the fly ash dissolution rate. These experiments investigated such parameters as : the fly ash type and source, the hydroxide concentration in the slurry, the slurry temperature, and the particle size of the fly ash. The results from these experiments are discussed in detail in the following sections.

6.1 Effect of fly ash type

Most of the previous investigations of the reaction of fly ash with $Ca(OH)_2$ to produce solids for use in FGD were performed using low-calcium fly ashes. A significant fraction of the fly ashes produced in the USA are high-calcium fly ashes, however, and these ashes seem to be more beneficial for use in FGD because some of the calcium present in the fly ash can be converted to materials which are reactive towards SO_2 (Petersen et al., 1988, Peterson and Rochelle, 1988A). These high-calcium fly ashes are usually derived from low-sulfur subbituminous coal which may be increasingly utilized if electric utilities switch coal sources to help meet lower SO_2 emission standards in the future. Therefore, the present investigation encompassed a variety of fly ashes.

Ten different fly ashes were used to determine the effect of fly ash type on the dissolution rate of the fly ash. These ashes included four low-calcium, three

medium-calcium, and three high-calcium fly ashes. The chemical compositions of these fly ashes are given in Table 5.1. The fly ashes were slurried for up to 6 hours at 90 °C in 0.1 M NaOH solution which contained Na_2EDTA to complex the calcium which dissolves from the fly ash in order to prevent the precipitation of calcium-based materials on the surface of the fly ash. The rates of fly ash dissolution were determined by analyzing the solution for dissolved calcium, aluminum and silicon. The results from these experiments are shown in Figures 6.1 and 6.2.

Figure 6.1 shows the effect of fly ash type on the dissolution rate of aluminum from the fly ash. The data show that the initial dissolution rate of the fly ash is a strong function of the fly ash type, but only a weak function of fly ash source. That is, all of the high-calcium fly ashes behaved similarly, but their behavior was different from the low- and medium-calcium fly ashes. The data show that greater than 50% of the aluminum present in the high-calcium fly ashes dissolves instantly, while the low- and medium-calcium fly ashes dissolve uniformly. However, after the initial period of rapid dissolution, the high-calcium fly ashes dissolved like the low- and medium-calcium fly ashes. Similar results were observed for the dissolution rate of silicon from the fly ash, but the fraction of silica which dissolved instantly from the high-calcium fly ashes was approximately 25 percent (Figure 6.2).

These data indicate that there is some very reactive material in the high-calcium fly ash which is not present in the low-calcium fly ash. This would suggest that the high-calcium fly ashes are more reactive towards $Ca(OH)_2$ and therefore would be more beneficial than low-calcium fly ashes for producing solids for flue gas desulfurization. Later results will show, however, that the preferred component of the fly ash is silicon, not aluminum, and that the presence of reactive forms of aluminum actually leads to the formation of solids which are unreactive towards SO_2. Therefore, the highly reactive nature of the high-calcium fly ashes can actually lead to the production of material which is unreactive towards SO_2.

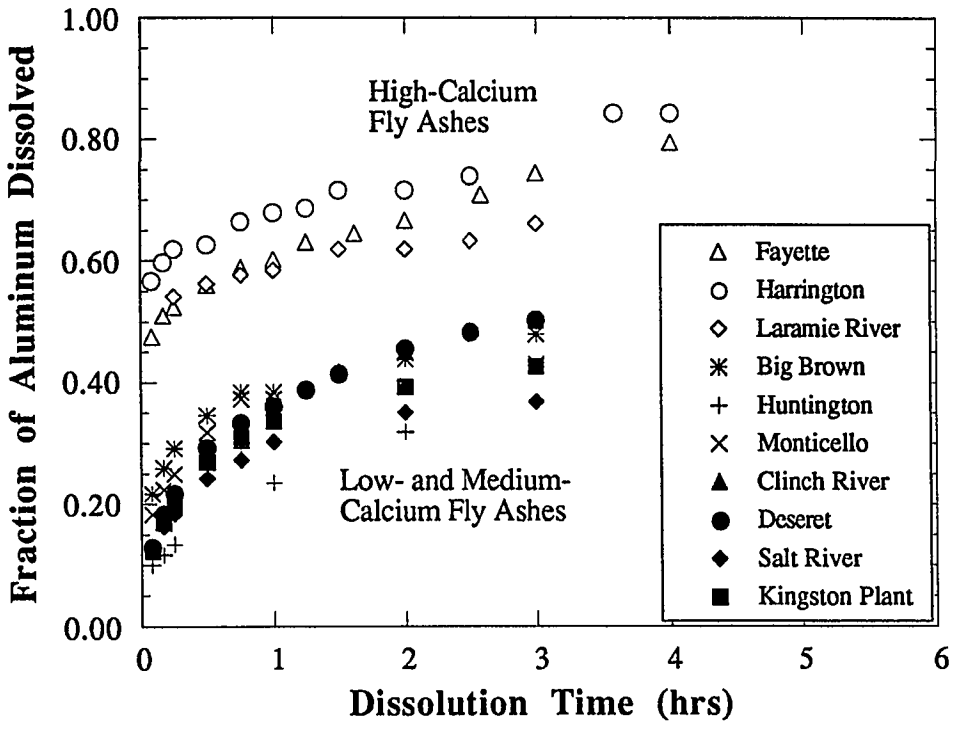

Figure 6.1 Effect of fly ash type on aluminum dissolution from the fly ash. 90 °C, 1.25 g fly ash/liter; 5 g Na_2EDTA/liter; 0.1 M NaOH, stir speed : 1000 rpm.

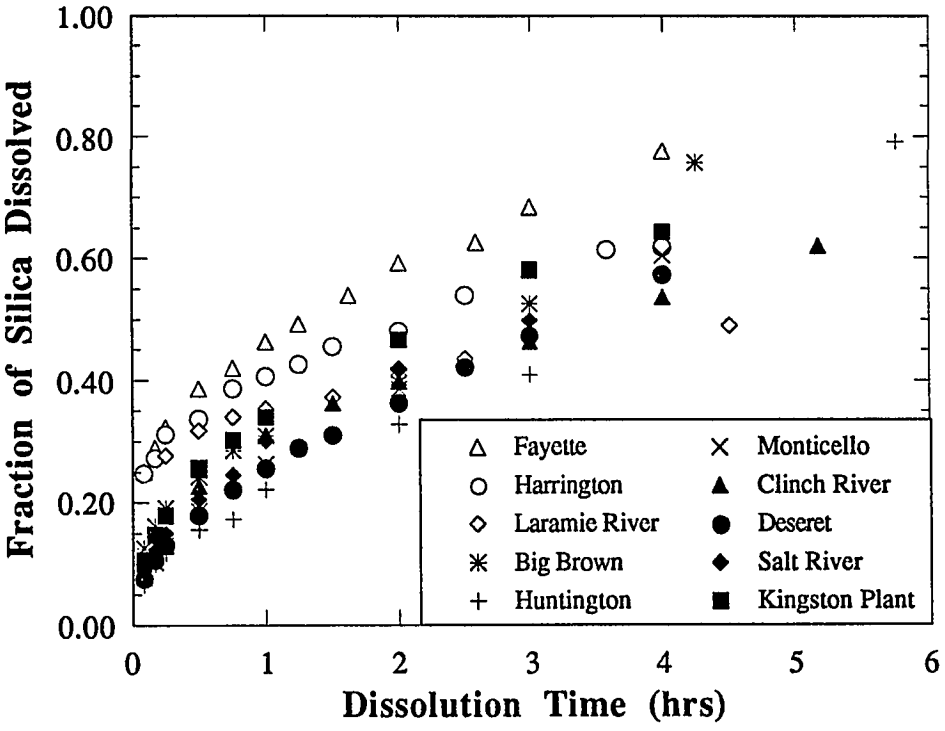

Figure 6.2 Effect of fly ash type on silica dissolution from the fly ash. 90 °C, 1.25 g fly ash/liter; 5 g Na_2EDTA/liter; 0.1 M NaOH, stir speed : 1000 rpm.

The highly reactive nature of the high-calcium fly ashes has been observed before in studies related to the use of fly ash in concrete (see Chapter III). Mehta (1989) indicates that the reason for the difference in the reactivity of the low and high-calcium fly ashes relates to the structure of the glass present in the fly ash. The author cited several studies to show that the low and high-calcium fly ashes contained roughly the same alumino-silicate glassy matrix, but the high-calcium fly ashes had higher contents of cation modifiers (i.e. Ca, Na, and K). These modifiers break the alumino-silicate chains present in the fly ash to produce shorter chains which are more reactive than the longer chains found in the low-calcium fly ashes.

Evidence of the effect of these modifiers was presented in Chapter III which showed that an indication of the chain length of the alumino-silicate matrix is found in the x-ray diffraction pattern of the fly ash. The position of the amorphous hump shifts to higher diffraction angles as the chains are shortened. Figure 6.3 shows the effect of the fly ash type on the position of the amorphous hump determined by x-ray diffraction for the fly ashes used in the dissolution experiments. This data agrees with that of McCarthy et al.,(1984) which showed that the position of the amorphous hump varied from 25 to 31 degrees two-theta as the calcium content in the fly ash varied from 1 to 31 %. These data show that the high-calcium fly ashes have shorter alumino-silicate chains which probably accounts for their high dissolution rates observed in the fly ash dissolution experiments.

The above data on fly ash dissolution leave a little to be desired because fly ash is not a homogeneous substance. The chemical composition and glass structure vary from ash to ash and from particle to particle within each ash. The above data show that the high-calcium fly ashes dissolve much faster than the low-calcium fly ashes in the initial stages of the experiment, but in the later stages of the experiment the dissolution rates are similar. The explanation for this behavior may lie in the inhomogeneity of the fly ash.

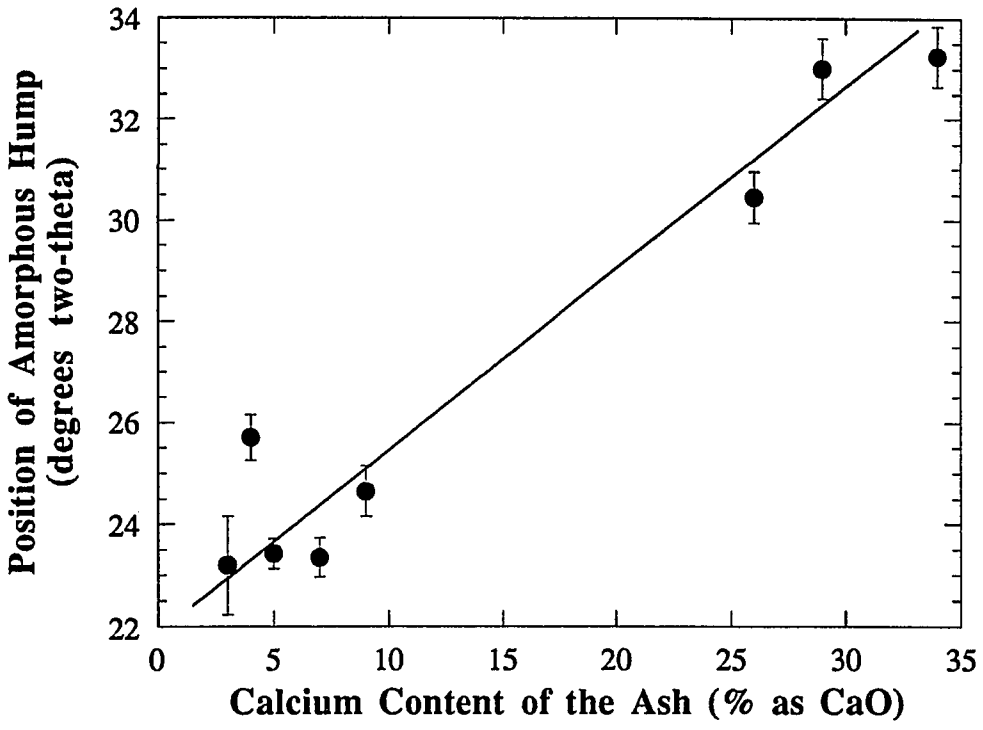

Figure 6.3 Effect of fly ash type on the position of the amorphous hump determined by x-ray diffraction.
Copper K^{α} radiation.

Hemmings and Berry (1986) have shown that the composition of the glass present in fly ash varies from particle to particle. They separated a medium-calcium fly ash by density to show that the heaviest fraction was made up of high-calcium particles while the lighter fractions consisted of low-calcium particles. They performed powder x-ray diffraction experiments on the various fractions and found that the position of the amorphous hump increased with the density (i.e. the calcium content) of the fraction.

It may therefore be possible to classify all fly ash particles into two broad groups : low- and medium-calcium fly ash particles which have long-chain alumino-silicate structures (slow dissolution); and high-calcium particles which have short-chain alumino-silicate structures (fast dissolution). Both types of these particles are probably present to some degree in all fly ashes regardless of the calcium content of the bulk fly ash.

6.2 Effect of NaOH concentration

It has been shown that the reactivity of the lime/fly ash solids towards SO_2 can be improved by the addition of NaOH to the lime/fly ash slurry (Chapter II). The NaOH is believed to increase the dissolution rate of the fly ash thereby increasing the reaction rate of the fly ash with the $Ca(OH)_2$ in solution. Fly ash dissolution experiments were performed to quantify the effect of the NaOH on the dissolution rate of the fly ash.

The effect of NaOH concentration on the dissolution rate of fly ash was investigated using low- and high-calcium fly ashes slurried at 90 °C. The NaOH concentration in the solution was varied from 0.0 to 0.5 M and the rate of fly ash dissolution was determined by monitoring the solution for dissolved silicon and aluminum metals. The results from these experiments are shown in Figures 6.4 to 6.10

Figure 6.4 shows the effect of NaOH concentration on the conversion rate of silicon from the low-calcium fly ash. The data show that the conversion

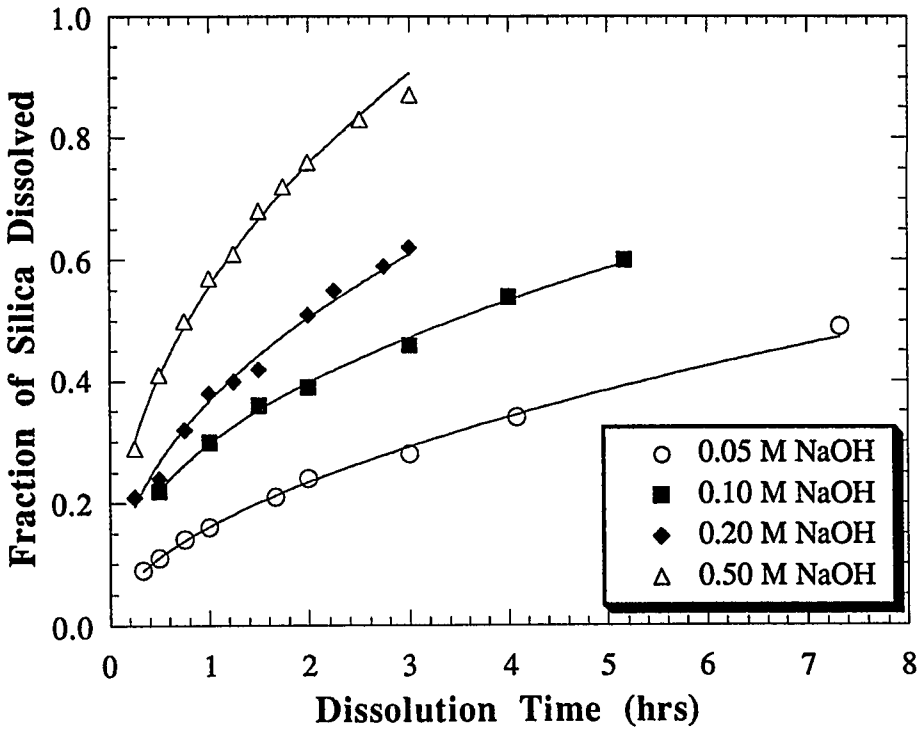

Figure 6.4 Effect of NaOH on the dissolution of silica from a low calcium fly ash.
90 °C, 1.25 g Clinch River fly ash/liter; 5 g Na_2EDTA/liter; 0.1 M NaOH, stir speed : 1000 rpm.

increases with slurry time and with NaOH concentration. Figure 6.5 shows the conversion of the silicon in this fly ash versus a reduced time. The reduced time is defined here as the time of dissolution divided by the time to a specified conversion (t_x) of the silicon in the fly ash. As Figure 6.5 shows, plotting the data this way collapses all of the data from the dissolution experiments onto the same curve. Since all of the data collapse, it is possible to determine the order of reaction with respect to the hydroxide concentration by plotting $1/t_x$ versus the concentration of NaOH in the slurry on a log-log graph (see Appendix C). Figure 6.6 shows that the dissolution of silica from the low-calcium fly ash is approximately first order with respect to the hydroxide concentration in the slurry. However, as illustrated in Figure 6.6, the calculated reaction order depends upon the specified conversion. For very low conversions (e.g. 15%) the uncertainty in the time required for the conversion is high and the data are not linear. As a result, the reaction orders calculated for the low conversion data are significantly higher than 1.0. For higher specified conversions, the errors associated with the determination of the time to the specified conversion are lower, the data are more linear, and the calculated reaction orders are very close to 1.0.

The dissolution rate of aluminum from the low-calcium fly ash was also found to increase with the NaOH concentration in the slurry. Figure 6.7 shows that for low silicon conversions (i.e. low NaOH concentrations), the conversion of the aluminum in the fly ash was higher than the conversion of silicon in the fly ash, but for high silicon conversions (high NaOH concentrations), the conversion of the aluminum was lower than the conversion of the silicon. This indicates that the dissolution of aluminum from the fly ash is not as dependent on the hydroxide concentration as is the dissolution of silicon from the fly ash. Through an analysis similar to that of the data for silicon conversion, the reaction order of aluminum dissolution with respect to hydroxide was found to be 0.86, slightly less than that for the dissolution of silica from the fly ash.

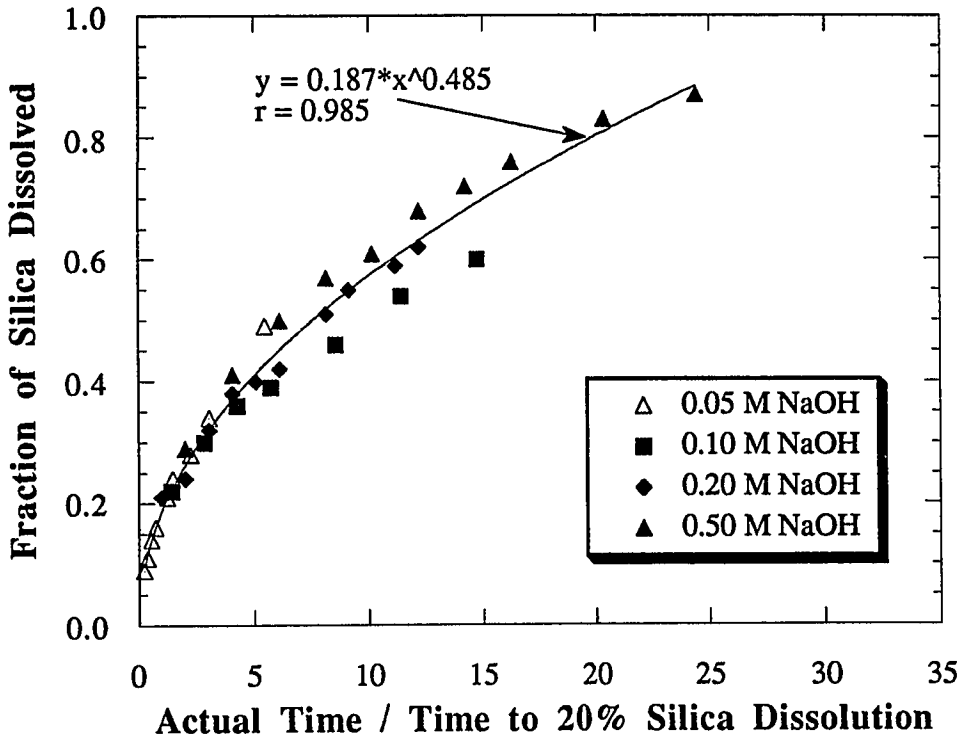

Figure 6.5 Collapsing the data for the effect of NaOH on the dissolution of silica from a low calcium fly ash.
90 °C, 1.25 g Clinch River fly ash/liter; 5 g Na_2EDTA/liter; 0.1 M NaOH, stir speed : 1000 rpm.

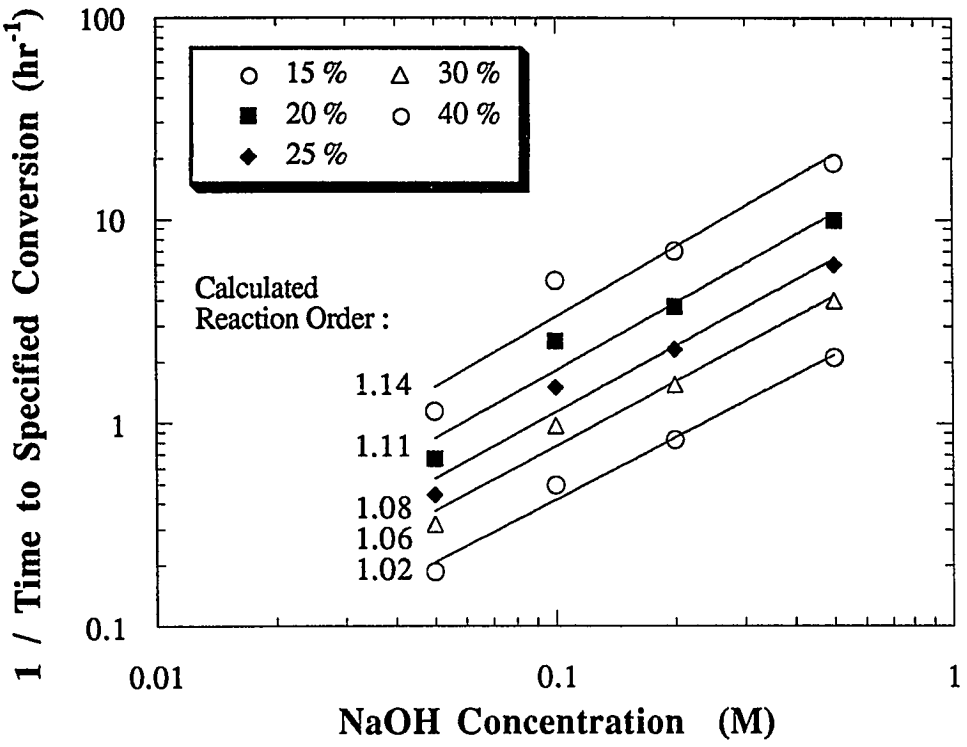

Figure 6.6 Determining the order of fly ash dissolution with respect to NaOH. 90 °C, 1.25 g Clinch River fly ash/liter; 5 g Na_2EDTA/liter; stir speed : 1000 rpm.

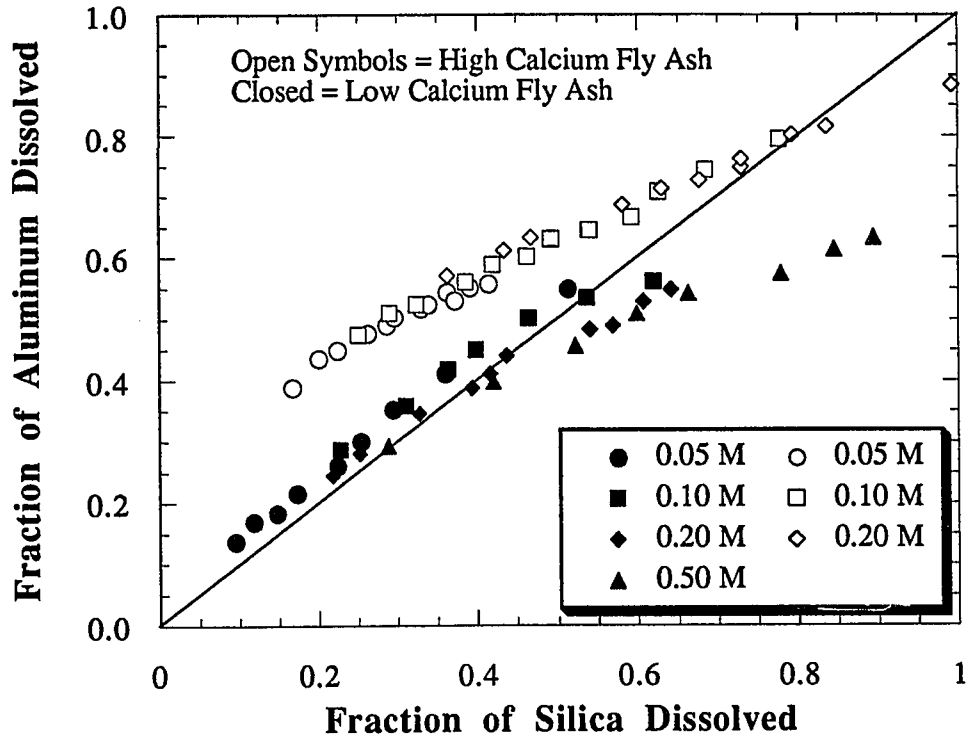

Figure 6.7 Comparing the rates of silicon and aluminum dissolution for low and high calcium fly ashes.
90 °C, 1.25 g Clinch River (low calcium) or Fayette (high calcium) fly ash/liter; 5 g Na_2EDTA/liter; stir speed : 1000 rpm.

Fly ash dissolution experiments studying the effect of the hydroxide concentration were also performed using a high-calcium fly ash. Figure 6.8 shows that the dissolution of silica from the high-calcium fly ash is a stronger function of the NaOH concentration than it was for the low-calcium fly ash. Figure 6.9 shows that the data for the high-calcium fly ash can be collapsed onto one curve as was done for the low-calcium fly ash, but Figure 6.10 shows that the calculated reaction order for the dissolution of silica from the high-calcium fly ash is approximately twice that for the low-calcium fly ash dissolution. The calculated reaction order was also much higher for the dissolution of aluminum from the fly ash ($\approx$ 2.5 vs 0.86 for the high- and low-calcium fly ashes, respectively).

The dissolution rate of silica from the fly ash increases with NaOH concentration because silica is more soluble at high pH and because the reaction for silica dissolution can be written as (Iler, 1979) :

$$(SiO_2)_x + 2\ H_2O \Leftrightarrow Si(OH)_4 + (SiO_2)_{x-1}$$

$$Si(OH)_4 + OH^- \Rightarrow Si(OH)_5^- \ (\text{or } HSiO_3^-) \qquad (1)$$

Iler indicates that the dissolution of silica in water is, in effect, a catalytic depolymerization through hydrolysis. The "catalyst" is a material which can be chemisorbed and increases the coordination number of a silicon atom on the surface to more than four, thus weakening the oxygen bonds to the underlying silica atoms. In alkaline solutions, the hydroxyl ion is the unique catalyst. Iler's proposed mechanism for the dissolution of silica is shown in Figure 6.11.

The dissolution of fly ash probably proceeds by a mechanism very similar to that proposed by Iler. The chief difference is that the glassy component of the fly ash consists of a silica glass that is highly substituted with aluminum and other metals. This high degree of substitution, along with the effects of cation modifiers, make the dissolution of fly ash more difficult to analyze than the dissolution of pure silica.

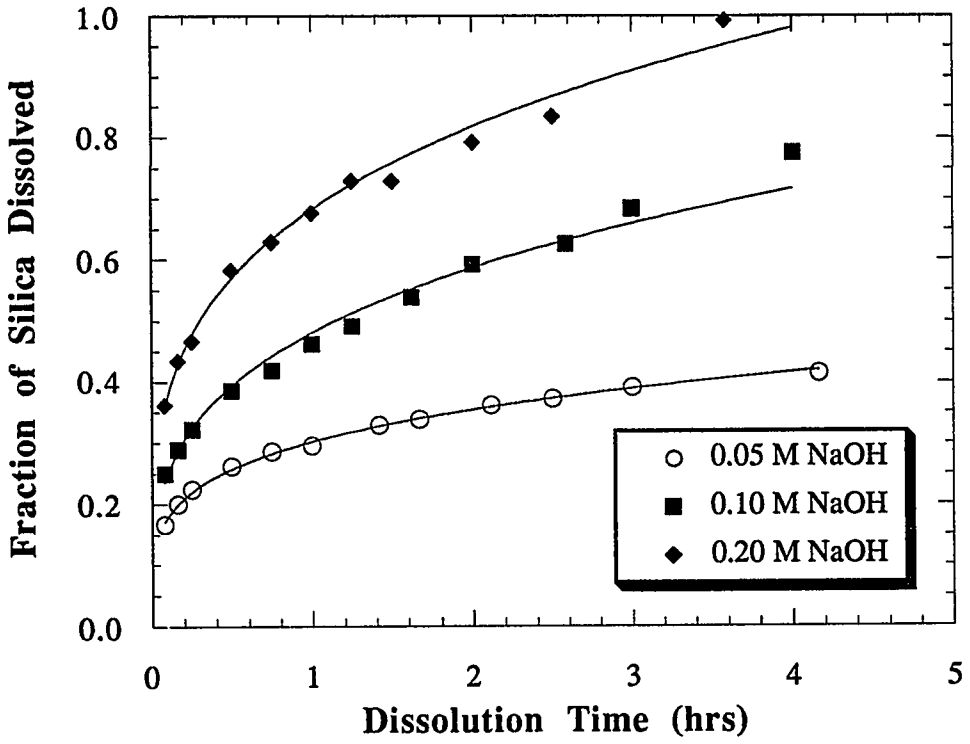

Figure 6.8 Effect of NaOH concentration on high calcium fly ash dissolution. 90 °C, 1.25 g Fayette fly ash/liter; 5 g Na_2EDTA/liter; stir speed : 1000 rpm.

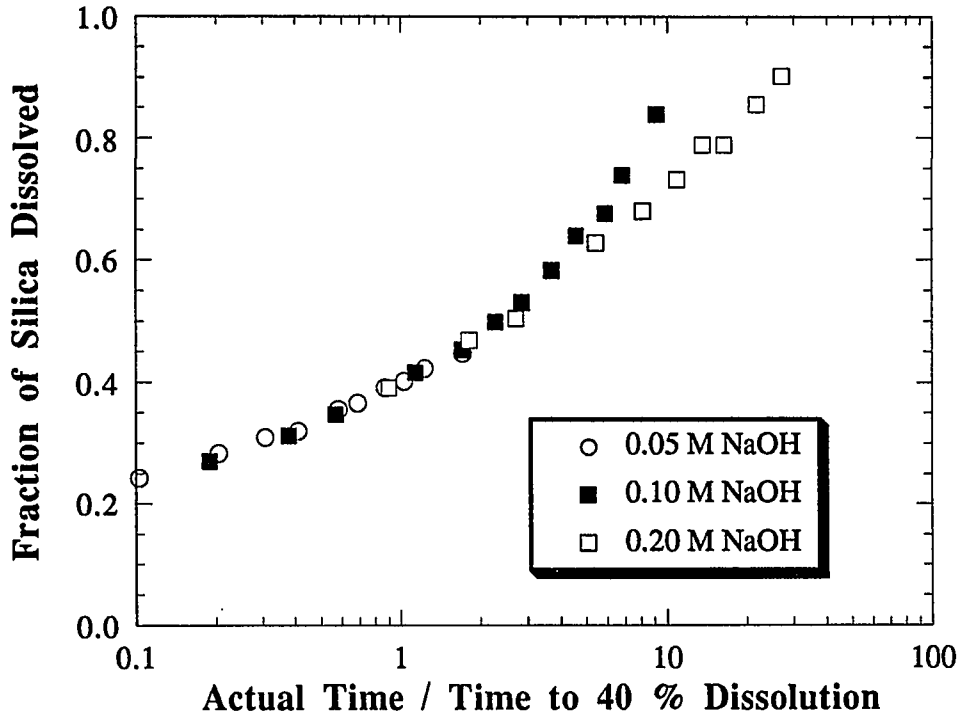

Figure 6.9 Collapsing the data for the effect of NaOH on the dissolution of silica from a high calcium fly ash.
90 °C, 1.25 g Fayette fly ash/liter; 5 g Na_2EDTA/liter;
stir speed : 1000 rpm.

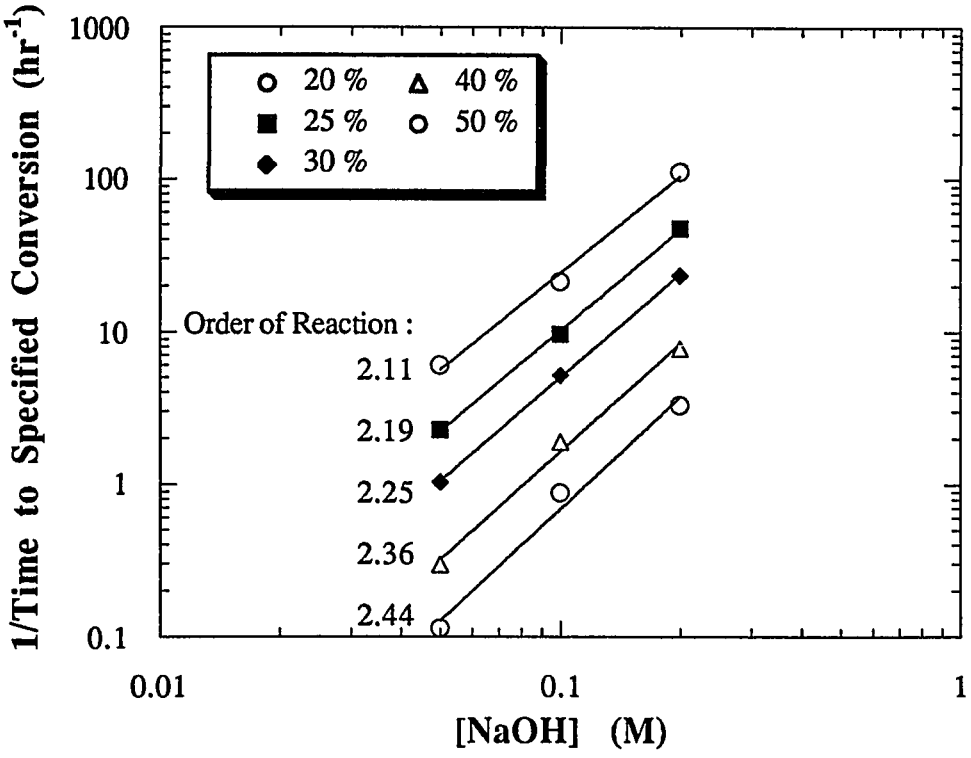

Figure 6.10 Determining the order of fly ash dissolution with respect to NaOH. 90 °C, 1.25 g Fayette fly ash/liter; 5 g Na_2EDTA/liter; stir speed : 1000 rpm.

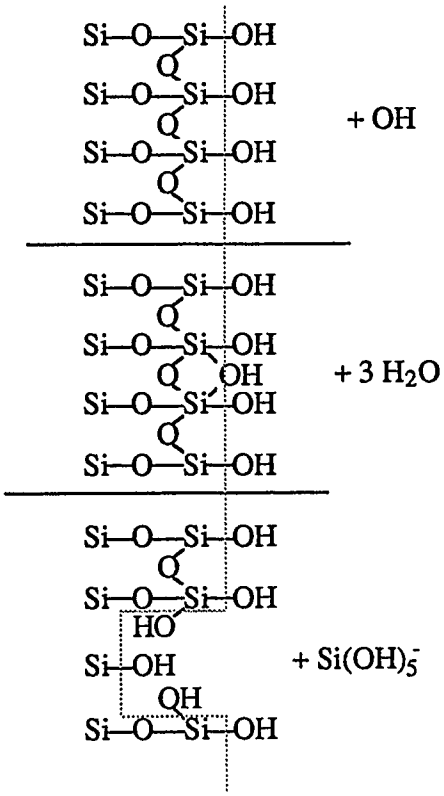

Figure 6.11 Proposed mechanism for the dissolution of amorphous silica under alkaline conditions. From Iler (1979).

The observation that the dissolution rate of silica from the low calcium fly ash is approximately first order in the hydroxide concentration agrees with the mechanism proposed by Iler and with some of the experimental data by Bauman (Taylor, 1979) who studied the dissolution of amorphous silica in the pH range of 2 to 9. Bauman found the dissolution rate to be proportional to the OH^- concentration for the pH range of 3 to 6. Above pH 6 the dissolution rate was not as strong a function of the hydroxide concentration, but Iler (1979) indicates that above this pH, the dissolution rate of amorphous silica is so great that the diffusion rate of silicic acid from the surface of the silica may limit the overall rate of dissolution. Since fly ash has a much lower surface area and reactivity than amorphous silica, it is logical that the dissolution rate would be proportional to the hydroxide concentration even at high pH.

The very strong effect of the hydroxide concentration on the silica and aluminum dissolution rates from the high-calcium fly ash probably relates to the structure of the glassy matrix of the fly ash. The highly reactive material present in the high-calcium fly ash dissolves almost instantaneously while the balance of the material dissolves more congruently (Figure 6.7). This makes an interpretation of the overall dissolution rate a difficult task.

6.3 Effect of slurry temperature

As was described in Chapter II, the reactivity of the lime/fly ash solids towards SO_2 generally improves as the slurry temperature increases. The reason for this increase relates to the dissolution rate of the fly ash. Higher slurry temperatures are believed to yield higher fly ash dissolution rates and therefore more reactive lime/fly ash solids. Fly ash dissolution experiments were performed to quantify the effect of temperature on the dissolution rate of the fly ash.

Clinch River fly ash was selected to determine the effect of temperature on the dissolution rate of the fly ash. The ash was slurried in 0.10 M NaOH at slurry temperatures from 25 to 90 °C for up to 6 hours. The fly ash dissolution rate was

determined by monitoring the solution for dissolved calcium, aluminum, and silicon concentrations. The results from these experiments are shown in Figures 6.12 and 6.13.

Figure 6.12 shows that the dissolution rate of silica from the fly ash increases with the slurry temperature. Similar results were found for the dissolution of aluminum from the fly ash. By treating the data in a manner similar to that of the previous section, one can determine the activation energy associated with the dissolution of the fly ash. Figure 6.13 shows the results of this data reduction. The plot is an Arrhenius plot in which the rate constant is defined as the time to a specified conversion of the product. The data show that the activation energy for the dissolution of silica from the fly ash is 20.8 kcal/mole and that for the dissolution of aluminum is 21.4 kcal/mole.

The activation energy for the dissolution of silica from the fly ash agrees very well with the data of previous researchers who studied the dissolution of various forms of silica in water and in alkaline solutions. Greenberg (1957) measured the dissolution rates of both quartz and amorphous silica powders in alkali and concluded that the energy of activation was 26.2 and 21.5 kcal/mole for quartz and amorphous silica, respectively. In a later study using only amorphous silica, O'Connor and Greenberg (1958) showed that the activation energy was 17.8 kcal/mole in water and 18 kcal/mole in alkali.

6.4 Effect of fly ash grinding

Petersen et al., (1988) showed that the reactivity of the lime/fly ash solids was greatly enhanced if the fly ash was ground before it was reacted with $Ca(OH)_2$. The grinding of the fly ash increased the surface area of the fly ash, which presumably increased the fly ash dissolution rate and the reactivity of the lime/fly ash solids. Fly ash dissolution experiments were conducted to quantify the effect of fly ash particle size on the dissolution rate of silica and aluminum from the fly ash.

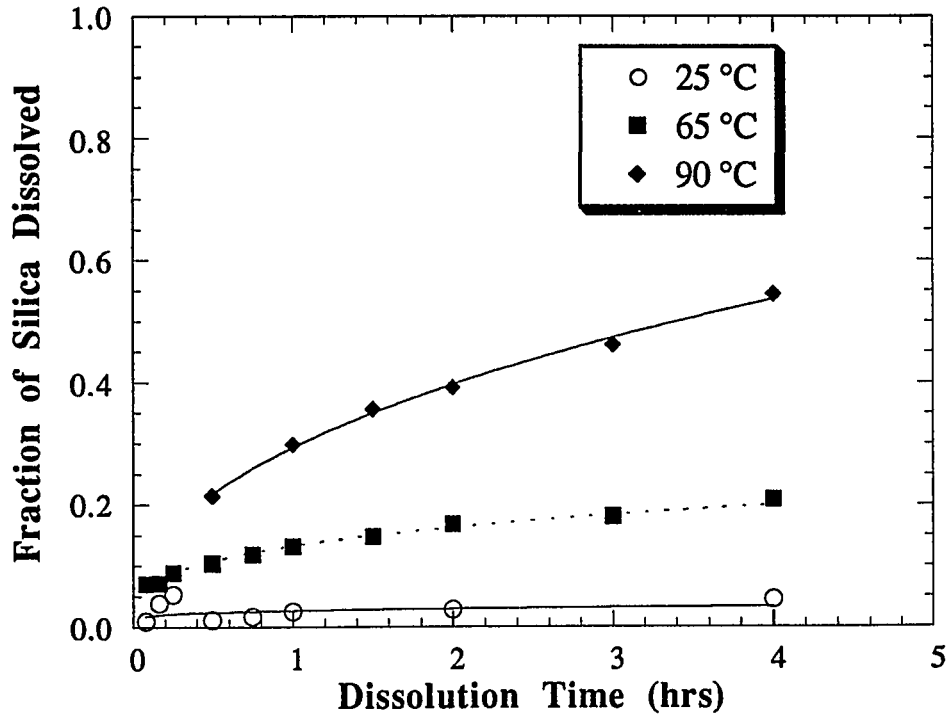

Figure 6.12 Effect of temperature on the dissolution of silica from a low calcium fly ash.
1.25 g Clinch River fly ash/liter; 5 g Na_2EDTA/liter;
stir speed : 1000 rpm.

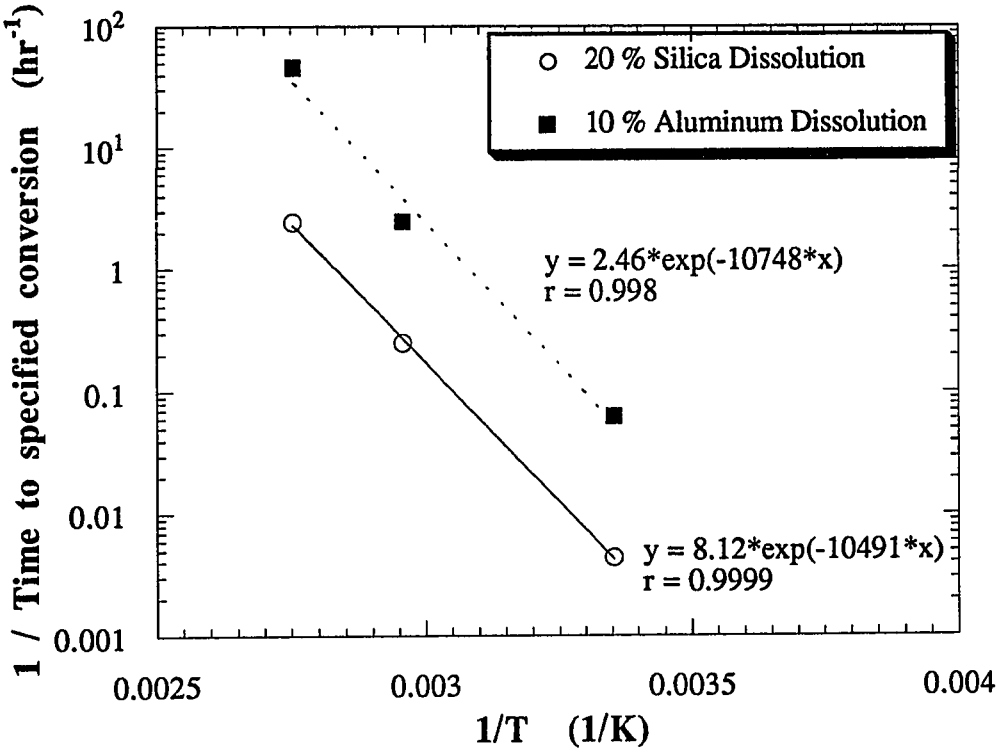

Figure 6.13 Arrhenius plots for the dissolution of low calcium fly ash. 1.25 g Clinch River fly ash/liter; 5 g Na_2EDTA/liter; stir speed : 1000 rpm.

Five samples of Clinch River fly ash were used to determine the effect of particle size on the dissolution rate of the fly ash. Three of the samples had been wet-ground in a pebble-mill grinder courtesy of Hans Karlsson and Tom Petersen of the University of Lund, Sweden. Another sample of the ash was dry ground in a disk-mill courtesy of the Texas State Highway department in Austin, Texas. The final sample of the ash was the unground fly ash, as received from the power plant.

The ashes were slurried in 0.10 M NaOH at slurry temperature of 90 °C for up to 6 hours. The fly ash dissolution rate was determined by monitoring the solution for dissolved calcium, aluminum, and silicon concentrations. The results from these experiments are shown in Figures 6.14 and 6.15.

Figure 6.14 shows the effect of fly ash grinding on the dissolution rate of silica from the low-calcium fly ash. As expected, the silica dissolution rate generally increased as the surface area of the fly ash increased. An analysis of the data showed that the initial dissolution rate of the fly ash was a linear function of the initial surface area of the fly ash (Appendix C).

The dissolution rate of aluminum from the fly ash was not a function of the initial surface area of the fly ash (Figure 6.15). This is a rather strange result, since it is assumed that the glassy phase of the fly ash consists of an alumino-silicate matrix. For this matrix, the dissolution rate of aluminum should increase if the dissolution rate of silica increases.

However, according to the model put forth by Hemmings and Berry (1989), when aluminum is substituted into the polymeric silica network, the network is broken and aluminum occupies the end of the polymeric silica chain. In that case, the aluminum atoms are already quite exposed to hydroxide attack, even in unground fly ash, while most of the silica is contained in the polymeric network. The grinding process exposes proportionately more "fresh" silica than aluminum, and the silica dissolution rate increases dramatically, while the aluminum dissolution rate is nearly unchanged.

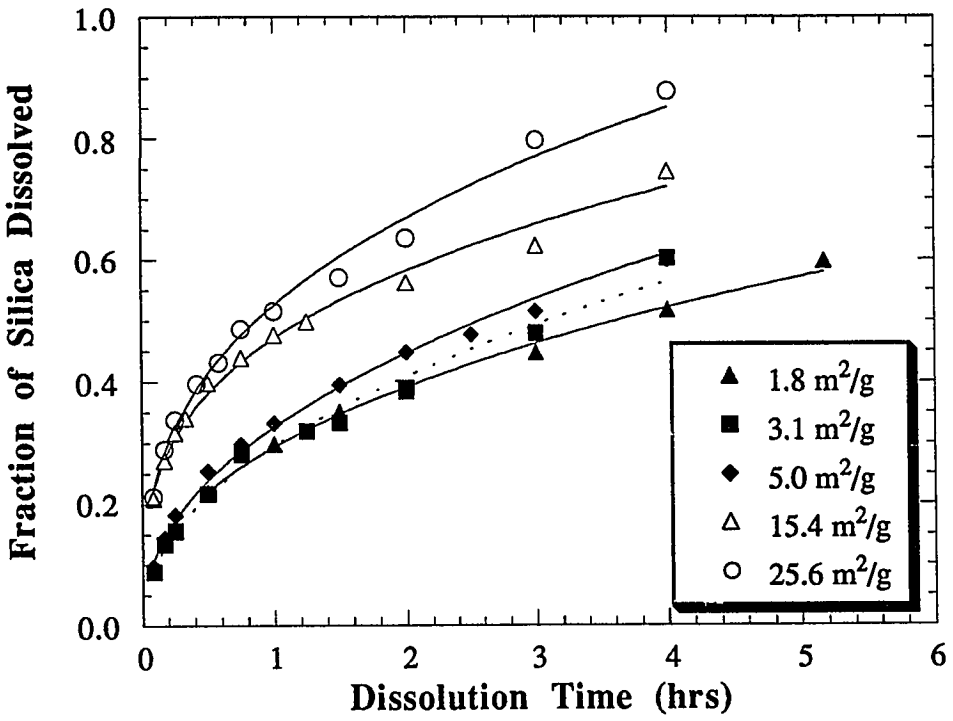

Figure 6.14 Effect of grinding on the dissolution rate of silica from a low calcium fly ash.
90 °C; 1.25 g Clinch River fly ash/liter; 5 g Na_2EDTA/liter; stir speed : 1000 rpm.

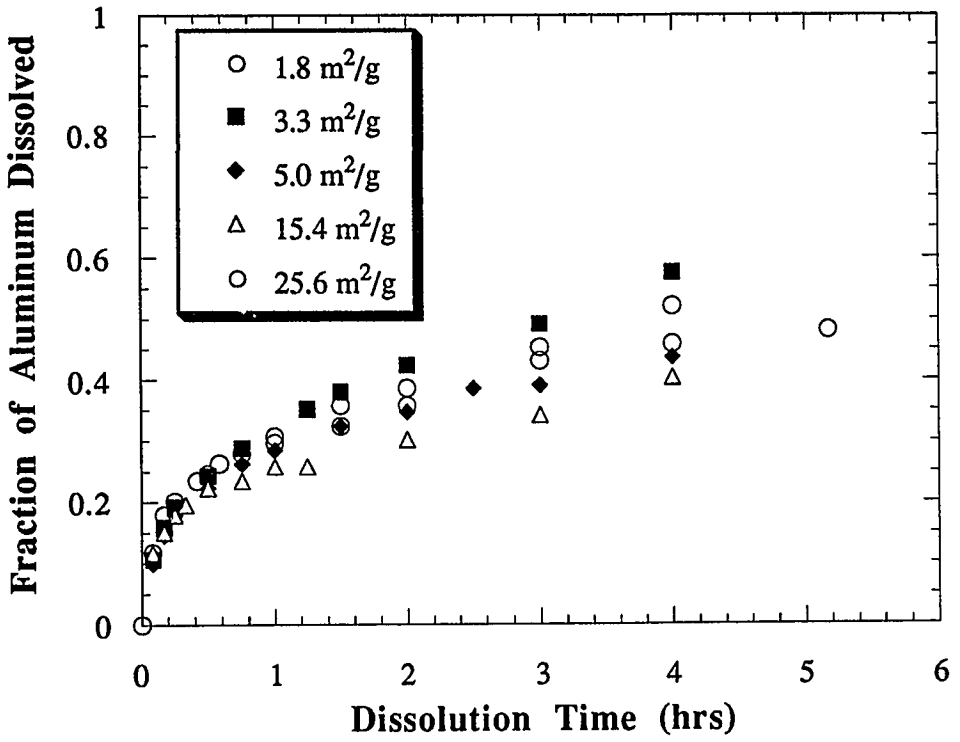

Figure 6.15 Effect of grinding on the dissolution rate of aluminum from a low calcium fly ash.
90 °C; 1.25 g Clinch River fly ash/liter; 5 g Na_2EDTA/liter;
stir speed : 1000 rpm.

Chapter VII

Experiments Using Reagent Chemicals

Because fly ash is a waste product, its chemical and mineralogical composition can vary greatly depending on the coal source and, to a lesser extent, on the boiler design and operation. This makes a detailed study of the chemistry of the lime/fly ash reaction a very complicated task. An attempt was made to reduce this complexity by performing experiments using reagent materials to simulate the major components of the fly ash.

The results that are discussed in this chapter are for 'normal' lime/fly ash experiments in which either silica fume or aluminum hydroxide was substituted for the fly ash. Silica fume was chosen over reagent chemicals such as precipitated SiO_2 and silicic acid because the surface area of these latter materials is usually very high (above 100 m^2/g), so these materials are less suitable to simulate the silica present in the low surface area fly ash (less than 1 m^2/g). Silica fume, a by-product from the manufacture of silicon metal, is formed under conditions similar to that of fly ash (i.e. high temperature fusion followed by rapid cooling) and has a surface area of approximately 20 m^2/g. The silica fume used in the following experiments consisted of approximately 92% amorphous SiO_2 (Table 7.1). The sample was obtained from Dr. Ramon Carrasquillo of the Department of Civil Engineering at The University of Texas at Austin.

Aluminum hydroxide ($Al(OH)_3$, certified grade from Fisher Scientific) was chosen over activated alumina (Al_2O_3, chromatographic grade, 80-200 mesh), which was used by Jozewicz and Rochelle (1986A, 1986B), because it was found

TABLE 7.1 CHARACTERIZATION OF REAGENT CHEMICALS.

Composition ($\%_{wt}$ as)	Silica Fume	$Al(OH)_3$
SiO_2	92	0
Al_2O_3	3	100
Fe_2O_3	2	0.1
CaO	0.1	Trace
Surface Area (m^2/g)	20	1.1
Source :	Univ. of Tx	Fischer Scientific

to be more reactive when tested under the "fly ash dissolution" experimental conditions which were described in Chapter V (Figure 7.1).

The methodology followed for the experimental program was to react $Ca(OH)_2$ with either silica fume or $Al(OH)_3$ to determine if these compounds react with $Ca(OH)_2$, and, if so, to determine what happens in the slurry while the materials are reacting. The solids produced in these slurries were characterized by the methods described in Chapter V and in Appendix A. After these initial studies were completed, several experiments were conducted in which $Ca(OH)_2$ was reacted with mixtures of silica fume and $Al(OH)_3$. These experiments were followed by an investigation of the effects of recycle materials (i.e. $CaSO_3$ and $CaSO_4$) on the above reactions.

7.1 Reaction of $Ca(OH)_2$ with silica

To determine the chemistry of the reaction of lime with fly ash to produce calcium silicate solids, reagent $Ca(OH)_2$ was slurried with silica fume in water at 90 °C and a 1:1 weight ratio. The total solids loading was 165 g/liter and the stirring speed was 700 rpm. Slurry samples were taken with time, vacuum

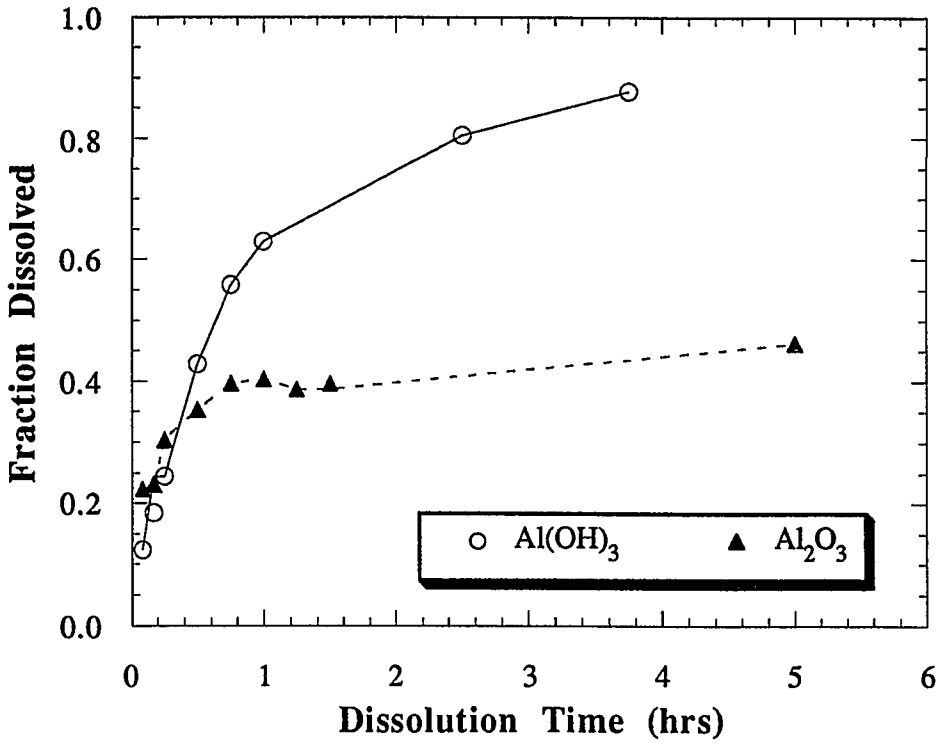

Figure 7.1 Comparing the dissolution rates of reagent aluminum sources.

90 °C, 0.1 M NaOH; 5 g Na_2EDTA/liter; stir speed : 1000 rpm.

filtered, and oven dried. The filtrates and the solids were stored for later analyses. The results from these experiments are shown in Figures 7.2 through 7.7.

Figure 7.2 compares the results from the filtrate analyses for the above slurry with those of Greenberg et al. (1960). The data show that both the pH of the solution (as measured at room temperature) and the dissolved calcium concentration decreased with slurry time and were below the level for a saturated solution of $Ca(OH)_2$ in water, even for short slurry times. The silicon concentration was less than 10 ppm for all slurry times, so it was immeasurable with atomic absorption. Greenberg et al. used a different method to analyze for silica, however, and were able to show that the solution behavior was totally determined by the solubility of CaH_2SiO_4. They determined that the solubility product for this species was $10^{-7.0}$ at 25 °C and somewhat less than that at 50 °C.

The data from the sugar dissolution analyses (Figure 7.3) show that the amount of unreacted $Ca(OH)_2$ in the product solids is very low for slurry times greater than three hours. The absence of $Ca(OH)_2$ at long slurry times was also confirmed by analyzing the above solids with powder x-ray diffraction - the diffraction lines attributed to $Ca(OH)_2$ were not present in the solids which were slurried for more than three hours (Figures 7.4 and 7.5). The x-ray diffraction data also indicate that the product solids are very amorphous, that is, they possess very little crystallinity. The only diffraction lines present for the solids which were slurried for long times were those for calcite ($CaCO_3$), which was probably formed by the reaction of atmospheric CO_2 with the $Ca(OH)_2$ during the sample preparation. The amorphous structure of the product solids makes it impossible to identify these solids using powder x-ray diffraction techniques.

All of the above data show that $Ca(OH)_2$ reacts rapidly with silica fume. The product solids were also tested for BET surface area and for reactivity towards SO_2. Figure 7.6 shows that these solids have a high surface area and are very reactive towards SO_2.

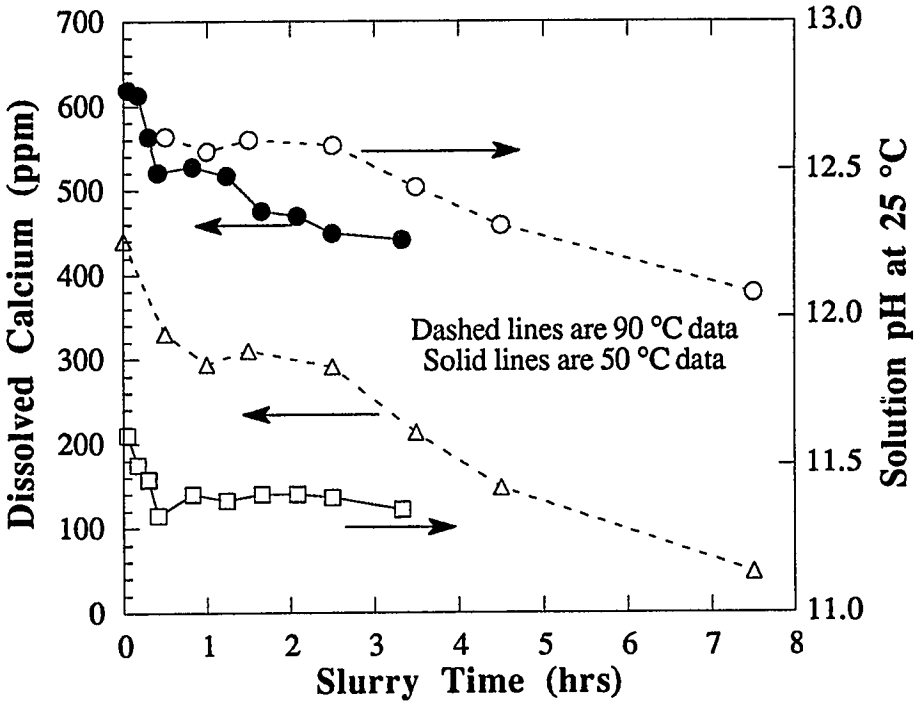

Figure 7.2 Filtrate analyses for silica fume reacting with $Ca(OH)_2$

33 g $Ca(OH)_2$ + 33 g Silica Fume + 400 ml H_2O;
90 °C ; Stir Speed = 700 rpm.

50 °C data are from Greenberg et al. (1960).

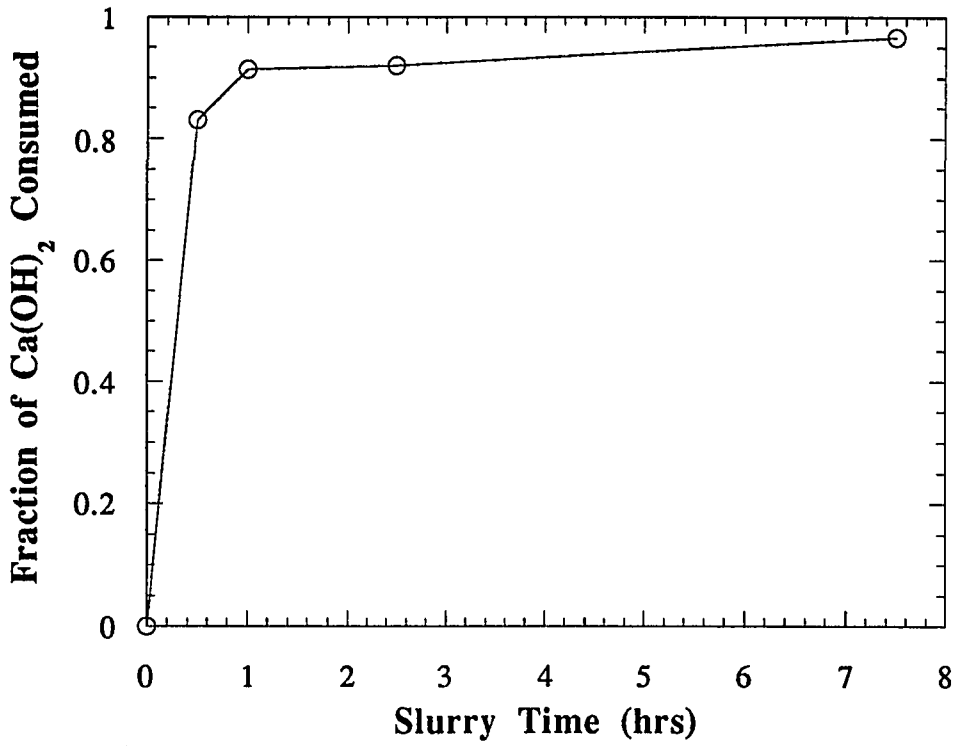

Figure 7.3 Silica fume reacting with $Ca(OH)_2$, sugar titration for residual $Ca(OH)_2$.

33.0 g silica fume + 33.0 g $Ca(OH)_2$ + 400 ml H_2O, 90 °C
stir speed : 700 rpm.

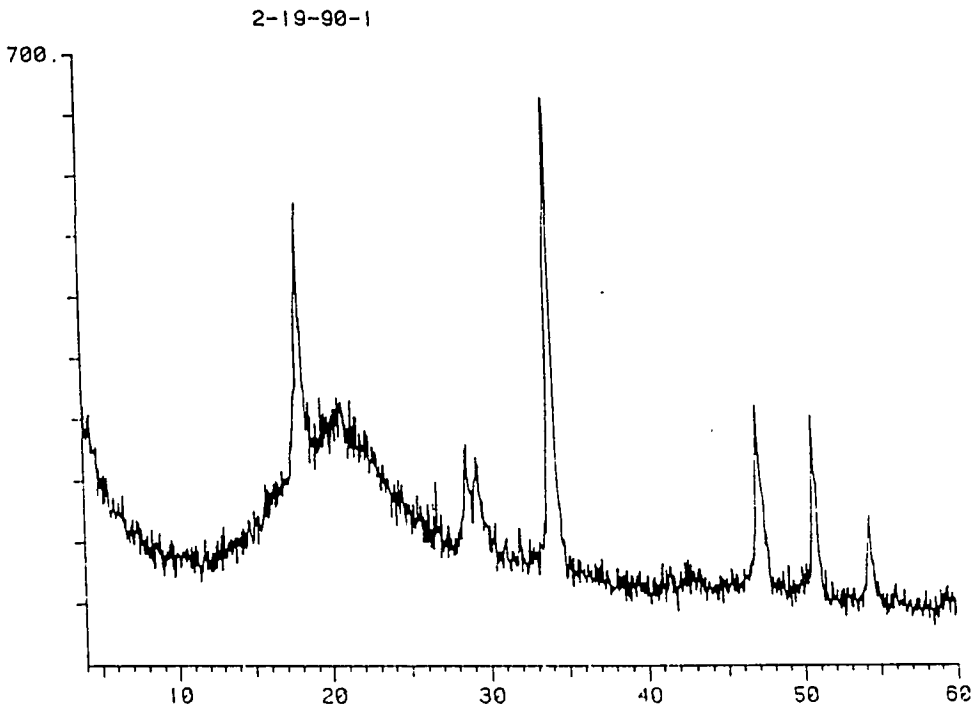

Figure 7.4 Powder x-ray diffraction pattern for solids produced by slurrying silica fume with $Ca(OH)_2$ for 0.5 hours.

33.0 g silica fume + 33.0 g $Ca(OH)_2$ + 400 ml H_2O, 90 °C
stir speed : 700 rpm.

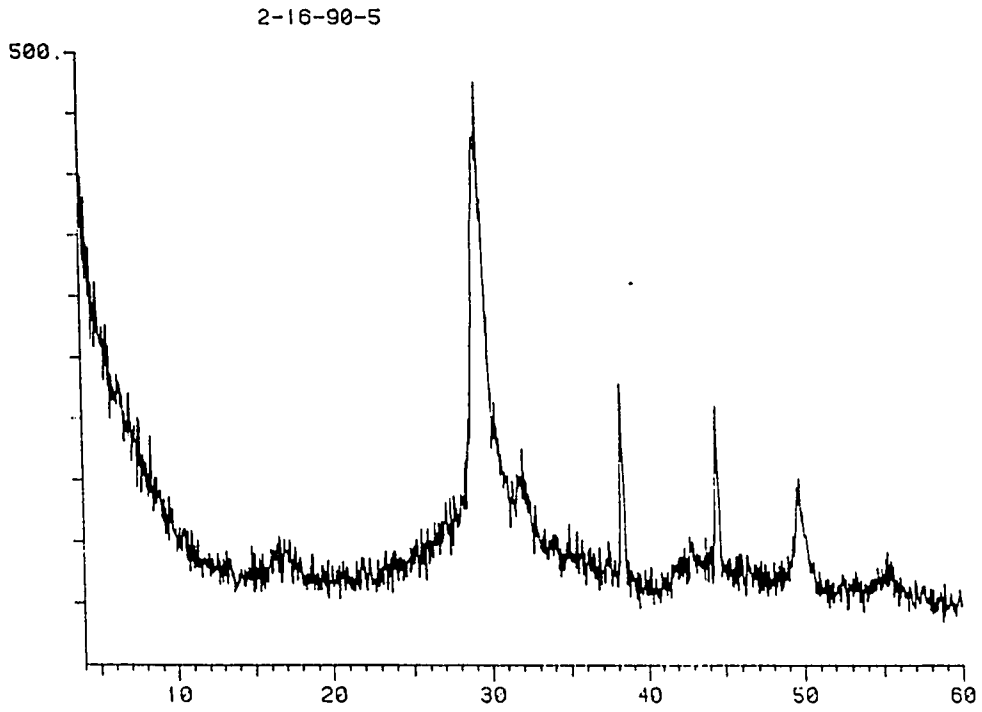

Figure 7.5 Powder x-ray diffraction pattern for solids produced by slurrying silica fume with $Ca(OH)_2$ for 7.5 hours.

33.0 g silica fume + 33.0 g $Ca(OH)_2$ + 400 ml H_2O, 90 °C
stir speed : 700 rpm.

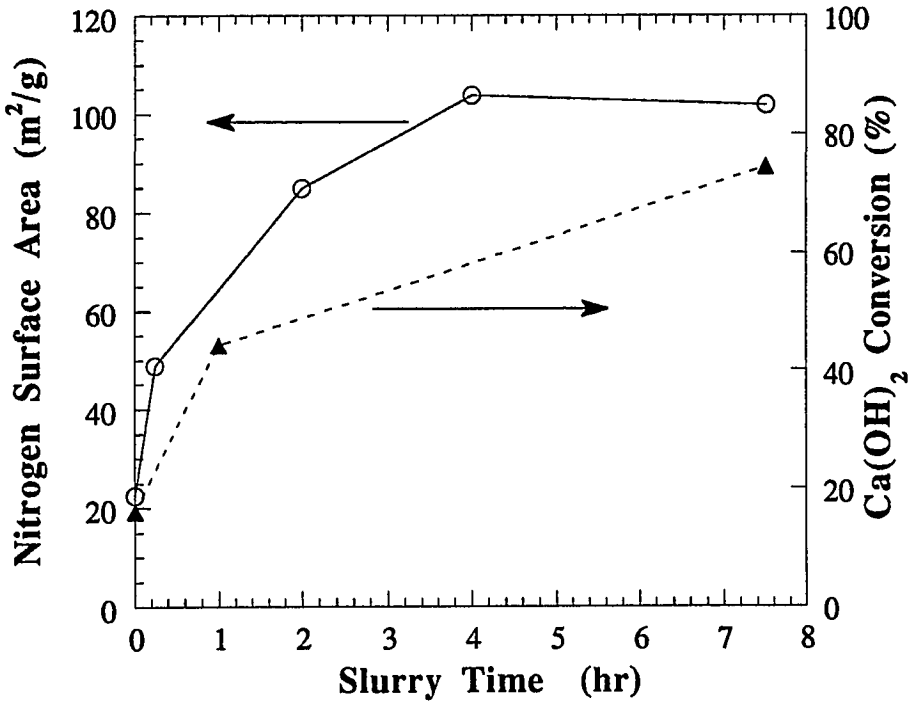

Figure 7.6 Reactivity and surface area of solids produced by reacting silica fume with $Ca(OH)_2$.

Slurry conditions :33.0 g silica fume + 33.0 g $Ca(OH)_2$ + 400 ml H_2O, 90 °C, stir speed : 700 rpm.
Reaction Conditions : 70 °C, 64% Relative Humidity, 5.0 slpm, 1000 ppm SO_2, 12 % O_2, 10% CO_2, 78% N_2 (dry basis).

These results indicate that the presence of silica in the fly ash is desirable since it reacts with $Ca(OH)_2$ to produce high surface area solids which are very reactive towards SO_2. The results also suggest that the reactive solids formed in the lime/fly ash reaction are amorphous, calcium silicate solids.

The above experimental results agree with the results of Jozewicz and Rochelle (1986A, 1986B) which showed that the reaction of $Ca(OH)_2$ with silicic acid or precipitated silica produced compounds which were very reactive towards SO_2. In another study using diatomaceous earth as a source of silica, Jozewicz et al. (1986A) also showed that there was an optimum $Ca(OH)_2$: SiO_2 ratio of 1:1 (mol/mol). In the current experiments, the ratio of $Ca(OH)_2$: SiO_2 was 0.88:1 (slightly less than the optimum value).

Although the current results agree with previous results, a positive identification of the calcium silicates formed in the slurry using x-ray diffraction was impossible because the solids were almost completely amorphous. Characterization of the solids was attempted by combining the data from the selective dissolution experiments with those of the sugar dissolution experiments as was described in Chapter V. The results from this procedure indicate that the calcium silicate solids have a $CaO:SiO_2$ ratio of approximately 1.3:1 (mol/mol).

The above analyses agree with previous data summarized by Taylor (1964) who stated that the calcium-silicate-hydrates include both well defined crystalline materials and ill-crystallized materials, which are often of somewhat indefinite composition. He states that reactions yielding calcium-silicate-hydrates below 100 °C normally give ill-crystallized materials. These materials are the main products formed by the hydration of Portland cement at room temperature.

According to Taylor, the ill-crystallized materials are subdivided into C-S-H(I) and C-S-H(II), where the initials C-S-H stand for "calcium-silicate-hydrates". C-S-H(I) denotes material having a Ca/Si molar ratio below 1.5, while C-S-H(II) denotes material with a ratio above 1.5. Within both categories considerable

variations are possible in the Ca/Si ratio, water content, degree of crystallinity, and other properties.

From the past and current results and the cement literature, one can conclude that the reactive products formed in the $Ca(OH)_2$ / silica fume system are type (I) calcium-silicate-hydrates. It is suspected that these calcium-silicate-hydrates also form when lime is reacted with fly ash.

7.2 Reaction of $Ca(OH)_2$ with aluminum

To determine if aluminum also reacts with $Ca(OH)_2$ to produce reactive solids, $Ca(OH)_2$ was slurried with $Al(OH)_3$ in water at a 1:1 or a 1:2 mole ratio. The total solids loading in the slurry varied from 185 to 288 g/liter and the slurry temperature varied from 25 to 92 °C. The stirring speed was constant at 700 rpm. Slurry samples were taken with time, filtered, and oven dried. The filtrates and the solids were stored for later analyses. The results from these experiments are shown in Figures 7.7 through 7.11.

Figure 7.7 shows the effect of slurry temperature on the dissolved calcium concentration for the slurry with a 1:2 weight ratio of $Ca(OH)_2$:$Al(OH)_3$. The data show that the dissolved calcium concentration decreases with slurry time for all slurry temperatures, as it did for the $Ca(OH)_2$ / silica fume experiments. However, in contrast to the $Ca(OH)_2$ / silica fume experiments, the dissolved calcium concentration reaches an equilibrium value. These data indicate that the dissolved calcium concentration is controlled by a solubility product of the calcium aluminate solids produced by the reaction. This is also indicated by the data from the sugar dissolution experiments (Figure 7.8) which show that a significant amount of unreacted $Ca(OH)_2$ is present in the solids even though the solution analyses indicate that the solution is not saturated with respect to $Ca(OH)_2$.

The calcium aluminate solids were also subjected to further characterization tests. The x-ray diffraction results showed that the product solids become increasingly crystalline with slurry time (Figures 7.9 and 7.10). The reaction

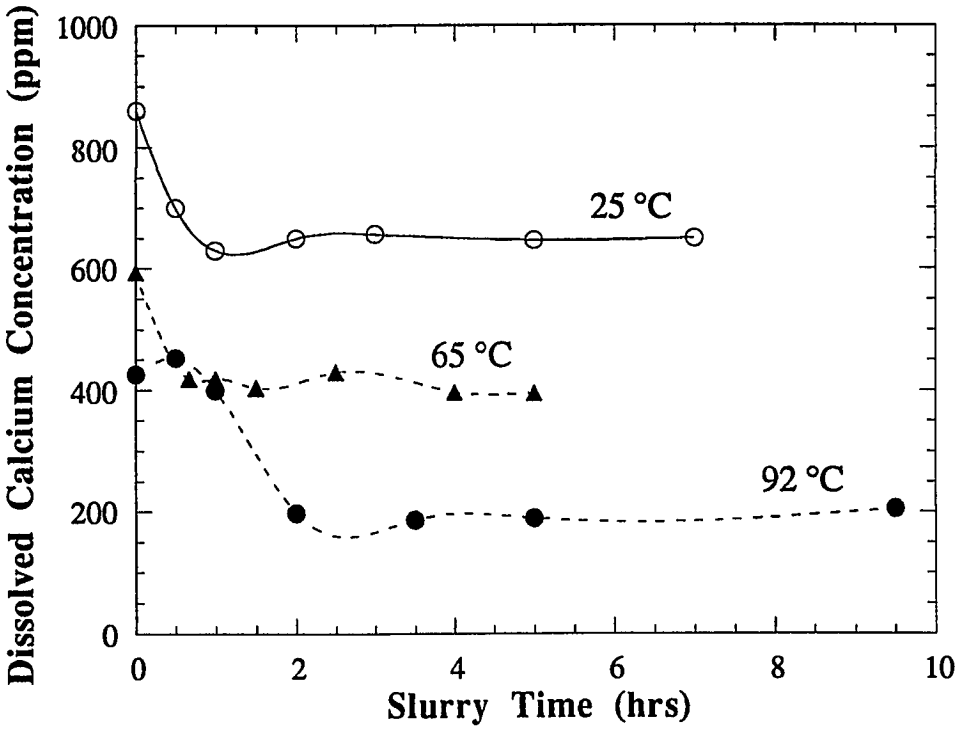

Figure 7.7 Solution composition for $Ca(OH)_2$ reacting with $Al(OH)_3$.

37.0 g $Ca(OH)_2$ + 78.0 g $Al(OH)_3$ + 400 ml H_2O, 90 °C
stir speed : 700 rpm.

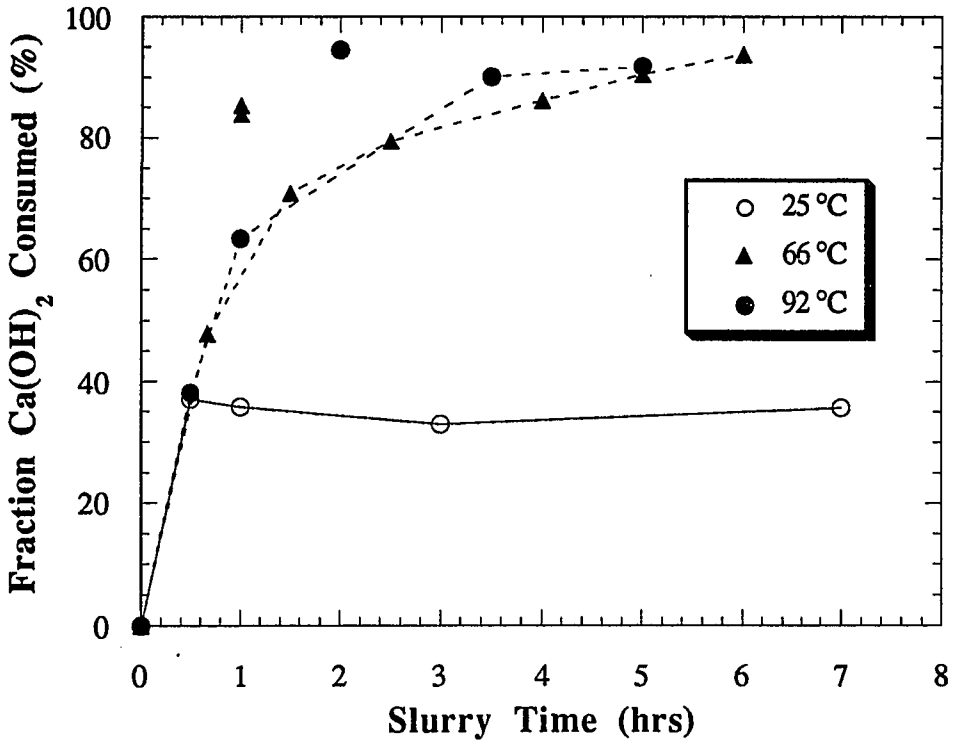

Figure 7.8 Effect of slurry temperature on solids free $Ca(OH)_2$ content.

37.0 g $Ca(OH)_2$ + 78.0 g $Al(OH)_3$ + 400 ml H_2O,
stir speed : 700 rpm

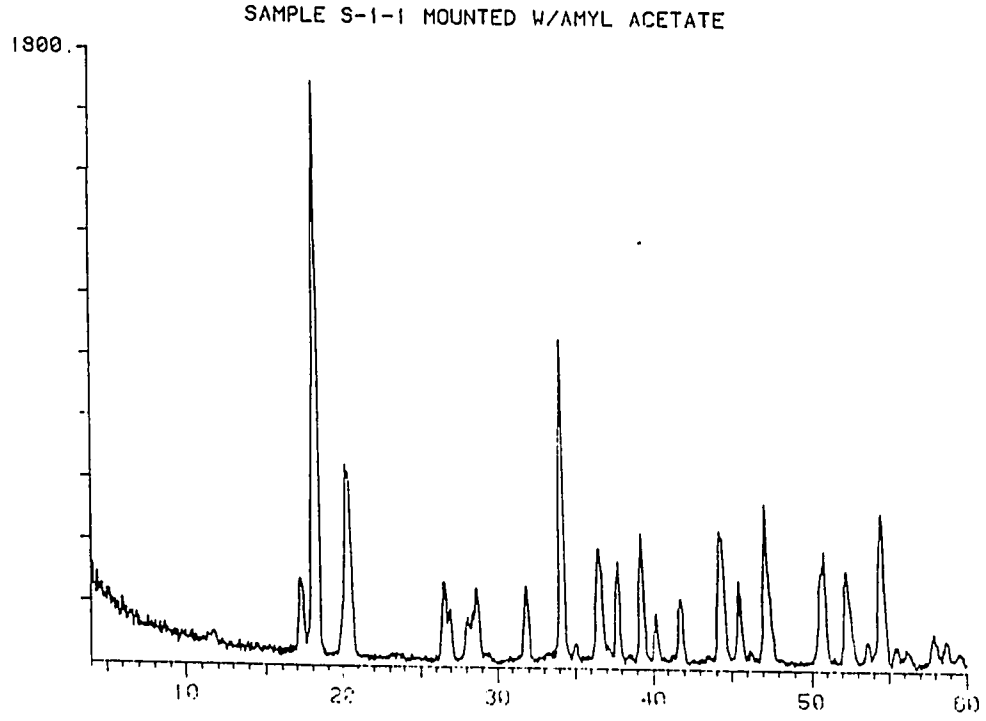

Figure 7.9 Powder x-ray diffraction pattern for solids produced by slurrying $Al(OH)_3$ with $Ca(OH)_2$ for 0.5 hours.

37.0 g $Ca(OH)_2$ + 78.0 g $Al(OH)_3$ + 400 ml H_2O,
stir speed : 700 rpm

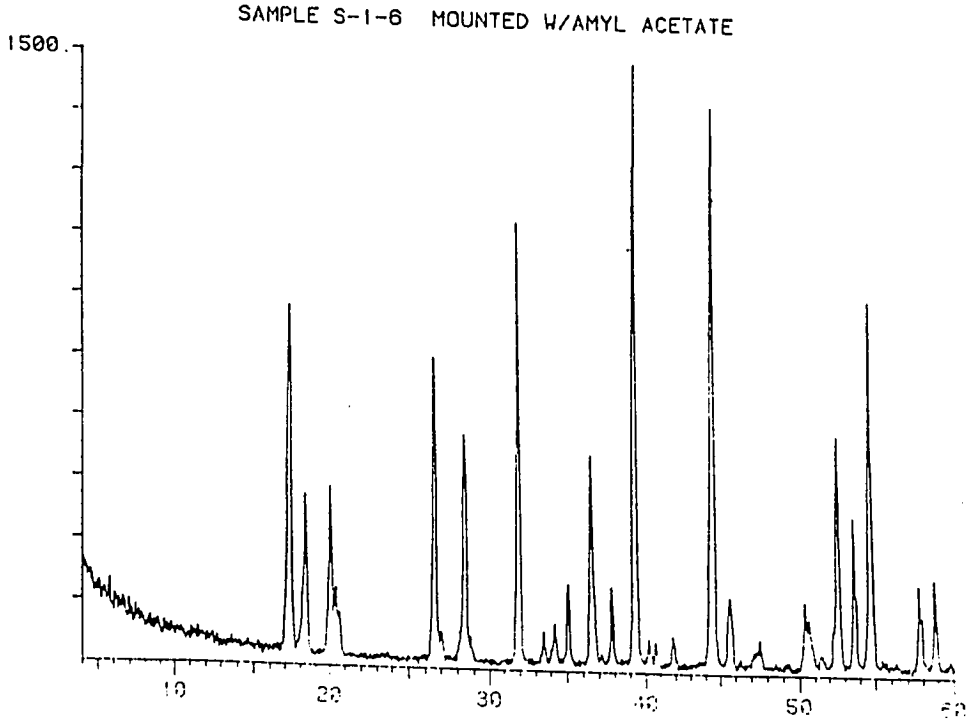

Figure 7.10 Powder x-ray diffraction pattern for solids produced by slurrying $Al(OH)_3$ with $Ca(OH)_2$ for 7.5 hours.

Slurry conditions : 37.0 g $Ca(OH)_2$ + 78.0 g $Al(OH)_3$ + 400 ml H_2O, stir speed : 700 rpm

product was identified as calcium aluminum hydroxide ($Ca_3Al_2(OH)_{12}$ JCPDS # 24-217). Taylor (1964) identified this material to be the only stable product in the calcium-aluminum-water system for temperatures of less than 225 °C.

This result is in sharp contrast to the data for the $Ca(OH)_2$/silica fume experiments, where the product solids were almost completely amorphous. Surface area and reactivity measurements show that the crystalline calcium aluminate solids have a low surface area and are unreactive towards SO_2 (Figure 7.11).

The above data indicate that the formation of calcium aluminates is not desirable for the formation of reactive lime/fly ash materials. This data, along with the data from Chapter VI, suggest that low-calcium fly ashes are more desirable for the production of lime/fly ash solids since the relative reactivity of silica to aluminum in these fly ashes is greater than that for high-calcium fly ashes. Presumably, the solids produced using fly ashes which have a large fraction of highly reactive aluminum would be low surface area solids which would be unreactive towards SO_2.

7.3 Reaction of $Ca(OH)_2$ with mixtures of silica and aluminum

After the initial investigations of the reaction of $Ca(OH)_2$ with silica fume and $Al(OH)_3$ were completed, several experiments were conducted to determine the effect of aluminum on the reaction of silica fume with $Ca(OH)_2$. This was undertaken because previous research has shown that the solubility of silica in water is dramatically lowered by the presence of minute amounts of aluminum in solution (Iler, 1973). A reduced silica solubility would presumably lead to a lower rate and extent of reaction between silica and $Ca(OH)_2$.

In this test series, 35 g of $Ca(OH)_2$ was slurried with 39 g of a mixture of silica fume with $Al(OH)_3$. The relative amount of each material was varied from 0 to 100% by weight. The solids were slurried in 400 ml of distilled water for up to

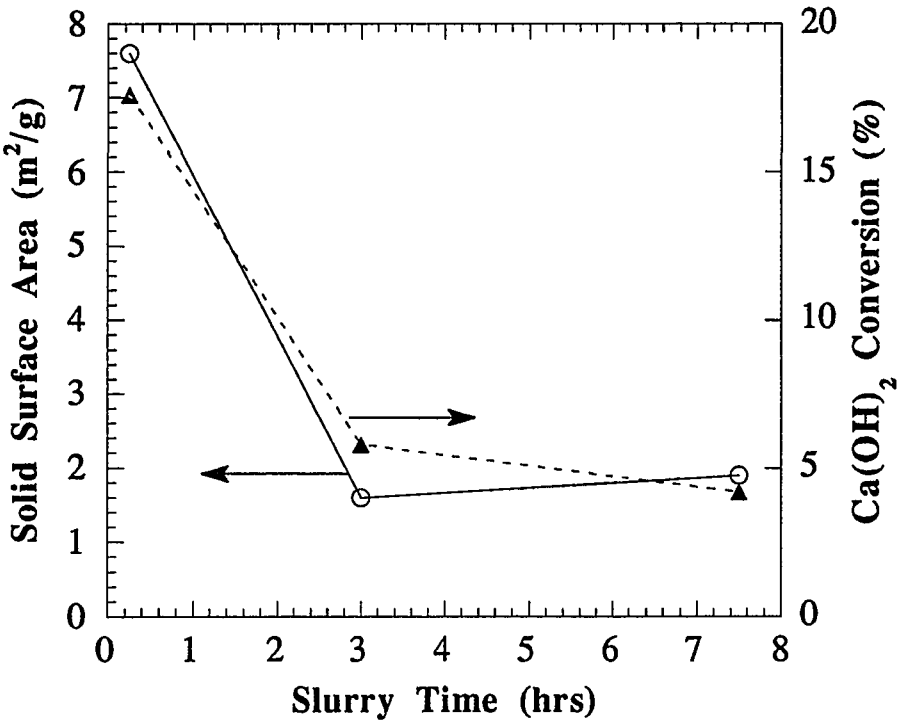

Figure 7.11 Results from surface area and solids reactivity experiments.

37.0 g $Ca(OH)_2$ + 78.0 g $Al(OH)_3$ + 400 ml H_2O, 90 °C
stir speed : 1000 rpm

Reaction Conditions : 70 °C, 64% Relative Humidity, 5.0 slpm,
1000 ppm SO_2, 12 % O_2, 10% CO_2, 78% N_2 (dry basis).

8 hours at 92 °C. The stirring speed was constant at 700 rpm. Slurry samples were taken with time, filtered, and dried. The results from these experiments are shown in Figures 7.12 through 7.14.

Figure 7.12 shows the data from the surface area analyses. This data shows that the surface area of the product solids decreases with increasing amounts of $Al(OH)_3$ added to the slurry. The surface area of the solids is generally highest for the solids created by slurrying $Ca(OH)_2$ with pure silica fume and lowest for the solids created by slurrying $Ca(OH)_2$ with pure $Al(OH)_3$. Note also that these data indicate that the presence of small amounts of aluminum in the slurry has no dramatic effect on the reaction of silica fume with $Ca(OH)_2$.

The solids reactivity data shown in Figure 7.13 support these data and indicate that the solids formed without silica fume present in the slurry are very unreactive towards SO_2. In fact, the data show that the calcium aluminate solids were even less reactive towards SO_2 than was unslurried $Ca(OH)_2$.

X-ray powder diffraction was used to identify the crystalline phases produced in one of the above slurries. This analysis was performed on the solids produced in a slurry of 35 g of $Ca(OH)_2$ with 19.5 g of silica fume and 19.5 g of $Al(OH)_3$. The slurry time was 5 hours and the slurry temperature was 92 °C. The only identifiable materials were $Al(OH)_3$ and $Ca_3Al_2(OH)_{12}$ (Figure 7.14). No $Ca(OH)_2$ was present and no calcium-aluminate-silicates were identified in this solid.

These data confirm the high reactivity of the calcium silicate solids and show that the presence of aluminum in the slurry does not decrease the reactivity of the silica fume towards the $Ca(OH)_2$. However, since the silica fume has a relatively high surface area (20 m^2/g) and reacts more quickly with the $Ca(OH)_2$ than does $Al(OH)_3$ (1.2 m^2/g), these data leave a little to be desired. Specifically, one needs to know the relative availability of silica to aluminum present in the fly ash. Indeed, this may be the reason some fly ashes produce more reactive lime/fly

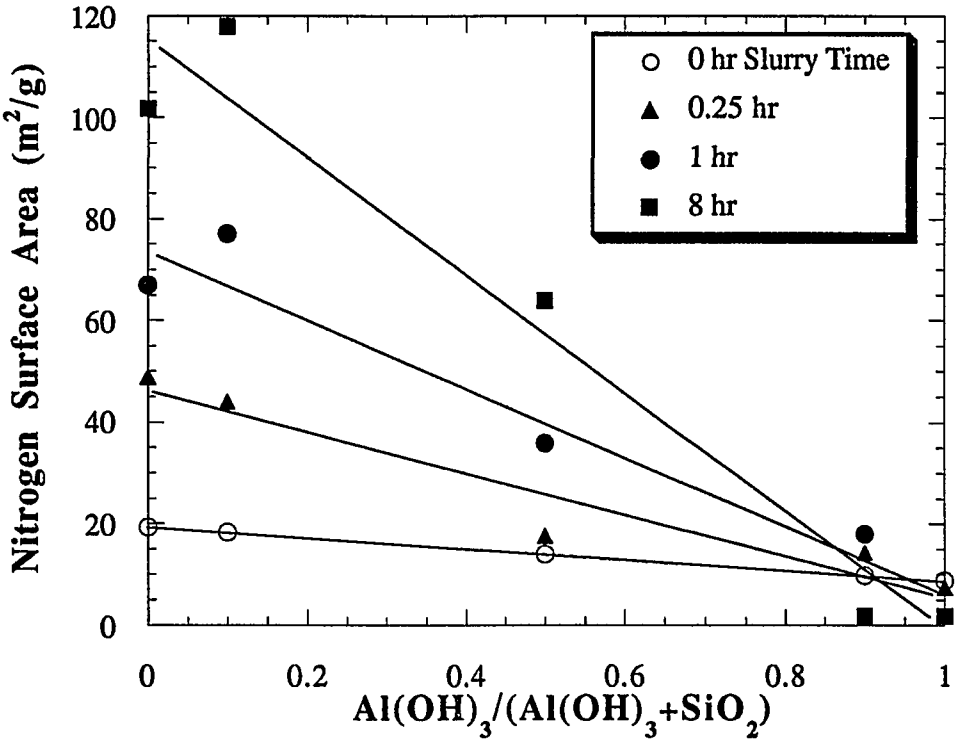

Figure 7.12 Effect of slurry time on solids surface area.

35.0 g $Ca(OH)_2$ + 39.0 g ($Al(OH)_3$+Silica Fume) + 400 ml H_2O
92 °C, 700 rpm

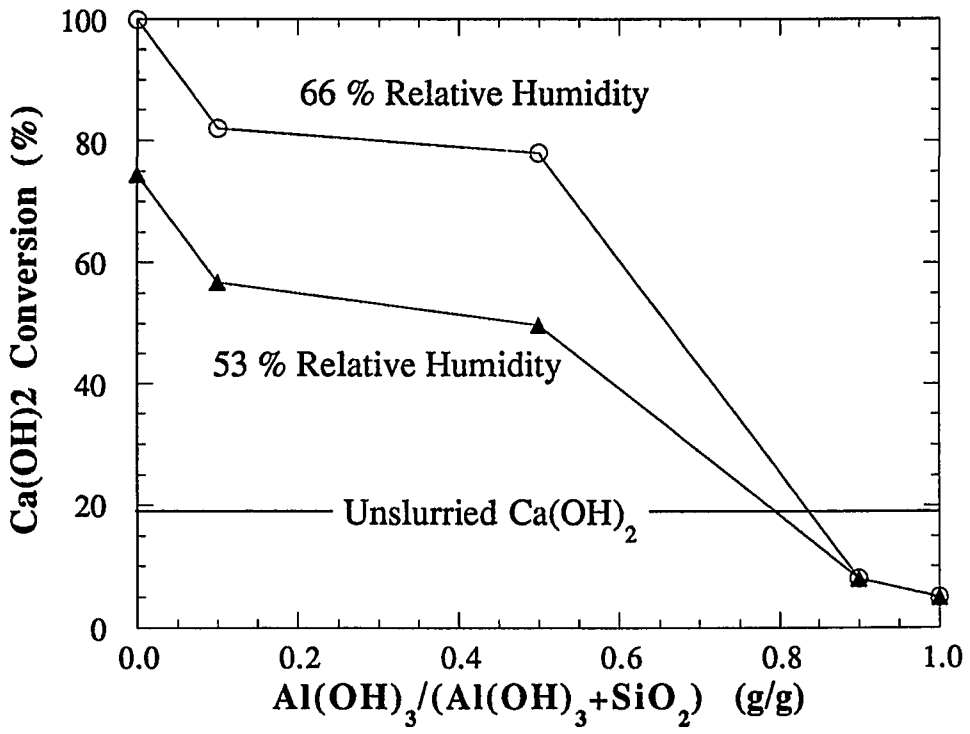

Figure 7.13 Reactivity of mixture solids towards SO_2.

35.0 g $Ca(OH)_2$ + 39.0 g ($Al(OH)_3$+Silica Fume) + 400 ml H_2O
Slurry temp. : 92 °C, stir speed : 700 rpm.

Reaction Conditions : 70 °C, 64% Relative Humidity, 5.0 slpm,
1000 ppm SO_2, 12 % O_2, 10% CO_2, 78% N_2 (dry basis).

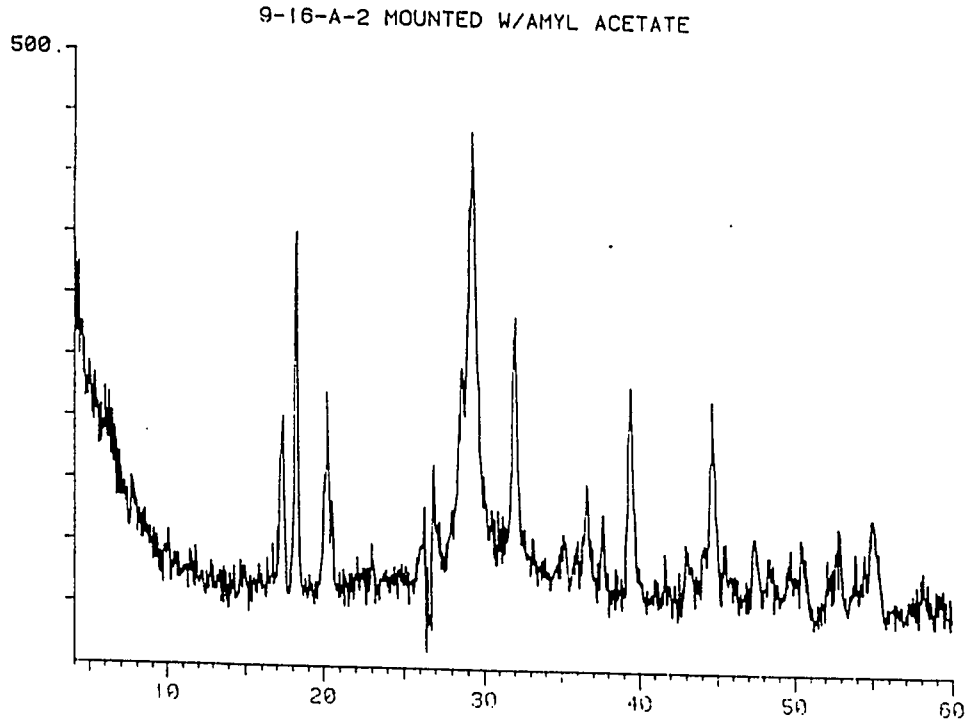

Figure 7.14 Powder x-ray diffraction pattern for solids produced by slurrying a mixture of $Al(OH)_3$ and silica fume with $Ca(OH)_2$ for 5 hours.

37.0 g $Ca(OH)_2$ + 19.05 g $Al(OH)_3$ + 19.5 g silica fume + 400 ml H_2O, stir speed : 700 rpm

ash solids than do others. The aluminum content of these "unreactive" fly ashes may be much more reactive than their silica content.

7.3 Effects of recycle materials

One of the goals of this research was to determine the effects of recycle materials on the reaction of lime with fly ash. These effects are important because a full scale FGD system using the lime/fly ash solids would probably recycle the solids collected in the particulate control device in order to utilize any unreacted lime/fly ash material. If this recycle material is sent to the lime/fly ash slurry tank, the sulfur compounds in the recycle stream may influence the reactivity of the lime/fly ash solids produced in this tank. The effects of these recycle compounds relate to the reaction of the sulfur species with the aluminum content of the fly ash to form calcium-alumino-sulfate materials, a reaction which is well documented by studies pertaining to cement and concrete (Taylor, 1964). It is not known if these calcium-alumino-sulfate materials form at the high temperatures of the lime/fly ash system, nor is it known how the formation of these materials affects the reactivity of the lime/fly ash material towards SO_2.

To determine if these materials form under the lime/fly ash reaction conditions, laboratory-produced calcium sulfite hemihydrate ($CaSO_3 \cdot 0.5H_2O$) or reagent quality gypsum ($CaSO_4 \cdot 2H_2O$) was added to slurries of $Ca(OH)_2$ with $Al(OH)_3$. Samples from these slurries were taken with time and vacuum filtered. The filtrates and the solids were stored and later analyzed. The results from these experiments are shown in Figures 7.15 through 7.22.

The results from the solution analyses (Figure 7.15) show that the presence of hemihydrate in the slurry does not dramatically affect the behavior of the dissolved calcium concentration. The dissolved calcium concentration decreases with time to reach an equilibrium value as was the case when hemihydrate was not present. However, the presence of gypsum in the slurry has a very strong effect. The dissolved calcium concentration was stable and was higher than for the base

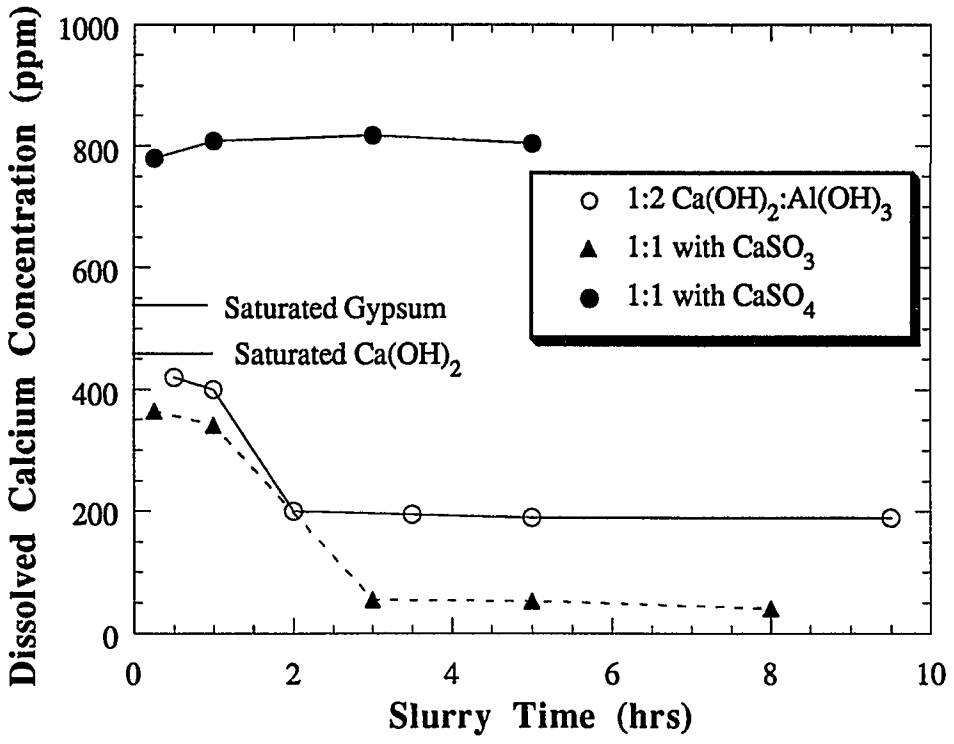

Figure 7.15 Effect of recycle materials on the solution composition for slurries of $Ca(OH)_2$ and $Al(OH)_3$.

Slurry Conditions : 37.0 g $Ca(OH)_2$ + 39.0 or 78.0 g $Al(OH)_3$ + 400 ml H_2O, 92 °C, stir speed : 700 rpm

with $CaSO_3$: 64.5 g $CaSO_3 \cdot 0.5H_2O$ added to slurry
with $CaSO_4$: 86.0 g $CaSO_4 \cdot 2H_2O$ added to slurry

case run without recycle. These effects are attributed to the relatively high solubility of gypsum compared to $Ca(OH)_2$ and hemihydrate.

Figure 7.16 shows that the presence of gypsum in the slurry also had a very strong effect on the reactivity of the $Al(OH)_3$ towards $Ca(OH)_2$, while hemihydrate had no effect. The presence of gypsum in the slurry halts the reaction of hydrate with $Al(OH)_3$. This was also shown by the surface area development of the calcium aluminate solids when recycle materials are present in the slurry (Figure 7.17). The solids produced in the slurries which did not contain gypsum lost surface area as the slurry time increased. However, the presence of gypsum stopped this loss of surface area with time, presumably because gypsum stops the reaction of aluminum with $Ca(OH)_2$.

The above results show that the presence of hemihydrate in the slurry seems to have no effect on the reaction of hydrate with $Al(OH)_3$. However, the x-ray diffraction results (Figure 7.18) show that the presence of hemihydrate prohibits the formation of calcium aluminum hydroxide ($Ca_3Al_2(OH)_{12}$) solids. A new crystalline product is formed (indicated by new diffraction lines appearing), but it was not identified because the JCPDS files have no data for any calcium-aluminum-sulfite materials. It is assumed that this product is a calcium-alumino-sulfite material somewhat analogous to ettringite.

The x-ray diffraction results on the solids produced when gypsum was present in the slurry support the sugar dissolution data and indicate that $Ca(OH)_2$ is not fully utilized. A small amount of new crystalline material was produced, but identification of this phase was not possible. More than likely, this material is a transient phase which leads to an identifiable calcium-sulfo-aluminate such as ettringite.

One recycle experiment using gypsum was conducted by slurrying $Ca(OH)_2$ with an equal weight mixture of silica fume and $Al(OH)_3$ to determine whether gypsum interferes with the reaction of silica fume with $Ca(OH)_2$. The results from

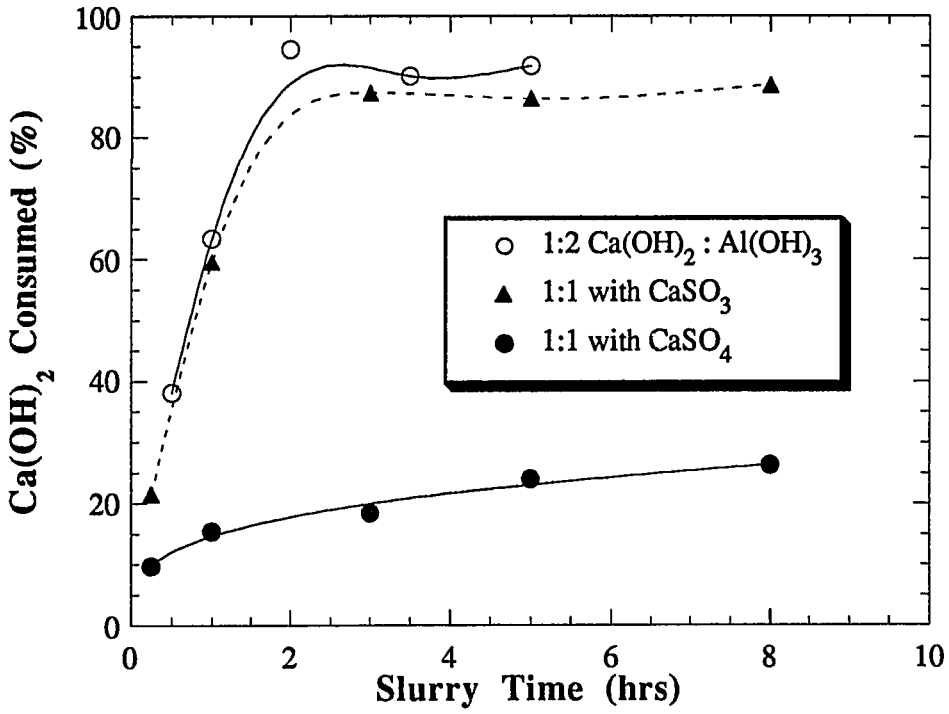

Figure 7.16 Effect of recycle materials on the reaction of $Ca(OH)_2$ with $Al(OH)_3$.

Slurry Conditions : 37.0 g $Ca(OH)_2$ + 39.0 or 78.0 g $Al(OH)_3$ + 400 ml H_2O, 92 °C, stir speed : 700 rpm

with $CaSO_3$: 64.5 g $CaSO_3 \cdot 0.5H_2O$ added to slurry
with $CaSO_4$: 86.0 g $CaSO_4 \cdot 2H_2O$ added to slurry

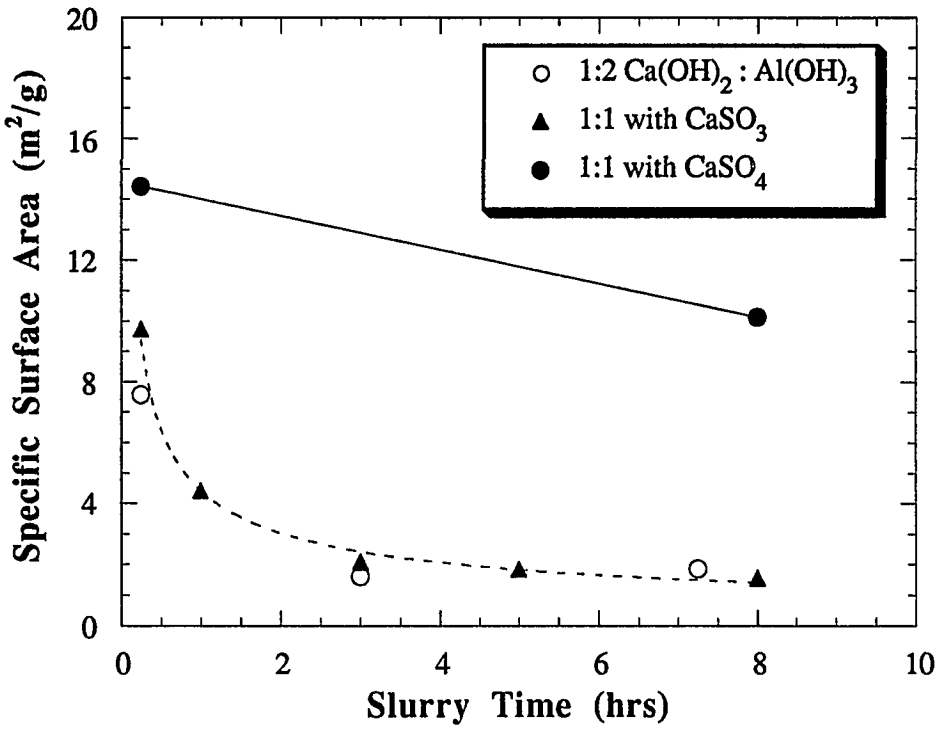

Figure 7.17 Effect of recycle materials on the development of surface area for calcium aluminate solids.

Slurry Conditions : 37.0 g $Ca(OH)_2$ + 39.0 or 78.0 g $Al(OH)_3$ + 400 ml H_2O, 92 °C, stir speed : 700 rpm

with CaSO3 : 64.5 g $CaSO_3 \cdot 0.5H_2O$ added to slurry
with CaSO4 : 86.0 g $CaSO_4 \cdot 2H_2O$ added to slurry

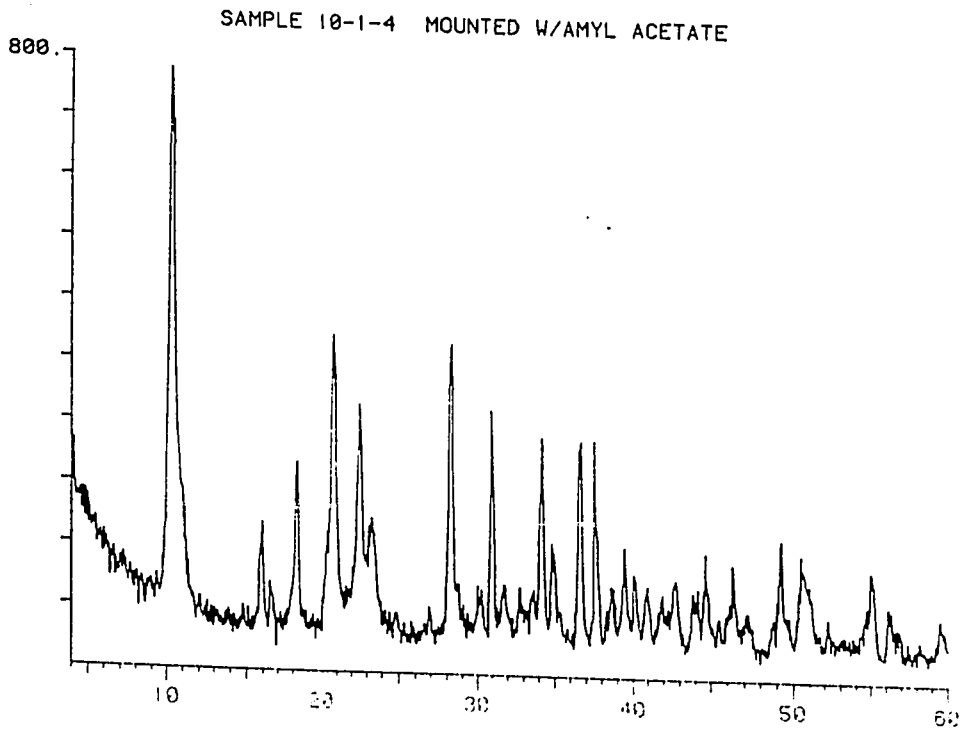

Figure 7.18 Powder x-ray diffraction pattern for solids produced by slurrying a mixture of $Al(OH)_3$, $CaSO_3 \cdot 0.5H_2O$, and $Ca(OH)_2$ for 5 hours.

37.0 g $Ca(OH)_2$ + 39 g $Al(OH)_3$ + 64.5 g $CaSO_3 \cdot 0.5H_2O$ + 400 ml H_2O, stir speed : 700 rpm

this experiment are plotted along with data from a control experiment in Figures 7.19 and 7.20. The data show that the presence of gypsum does not interfere with the reaction of silica fume with $Ca(OH)_2$ to form high surface area solids. In fact, the surface area data suggest that the presence of gypsum in the slurry serves as a method to decrease the formation of non-reactive calcium aluminates and produce more of the very reactive calcium silicate materials. This is evidenced by noting that the surface areas of the solids which were produced in the slurry that contained gypsum were higher than those which were produced with no gypsum present in the slurry.

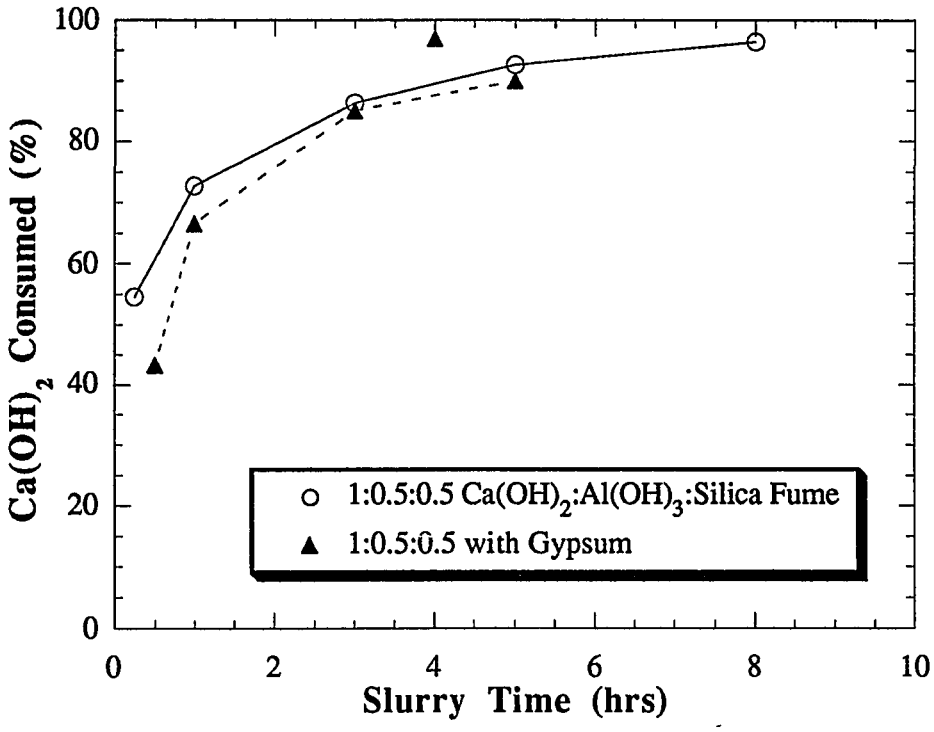

Figure 7.19 Effect of gypsum on the reaction of $Ca(OH)_2$ with a mixture of $Al(OH)_3$ and silica fume.

Slurry Conditions : 37.0 g $Ca(OH)_2$+19.5 g $Al(OH)_3$+19.5 g silica fume. 400 ml H_2O, 92 °C, stir speed : 700 rpm

with Gypsum : 16.3 g $CaSO_4 \cdot 2H_2O$ added to slurry

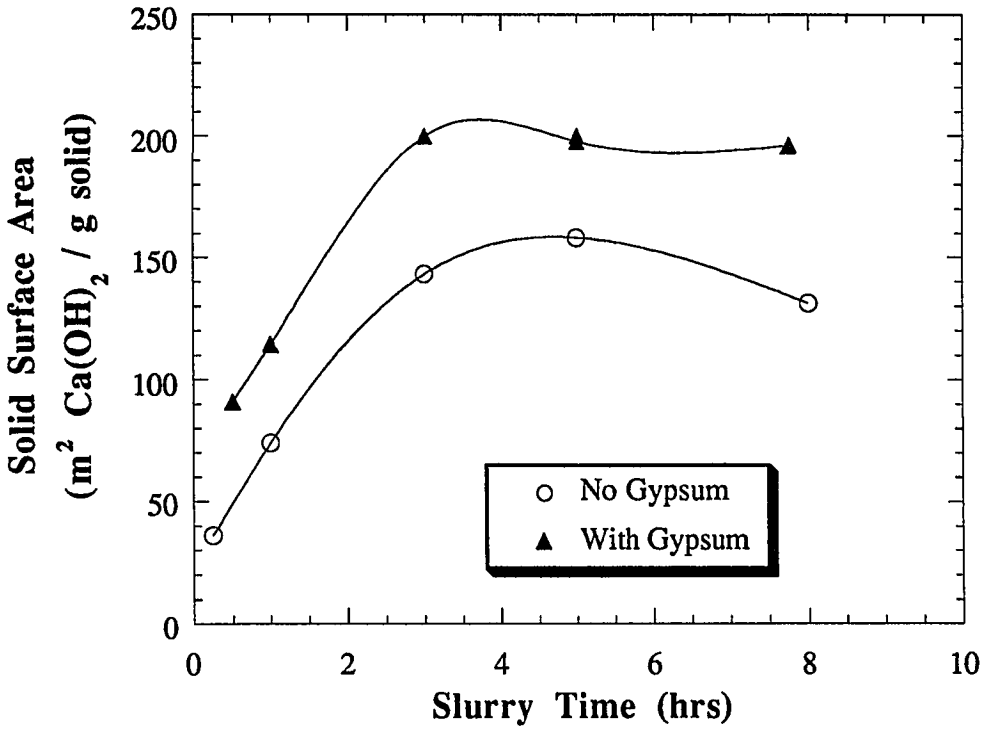

Figure 7.20 Effect of gypsum on the reaction of $Ca(OH)_2$ with a mixture of $Al(OH)_3$ and silica fume.

Slurry Conditions : 37.0 g $Ca(OH)_2$+19.5 g $Al(OH)_3$+19.5 g silica fume. 400 ml H_2O, 92 °C, 700 rpm

with Gypsum : 16.3 g $CaSO_4 \cdot 2H_2O$ added to slurry

Chapter VIII

Experiments Using Lime/Fly Ash Solids

The experiments described in the previous chapters were meant to provide a fundamental understanding of the reactions which occur when lime is reacted with fly ash. To complement these experiments, lime/fly ash solids were created by slurrying $Ca(OH)_2$ with fly ash in water at high temperature. The reactions were followed by analyzing the solution composition and the product solids with time. These lime/fly ash experiments investigated the effects of fly ash type, fly ash grinding, and the presence of recycle materials in the slurry. The results from these experiments are described in the following sections.

8.1 Effect of fly ash type

To determine the effect of fly ash type on the reaction of $Ca(OH)_2$ with fly ash, nine different fly ashes were slurried with $Ca(OH)_2$ in water at 92 °C. The total solids loading was 350 g solids/liter (35 g $Ca(OH)_2$ + 105 g fly ash + 400 ml H_2O) and the stirring speed was 700 rpm. Slurry samples were taken with time and vacuum filtered. The solids were oven dried and then characterized by the methods described in Chapter V. The filtrates were analyzed for pH and dissolved metal concentrations using atomic absorption spectroscopy. The results from these experiments are shown in Figures 8.1 through 8.18.

8.1.1 Solution analyses

Figure 8.1 shows the effect of fly ash type on the dissolved calcium concentration in the slurry. The data show that, for all of the fly ashes tested, the dissolved calcium concentration decreases rapidly during the first two hours of reaction and then stabilizes at a fairly constant level. These results are similar to those obtained for the slurries of $Ca(OH)_2$ with either silica fume or $Al(OH)_3$ (Chapter VII), so one might conclude that the solution composition was controlled by a calcium-silicate-hydrate material in a manner similar to the reaction of $Ca(OH)_2$ with silica fume.

However, the hydroxide concentration in the solution also changes during the course of the reaction. Figure 8.2 shows the effect of fly ash type on the pH of the slurry solution. The data show that the pH of the solution increases with time for all of the fly ashes tested, regardless of the fly ash type or source. This data is in contrast with the data from the reagent chemical experiments (Chapter 8) which showed that the pH of the solution dropped with time as the $Ca(OH)_2$ reacted with either silica fume or $Al(OH)_3$. Figure 8.3 shows that the increase in the solution pH is due to alkali materials which are present in the fly ash. The data show that the sodium which is present in the fly ash (presumably as Na_2O) dissolves from the fly ash and reacts with water to produce hydroxide and sodium ions. Even though the sodium content of this fly ash was responsible for the increase in the solution pH, the presence of other alkali metals (e.g. K) in the fly ash should have a similar effect on the solution pH. An analysis of the solution data indicate that all of the solutions were slightly supersaturated to $Ca(OH)_2$ (Figure 8.4). This is supported by the data from the sugar dissolution and x-ray powder diffraction analyses which indicated the presence of solid $Ca(OH)_2$ for most of the lime/fly ash solids.

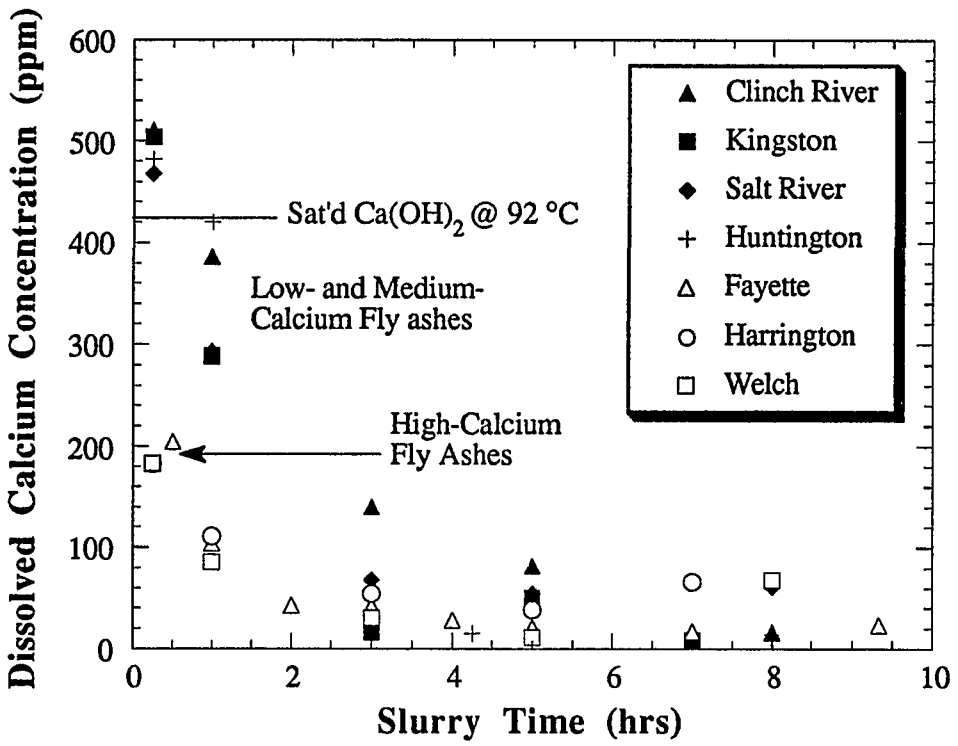

Figure 8.1 Effect of fly ash type on the dissolved calcium concentration in the slurry.

Slurry Conditions : 35 g $Ca(OH)_2$ + 105 g fly ash + 400 ml H_2O; 92 °C; 700 rpm.

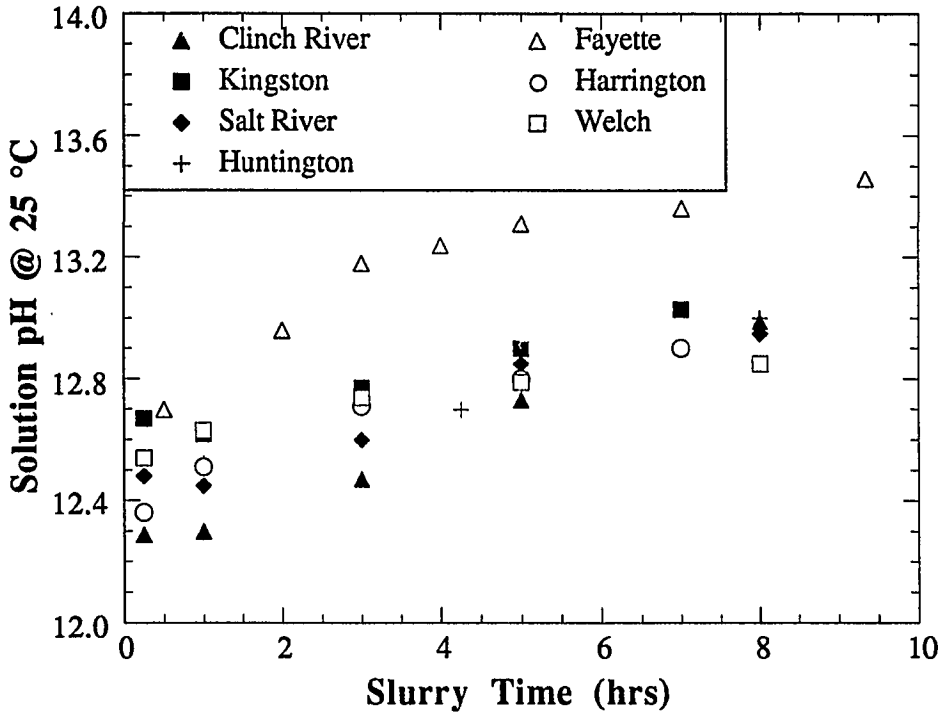

Figure 8.2 Effect of fly ash type on the solution pH for slurries of $Ca(OH)_2$ and fly ash.

Slurry Conditions : 35 g $Ca(OH)_2$ + 105 g fly ash + 400 ml H_2O; 92 °C; 700 rpm.

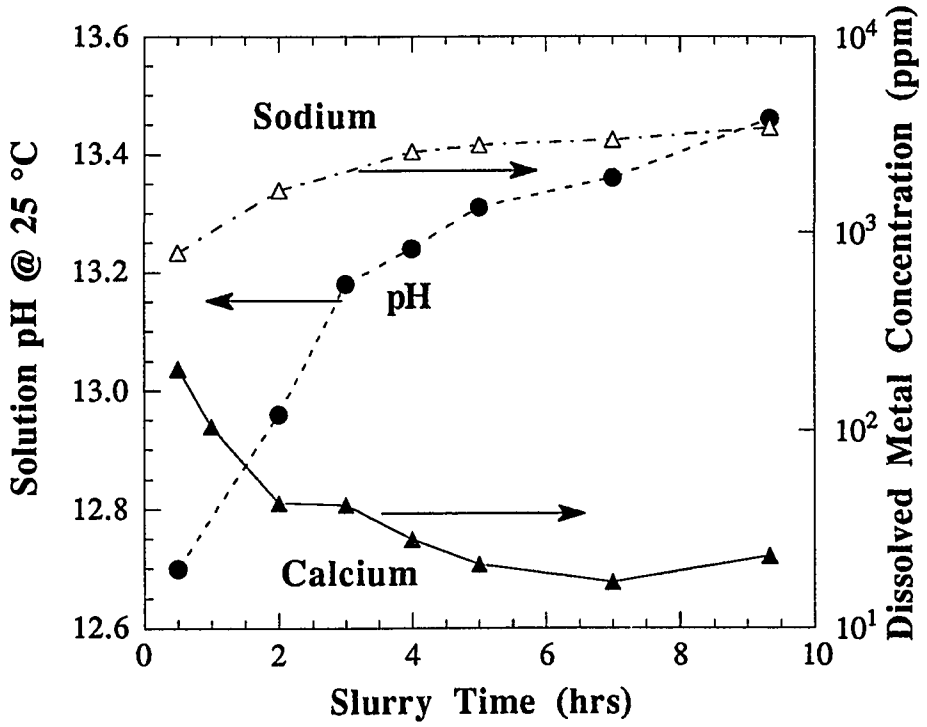

Figure 8.3 Solution composition for slurry of high calcium fly ash with $Ca(OH)_2$.

Slurry Conditions : 35 g $Ca(OH)_2$ + 105 g Fayette fly ash + 400 ml H_2O; 92 °C; 700 rpm.

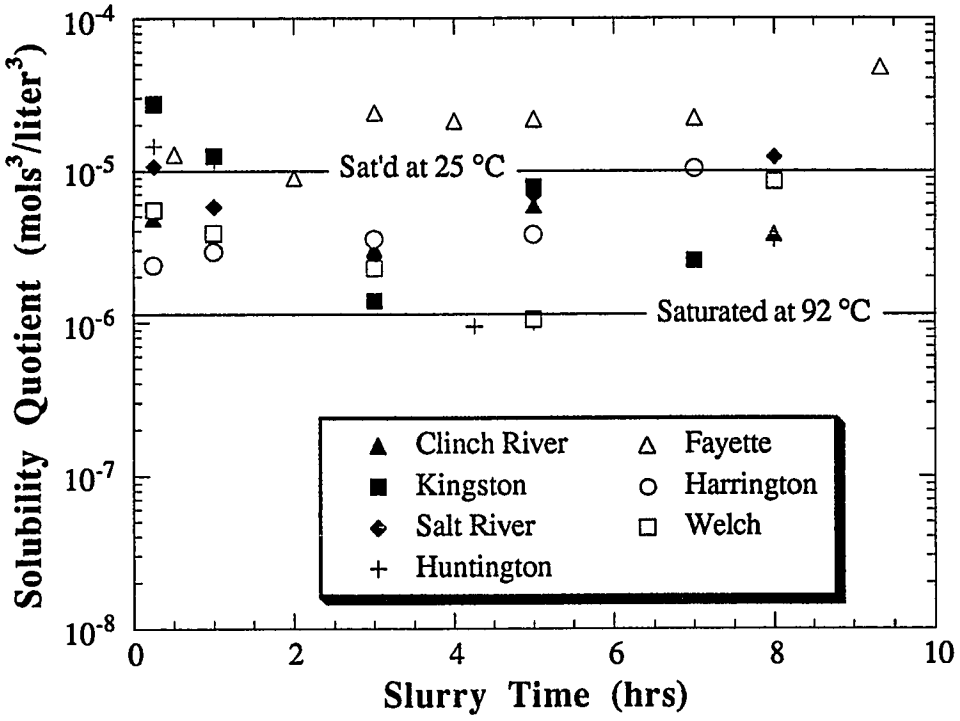

Figure 8.4 Determining the relative saturation with respect to $Ca(OH)_2$ for the lime/fly ash slurries.

Slurry Conditions : 35 g $Ca(OH)_2$ + 105 g fly ash + 400 ml H_2O; 92 °C; 700 rpm.

Solubility quotient defined as : $[Ca^{2+}]*[OH^-]^2$ (both in moles/liter)

8.1.2 Solids analyses

The data from the solids characterization experiments showed a strong effect of fly ash type. Figure 8.5 shows the effect of fly ash type on the reaction between fly ash and $Ca(OH)_2$. These data show that, for long slurry times, the low-calcium fly ashes consume much more of the original $Ca(OH)_2$ present in the slurry than do the medium- and high-calcium fly ashes. At short times, however, the high-calcium fly ashes consume more $Ca(OH)_2$ than the low- and medium-calcium fly ashes.

These results can be explained by referring to the chemical composition of the fly ashes and by using the results from the fly ash dissolution experiments. The medium- and high-calcium fly ashes contain less total silica and alumina than the low-calcium fly ashes, so for long reaction times it is not surprising that the low-calcium fly ashes consume more $Ca(OH)_2$ (Figure 8.6). For short reaction times, recall that the high-calcium fly ashes contain a large fraction of material that dissolves instantaneously in the fly ash dissolution experiments. A portion of this reactive alumino-silicate material probably dissolves rapidly into the lime slurry and precipitates calcium-aluminates and calcium-silicates onto the surface of the undissolved fly ash particles. This reactive material accounts for the consumption of a relatively large portion of the $Ca(OH)_2$ present in the slurry for short reaction times.

A significant disadvantage of the sugar dissolution method is that it does not account for the reactivity of the calcium that is present in the fly ash, and therefore understates the actual amount of calcium that has been consumed by the silica and aluminum. However, the data from the selective dissolution experiments quantifies the reactive fraction of the calcium which is present in the fly ash. Table 8.1 shows that the amount of reactive calcium present in the fly ash varies from 0.0 to 17.5 percent depending upon the fly ash type. When this calcium is taken into account, the high-calcium fly ashes definitely consume more $Ca(OH)_2$ than do the low- and medium-calcium fly ashes in the early stages of reaction (Figure 8.7).

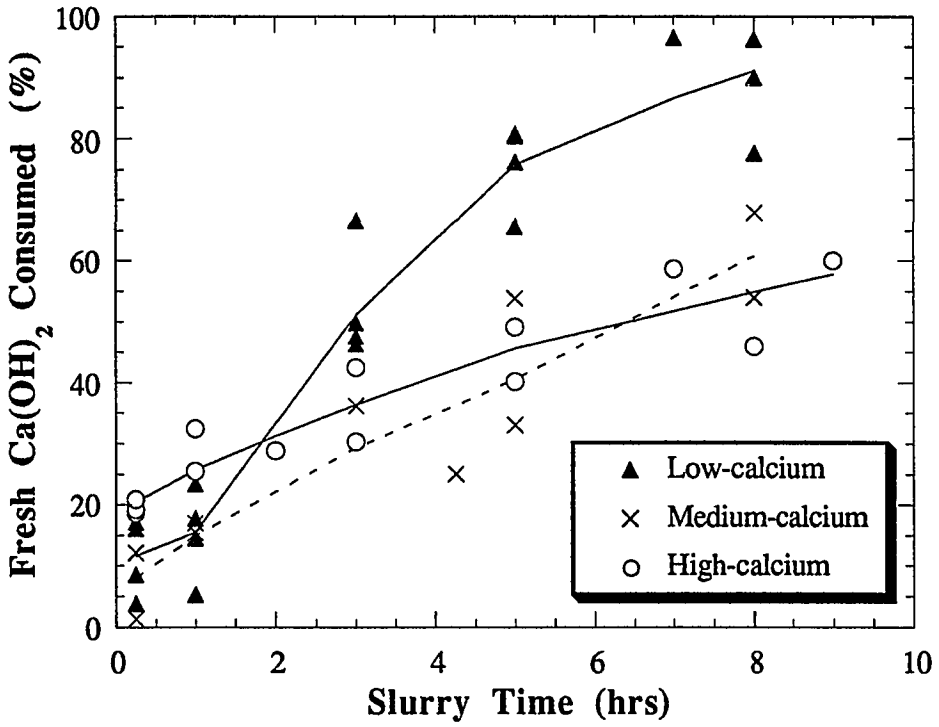

Figure 8.5 Effect of fly ash type on its reactivity towards $Ca(OH)_2$.

Slurry Conditions : 35 g $Ca(OH)_2$ + 105 g fly ash + 400 ml H_2O; 92 °C; 700 rpm.

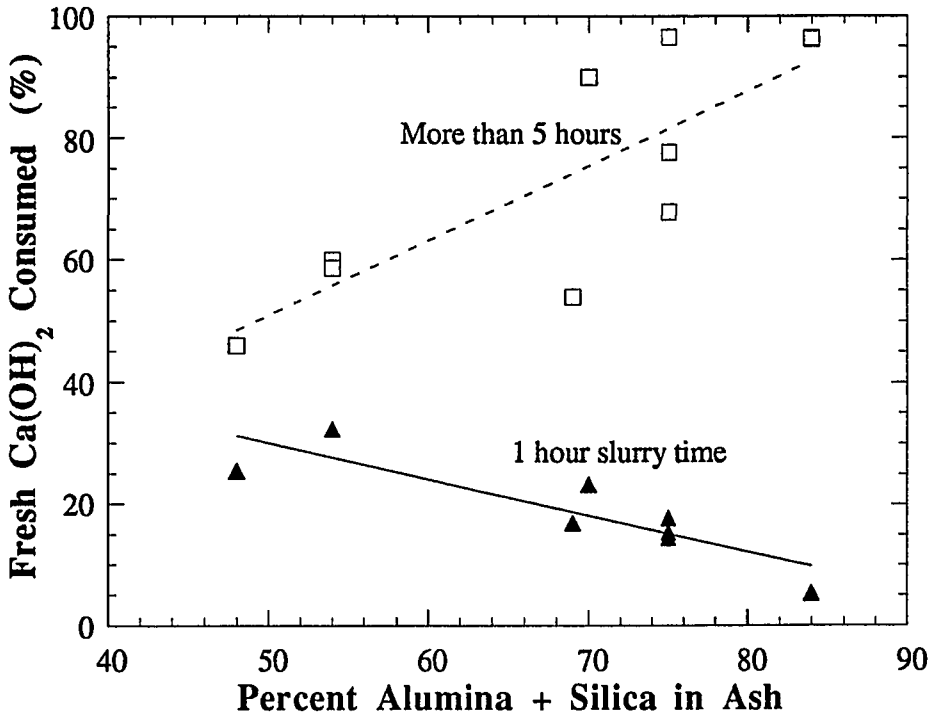

Figure 8.6 Effect of fly ash chemical composition on its reactivity towards $Ca(OH)_2$.

Slurry Conditions : 35 g $Ca(OH)_2$ + 105 g fly ash + 400 ml H_2O; 92 °C; 700 rpm.

TABLE 8.1 DETERMINATION OF REACTIVE CALCIUM CONTENT OF SEVERAL FLY ASHES.

Fly Ash	Slurry Time (hrs)	Fresh[a] $Ca(OH)_2$ Recovery	Total[b] $Ca(OH)_2$ Recovery	Percent[c] Reactive Calcium
Clinch River	0.25	111.4	96.5	2.9
Clinch River	1.0	107.8	93.4	2.0
Clinch River	3.0	108.9	94.3	2.2
Clinch River	8.0	110.2	95.4	2.6
Deseret	0.25	102.0	89.0	0.5
Deseret	1.0	105.7	92.2	1.4
Deseret	3.0	100.1	87.4	0.0
Deseret	5.0	97.3	84.9	(-0.7)
Deseret	8.0	100.7	87.9	0.2
Salt River	0.25	104.6	90.6	1.2
Salt River	1.0	101.3	87.7	0.3
Salt River	3.0	96.2	83.4	(-1.0)
Salt River	5.0	100.5	87.0	0.1
Salt River	8.0	108.3	93.8	2.1
Monticello	0.25	96.8	75.9	(-0.8)
Monticello	1.0	98.5	77.2	(-0.4)
Monticello	3.0	100.7	78.9	0.2
Monticello	5.0	101.1	79.2	0.3
Monticello	8.0	99.1	77.7	(-0.2)
Huntington	0.25	114.3	84.7	3.6
Huntington	1.0	113.0	83.9	3.3
Huntington	3.0	114.5	85.0	3.7
Huntington	4.25	115.8	86.0	4.0
Huntington	8.0	111.5	82.7	2.9
Harrington	0.25	166.8	76.4	16.8
Harrington	1.0	163.4	74.8	16.0
Harrington	3.0	145.1	66.5	11.4
Harrington	5.0	165.9	76.0	16.6
Harrington	8.0	163.7	75.0	16.1
Welch	0.25	162.9	69.5	15.9
Welch	1.0	167.6	71.5	17.0
Welch	3.0	173.7	74.1	18.6
Welch	5.0	171.7	73.2	18.1
Welch	8.0	170.5	72.7	17.8

[a] percentage based on $Ca(OH)_2$ added to the slurry

[b] percentage including all of calcium present in the fly ash

[c] calculated value = g CaO / 100 g fly ash

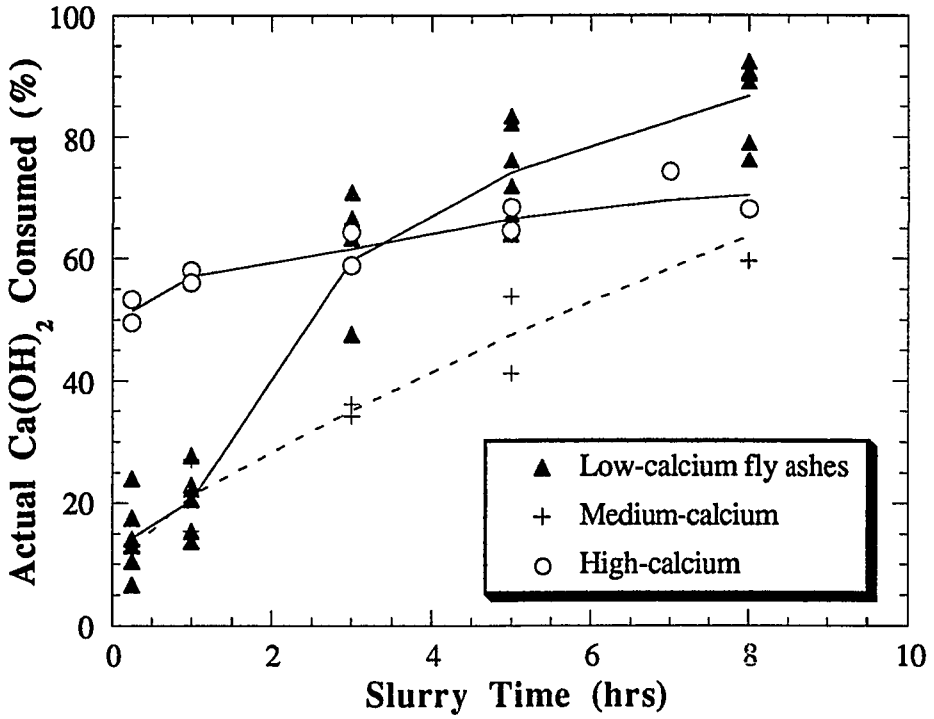

Figure 8.7 Effect of fly ash type on its reactivity towards $Ca(OH)_2$.

Slurry Conditions : 35 g $Ca(OH)_2$ + 105 g fly ash + 400 ml H_2O; 92 °C; 700 rpm.

The effect of fly ash type was also evident in the surface area development of the fly ash. Figure 8.8 shows that the use of medium- and high-calcium fly ashes generally led to the production of lower surface area materials. This result probably relates to the chemical composition of the fly ashes and to the relative reactivities of the silica and aluminum present in the fly ashes. The data in Chapter VI showed that the high-calcium fly ashes contain a larger fraction of reactive aluminum than reactive silica. These reactive aluminates were shown in Chapter VII to lead to the formation of low surface area materials. The very reactive aluminum compounds present in the high-calcium fly ash evidently react with the $Ca(OH)_2$ quickly to tie-up the $Ca(OH)_2$ before it can react with the silica present in the fly ash. The high-calcium fly ashes also have less total silica available for reaction with the $Ca(OH)_2$ to form high surface area materials. These two features lead to the production of the lower surface area materials shown in Figure 8.8.

The lime/fly ash solids were also tested for reactivity towards SO_2 in a sandbed reactor. The results from these tests are shown in Figures 8.9 and 8.10. The data presented in Figure 8.9 show that the reactivity of the lime/fly ash solids towards SO_2 increases with slurry time for all of the fly ashes tested and that there is only a slight effect of fly ash type on the solids' reactivity towards SO_2. The solids produced using the low- and medium-calcium fly ashes were slightly more reactive towards SO_2 than the solids produced using the high calcium fly ash.

It should be noted, however, that the reactivity shown in Figure 8.9 assumes that none of the calcium present in the fly ash reacts with the SO_2. This is probably a poor assumption, because previous researchers have shown that the calcium present in fly ash can be activated for reactivity towards SO_2 by slurrying the fly ash in hot water (Peterson and Rochelle, 1988). Furthermore, the fly ash dissolution experiments showed that approximately 60 percent of the calcium present in the high calcium fly ash dissolves instantaneously. If we assume that the data from the selective dissolution experiments approximates the calcium that is

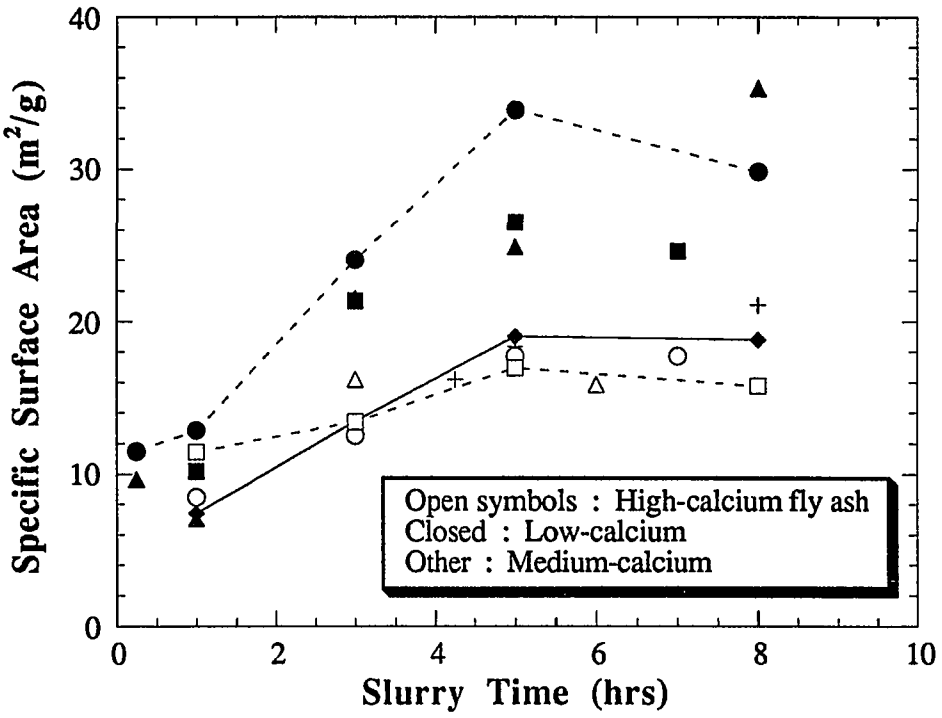

Figure 8.8 Effect of fly ash type on surface area development of lime/fly ash solids.

Slurry Conditions : 35 g $Ca(OH)_2$ + 105 g fly ash + 400 ml H_2O; 92 °C; 700 rpm.

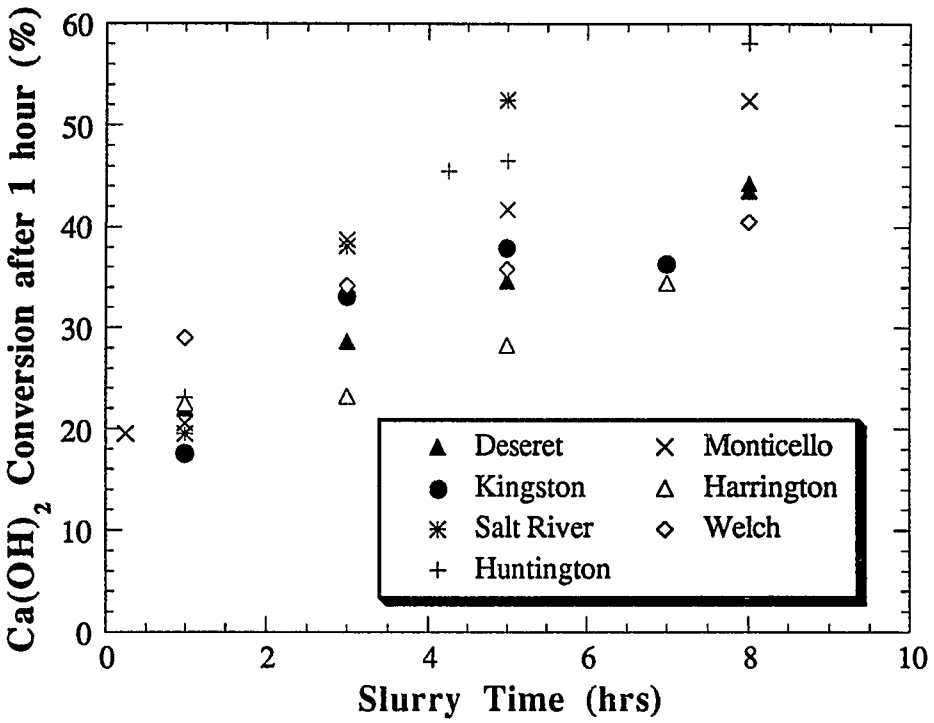

Figure 8.9 Effect of fly ash type on lime/fly ash solids reactivity towards SO_2.

Slurry Conditions : 35 g $Ca(OH)_2$ + 105 g fly ash + 400 ml H_2O; 92 °C; 700 rpm.

Reaction Cond.: 70 °C, 64% Relative Humidity, 5.0 slpm, 1000 ppm SO_2, 12 % O_2, 10% CO_2, 78% N_2.

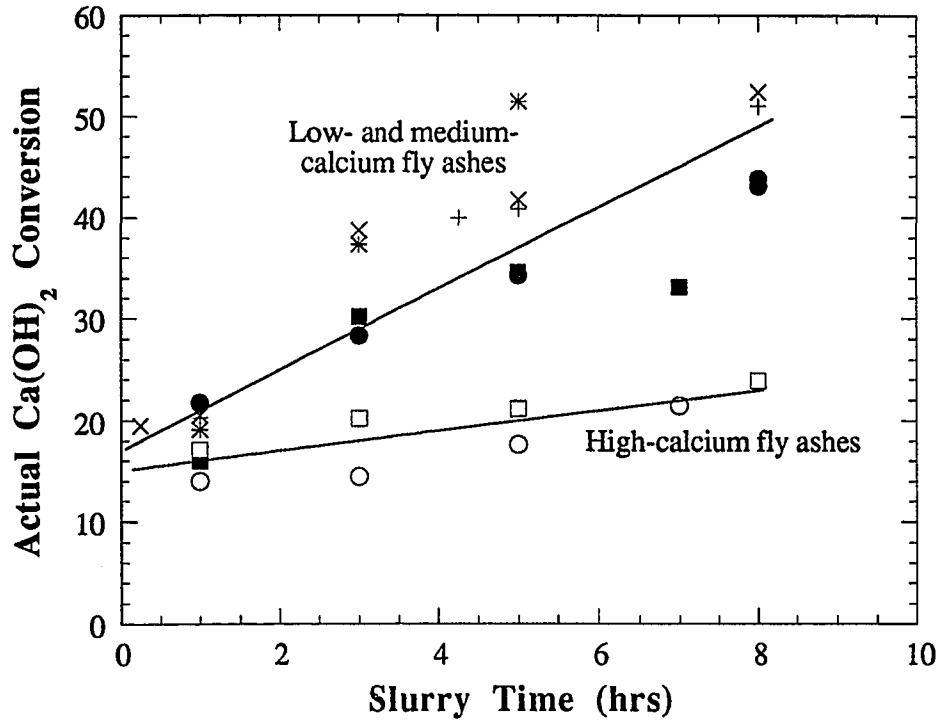

Figure 8.10 Effect of fly ash type on the reactivity of lime/fly ash solids towards SO_2. Values adjusted for the reactive calcium content of the fly ash.

Slurry Conditions : 35 g $Ca(OH)_2$ + 105 g fly ash + 400 ml H_2O; 92 °C; 700 rpm.

Reaction Cond.: 70 °C, 64% Relative Humidity, 5.0 slpm, 1000 ppm SO_2, 12 % O_2, 10% CO_2, 78% N_2.

present in the fly ash is in a reactive form, the low- and medium-calcium fly ashes perform much better than the high-calcium fly ashes (Figure 8.10).

8.1.3 Chemical and mineralogical characterization of solids

The chemical composition of the lime/fly ash solids was determined by combining the data from the selective dissolution experiments with the data from the sugar dissolution analyses. The data for seven different fly ashes are shown in Figure 8.11. This figure shows the experimentally obtained ratio of calcium-to-total pozzolanic material present in the reaction product of the lime/fly ash solids as a function of slurry time. The pozzolanic material is defined here as the amount of silica plus the amount of aluminum and the ratio is defined on a mole basis. The data are very scattered for the shorter slurry times (where the errors for the selective dissolution experiments are relatively high), but are less so for the longer slurry times (where the selective dissolution errors are lower). The analyses indicate that the ratio of calcium to total pozzolan for long slurry times is approximately 1.1 (mol:mol) with a standard deviation of 0.1.

Some of the lime/fly ash solids were also characterized with scanning electron microscopy (SEM) and with powder x-ray diffraction. The SEM data are shown in Figures 8.12 through 8.15 and the data from the x-ray diffraction analyses are tabulated in Appendix B.3. Figures 8.12 and 8.13 show the lime/fly ash solids created from a low-calcium fly ash at slurry times of 0.25 and 8 hours, respectively. The data show the presence of smooth fly ash spheres and rough $Ca(OH)_2$ particles for the 0.25 hour slurry time. The specific surface area for this mixture was 9.7 m^2/g which is fairly close to the value for a dry mixture of fly ash and $Ca(OH)_2$ (7.8 m^2/g). For the 8 hour slurry time, no $Ca(OH)_2$ particles were visible and the fly ash particles were coated with a gel-like substance. This coating is the amorphous, calcium-silicate material which gives the lime/fly ash materials their high surface area (35.3 m^2/g for the solids in Figure 8.13) and is responsible for the solids high reactivity towards SO_2.

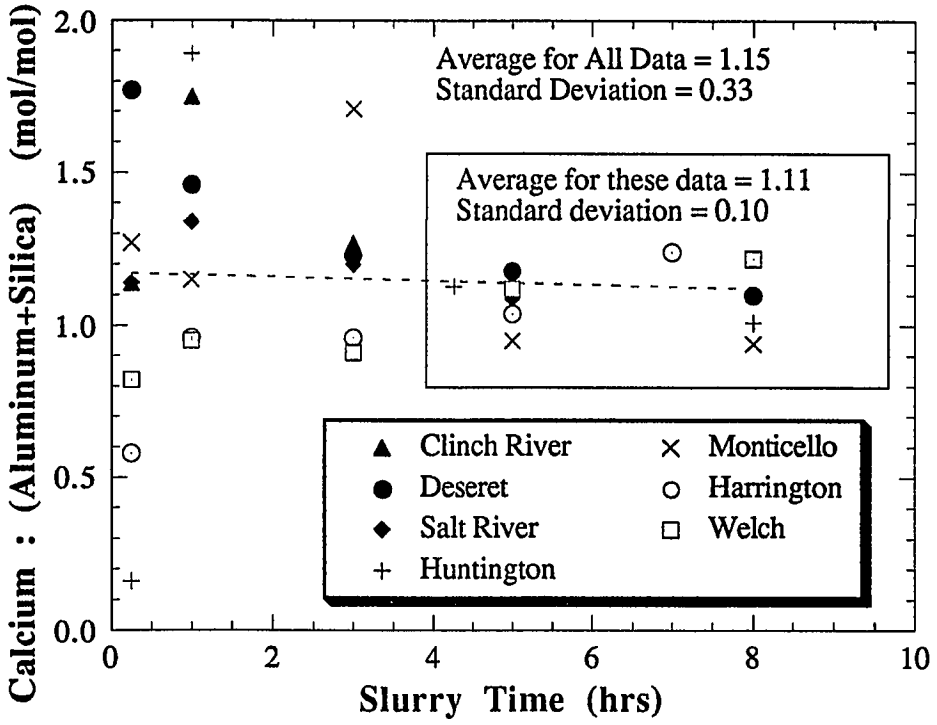

Figure 8.11 Approximation of the chemical composition of the lime/fly ash products.

Slurry Conditions : 35 g $Ca(OH)_2$ + 105 g fly ash + 400 ml H_2O; 92 °C; 700 rpm.

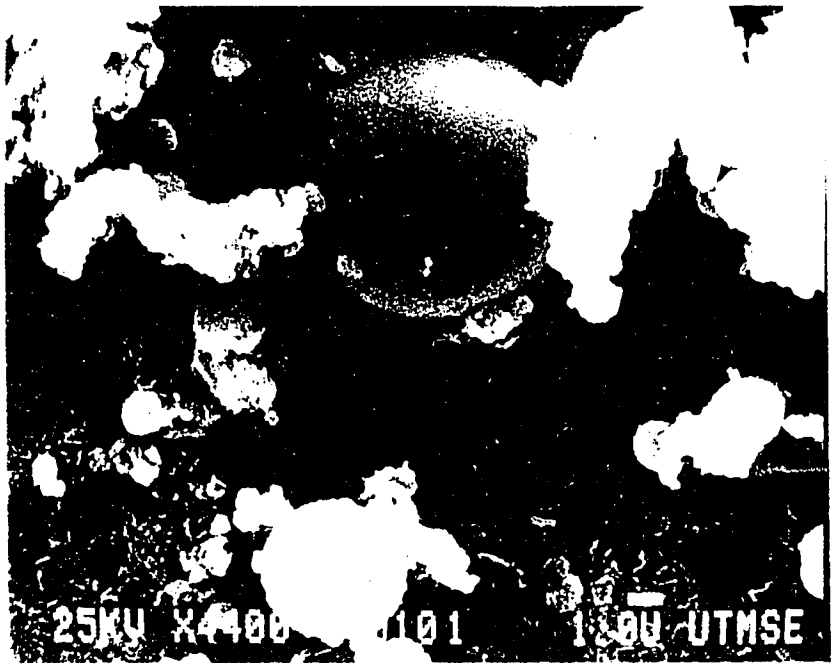

Figure 8.12 SEM photograph of low-calcium fly ash/$Ca(OH)_2$ mixture after 0.25 hours of slurrying.

Slurry Conditions : 35 g $Ca(OH)_2$ + 105 g fly ash + 400 ml H_2O; 92 °C; 700 rpm.

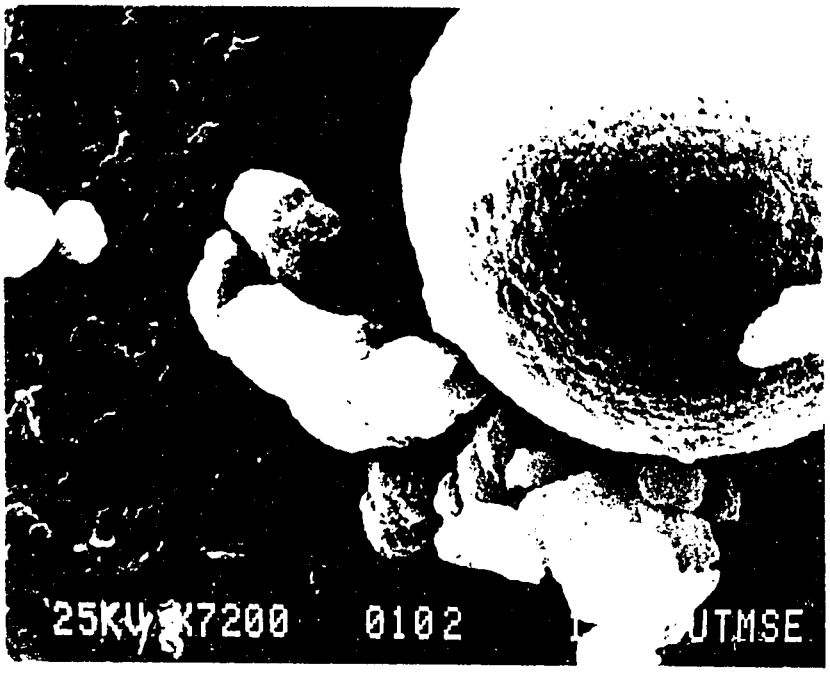

Figure 8.13 SEM photograph of low-calcium fly ash/$Ca(OH)_2$ mixture after 8 hours of slurrying.

Slurry Conditions : 35 g $Ca(OH)_2$ + 105 g fly ash + 400 ml H_2O; 92 °C; 700 rpm.

Figures 8.14 and 8.15 show similar data for a lime/fly ash solid created with a high calcium fly ash. The data for the 0.25 hour slurry time show the presence of both smooth and coated fly ash particles as well as rough $Ca(OH)_2$ particles. The surface area for this mixture was 8.0 m^2/g. For the 8 hour slurry time, all of the fly ash particles are coated with a gel-like substance and the surface area increased to 17.7 m^2/g.

The presence of coated fly ash spheres at short slurry times for the high calcium fly ash gives a qualitative confirmation of the sugar dissolution data which showed that a large fraction of the $Ca(OH)_2$ was consumed in the first hour of reaction. The resulting product material was probably precipitated onto the surface of the fly ash particles as is shown in Figure 8.14.

The data from the x-ray diffraction analyses showed that unreacted $Ca(OH)_2$ was present in most of the lime/fly ash solids (Table 8.2). The maximum observed intensities varied from less than 200 to approximately 400 counts per second. These low intensities indicate that the product solids are generally non-crystalline or are made up of very small crystals which do not give good x-ray diffraction patterns. However, for long slurry times, $Ca_3Al_2(SiO_4)(OH)_8$ (JCPDS No. 38-368) was identified in all of the lime/fly ash solids regardless of the fly ash type. Note that this material has a calcium-to-total pozzolan ratio of 1.0, which is very close to the measured value of 1.1.

8.1.4 Comparing reaction with fly ash dissolution

The data from the selective dissolution experiments were used to calculate a chemical composition for the product solids and to compare the rate of lime/fly ash reaction with the rate of fly ash dissolution. The results from these analyses are presented in Figures 8.16 through 8.18.

Figure 8.16 shows the effect of fly ash type on the molar ratio of silica to aluminum in the lime/fly ash product solids. The data show that, for long times, this ratio is much higher for the solids prepared using the low- and medium-calcium

TABLE 8.2 SUMMARY OF THE X-RAY DIFFRACTION ANALYSES FOR SOME LIME/FLY ASH SOLIDS.

Fly Ash	Slurry Time (hrs)	$Ca(OH)_2$ Intensity[a]	$Ca_3Al_2(SiO_4)(OH)_8$ Probability[b]	Peaks Matched[c]
Clinch River	0.25	100	Very Poor	0/12
Clinch River	1.0	100	Very Poor	0/12
Clinch River	8.0	0	Fair	6/12
Deseret	8.0	20	Fair	5/12
Fayette	1.0	100	Very Poor	0/12
Fayette	2.0	100	Very Poor	0/12
Fayette	3.0	100	Very Good	11/12
Fayette	4.0	100	Very Good	11/12
Fayette	7.0	100	Very Good	11/12
Harrington	1.0	100	Fair	6/12
Harrington	3.0	100	Good	10/12
Harrington	8.0	100	Very Good	11/12
Salt River	8.0	58.5	Good	9/12
Welch	8.0	100	Very Good	11/12

[a] relative intensity of strongest $Ca(OH)_2$ peak (100 = most intense peak)

[b] subjective rating based on the number of peaks matched

[c] number of peaks matched / 12 strongest peaks from JCPDS card no. 38-368

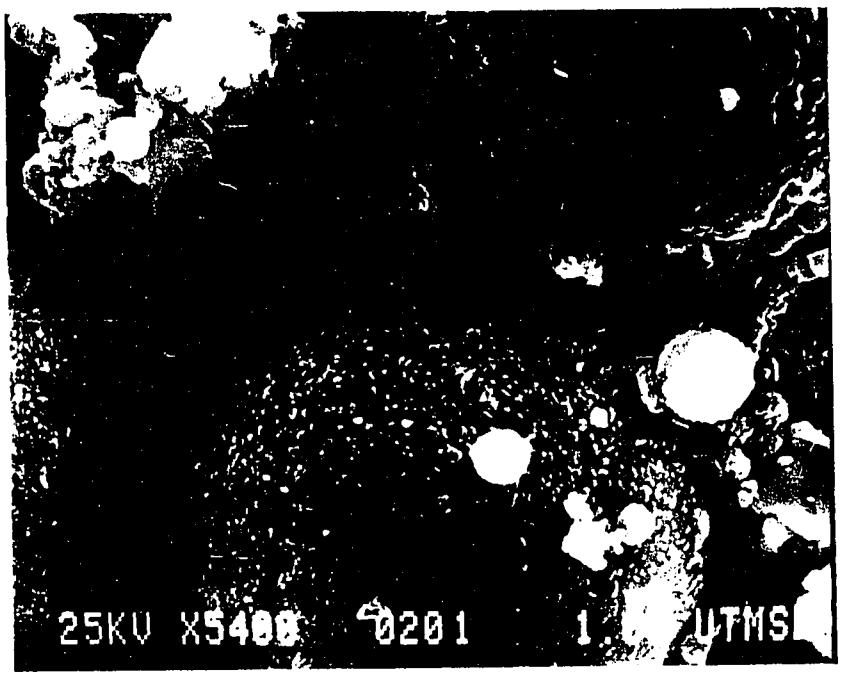

Figure 8.14 SEM photograph of high-calcium fly ash/$Ca(OH)_2$ mixture after 0.25 hours of slurrying.

Slurry Conditions : 35 g $Ca(OH)_2$ + 105 g fly ash + 400 ml H_2O; 92 °C; 700 rpm.

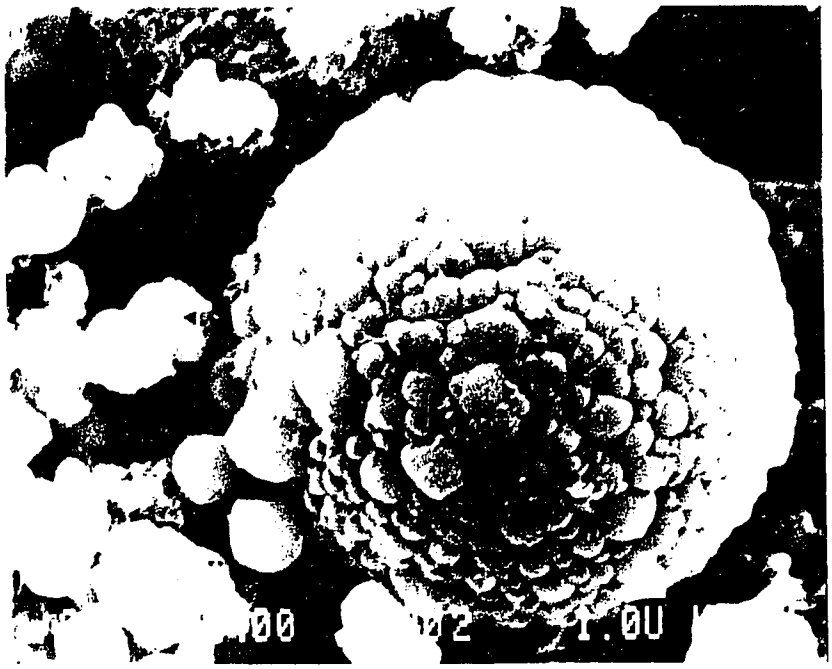

Figure 8.15 SEM photograph of high-calcium fly ash/$Ca(OH)_2$ mixture after 8 hours of slurrying.

Slurry Conditions : 35 g $Ca(OH)_2$ + 105 g fly ash + 400 ml H_2O; 92 °C; 700 rpm.

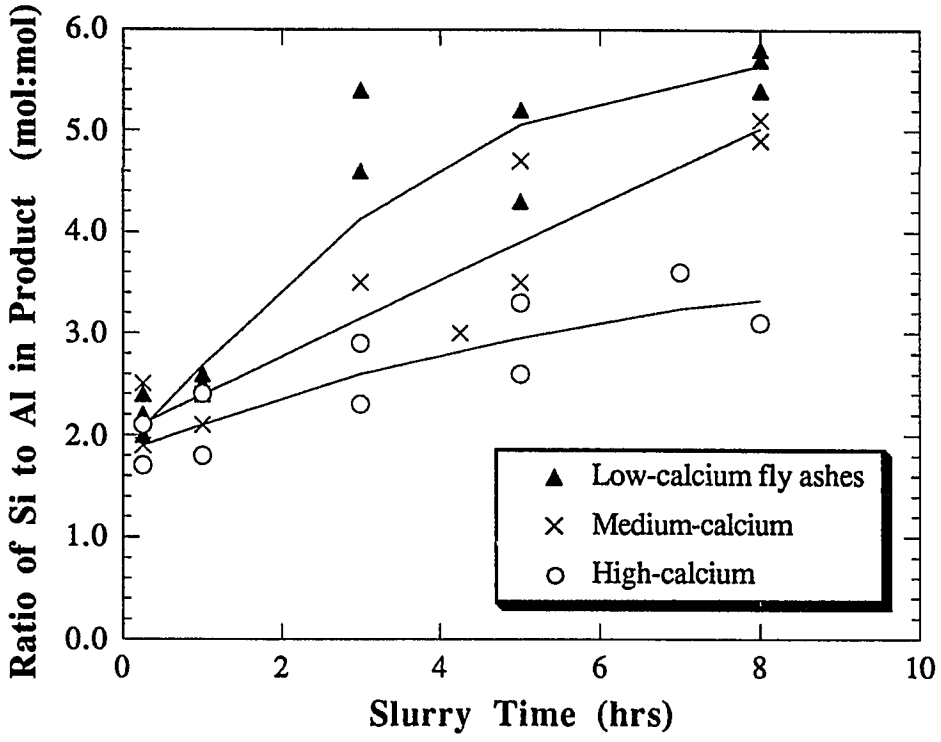

Figure 8.16 Effect of fly ash type on the chemical composition of the lime/fly ash solids. Composition determined by selective dissolution.

Slurry Conditions : 35 g $Ca(OH)_2$ + 105 g fly ash + 400 ml H_2O; 92 °C; 700 rpm.

fly ashes (5.5:1, 5.0:1) than for those materials prepared using the high-calcium fly ash (3:1). This effect of fly ash type may arise because the molar ratio of silica to alumina in the fly ashes is a function of fly ash type. The average ratios for the types of fly ashes tested are 1.7, 2.4, and 1.2 for the low-, medium-, and high-calcium fly ashes, respectively. Note that the experimentally determined ratio is higher than these average ratios for all the fly ashes tested (at long slurry times). A surprising result is that the experimentally determined ratio is not even close to the value present in the solids identified by x-ray diffraction (3.0 - 5.5 vs 0.5, respectively). This indicates that the crystalline material $Ca_3Al_2(SiO_4)(OH)_8$ is not the major product of the lime/fly ash reaction, even though it seems to be present in every reaction product. The results from the selective dissolution experiments suggest that the major reaction product is amorphous and contains much more silica than aluminum.

Figures 8.17 and 8.18 compare the data from the fly ash dissolution experiments (no precipitation possible) with those from the selective dissolution experiments (precipitation has occurred). For short slurry times, the fraction of silica that dissolved in the fly ash dissolution experiments was much greater than the fraction of silica that reacted to form lime/fly ash materials. For longer slurry times, however, the two fractions were approximately equal. This shows that the precipitation of calcium-silicate and calcium-aluminate materials on the surface of the fly ash particles retards the dissolution of the fly ash and therefore slows the production rate of lime/fly ash solids. The data also show that the conversion of silica is much greater than the conversion of alumina for the "reaction" experiments, but the reverse is true for the "dissolution" experiments. Also note that the amount of aluminum which is present in the lime/fly ash solids at short slurry times is much higher for the high-calcium fly ash than for the low-calcium fly ash.

The above results suggest that the dissolution of the fly ash, per se, is not the only limiting step of the reaction. A significant limitation seems to be the diffusion of the dissolved fly ash species through the product solids which coat the fly ash particles.

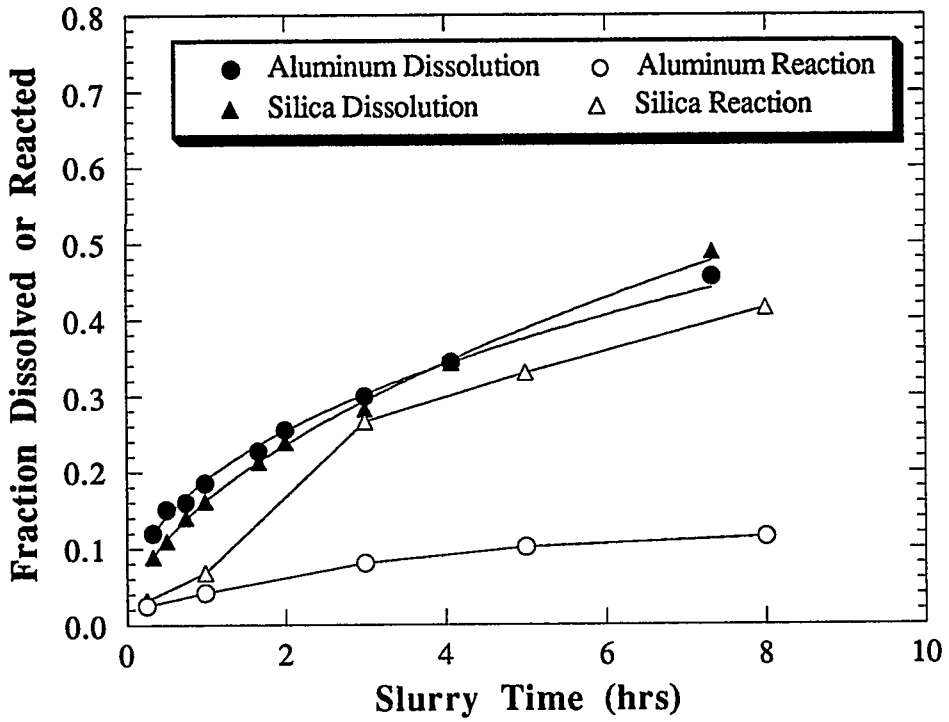

Figure 8.17 Comparison of reaction with dissolution for a low-calcium fly ash.

Slurry Conditions : 35 g $Ca(OH)_2$ + 105 g fly ash + 400 ml H_2O; 92 °C; 700 rpm.

Dissolution : 1.25 g fly ash/liter, 90 °C, 0.05 M NaOH 5.0 g Na_2EDTA/l.

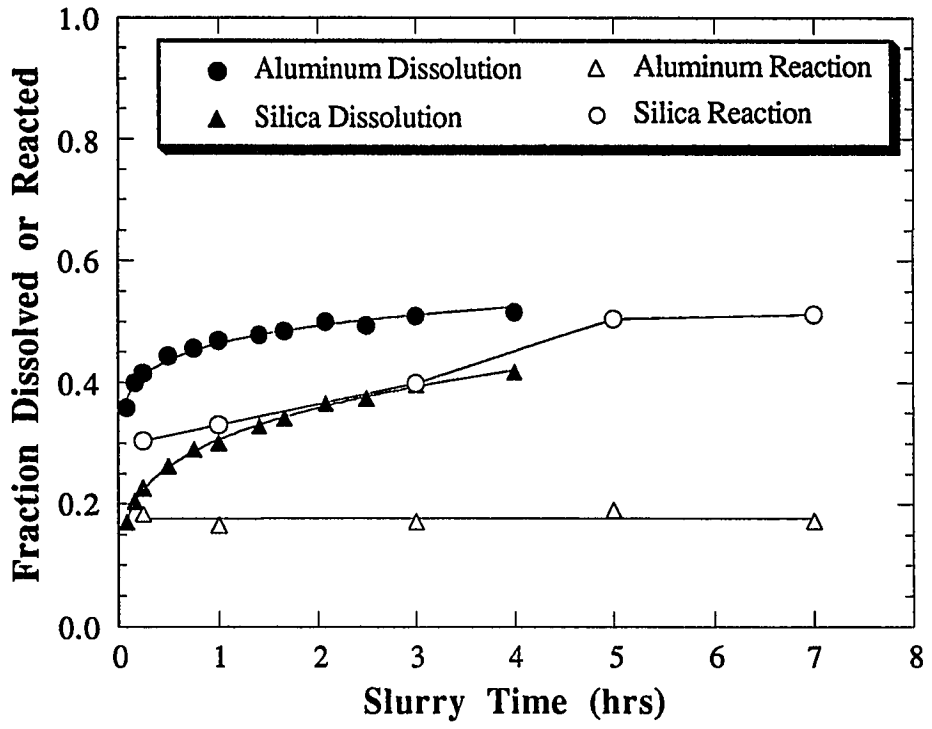

Figure 8.18 Comparison of reaction with dissolution for a high-calcium fly ash.

Slurry Conditions : 35 g $Ca(OH)_2$ + 105 g fly ash + 400 ml H_2O; 92 °C; 700 rpm.

Dissolution : 1.25 g fly ash/liter, 90 °C, 0.05 M NaOH 5.0 g Na_2EDTA/l.

8.2 Effect of recycle materials

One of the major objectives of this work was to determine the effect of recycle materials on the reaction of lime with fly ash. This topic is important because, for commercial systems, recycle materials are likely to be present in the lime/fly ash slurry tank and it is not known how the presence of these materials affects the reactivity of the lime/fly ash materials. Results have already been presented for a large number of experiments which studied the effect of recycle materials on the reaction of $Ca(OH)_2$ with $Al(OH)_3$ and silica fume (Chapter VII). The experiments described in this section were performed using fly ash to determine if the observed effects of the recycle materials on the reaction of $Ca(OH)_2$ with $Al(OH)_3$ also occur in the lime/fly ash system.

Most of the experiments studying the effect of the recycle materials were performed using high-calcium fly ashes because these ashes contain a large fraction of reactive aluminum which is able to interact with the sulfur species of the recycle materials. These experiments focused on the ability of gypsum to retard the reaction between $Ca(OH)_2$ and the aluminum content of the fly ash. Several experiments were also performed where $CaSO_3 \cdot 0.5\ H_2O$ was added to slurries of low- and high-calcium fly ashes with $Ca(OH)_2$. This work is significant because $CaSO_3 \cdot 0.5\ H_2O$ is likely to constitute a major fraction of the material present in the recycle solids.

8.2.1 Effect of gypsum

Figure 8.19 shows the solution composition for slurries of a high-calcium fly ash and $Ca(OH)_2$ that contained either gypsum or $CaSO_3 \cdot 0.5\ H_2O$. The data show that the presence of $CaSO_3 \cdot 0.5\ H_2O$ does not markedly influence the pH or the dissolved calcium concentration in the slurry solution. However, the presence of gypsum caused the dissolved calcium concentration to start and remain much higher and caused the pH to remain lower than the values for the base-case slurry.

These effects of gypsum on the solution behavior were also observed for two different high-calcium fly ashes at three different gypsum loadings.

The above results are similar to the results from the reagent chemical experiments (Chapter VII) and result, in part, from the relatively high solubility of the gypsum compared to $Ca(OH)_2$ and $CaSO_3 \cdot 0.5\ H_2O$.

The presence of recycle materials in the high-calcium fly ash slurry had various effects on the properties of the lime/fly ash solids produced in those slurries. Figure 8.20 shows that the presence of gypsum in the slurry did not affect the rate or extent of the reaction between $Ca(OH)_2$ and fly ash. This result is surprising because gypsum should inhibit the reaction rate of the aluminum species of the fly ash and therefore slow the rate of reaction between $Ca(OH)_2$ and fly ash. Gypsum also decreases the solution pH which should decrease the rate of fly ash dissolution and, therefore, the rate of lime/fly ash reaction.

However, the effects of gypsum were observed in the development of the specific surface areas and reactivities of the lime/fly ash solids. Figures 8.21 and 8.22 show the surface area development for lime/fly ash solids created using three different high-calcium fly ashes with and without gypsum present in the slurry. The data show that, in every case, the surface area of the lime/fly ash solids is higher when gypsum is present in the slurry.

The effects of gypsum on the properties of the lime/fly ash solids were also clearly evident in the reactivities of the lime/fly ash solids. Figure 8.23 shows the reactivity of the aforementioned lime/fly ash solids as determined in a sand-bed reactor. The data show that the solids that were produced in slurries containing gypsum were much more reactive towards SO_2 than were the base-case solids.

The above data agree with the hypothesis that the presence of gypsum in the slurry inhibits the formation of low surface area, unreactive, calcium-aluminate materials. The gypsum presumably functions by reacting with the aluminum present in some of the fly ash particles to form an impenetrable barrier to fly ash

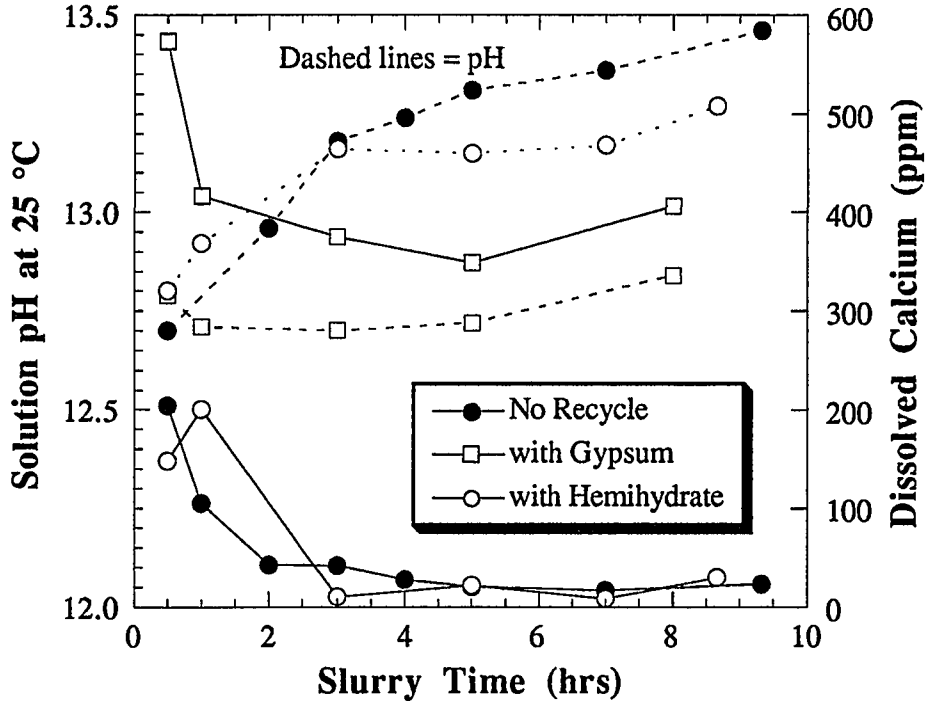

Figure 8.19 Effect of gypsum on the solution composition of lime/fly ash slurry for a high calcium fly ash.

Slurry Conditions : 105 g Fayette fly ash + 35 g $Ca(OH)_2$ + 400 ml H_2O; 92 °C; 700 rpm.

"with Gypsum" = 46.7 g $CaSO_4 \cdot 2H_2O$ added to slurry

"with Hemihydrate" = 35.0 g $CaSO_3 \cdot 0.5H_2O$ added to slurry

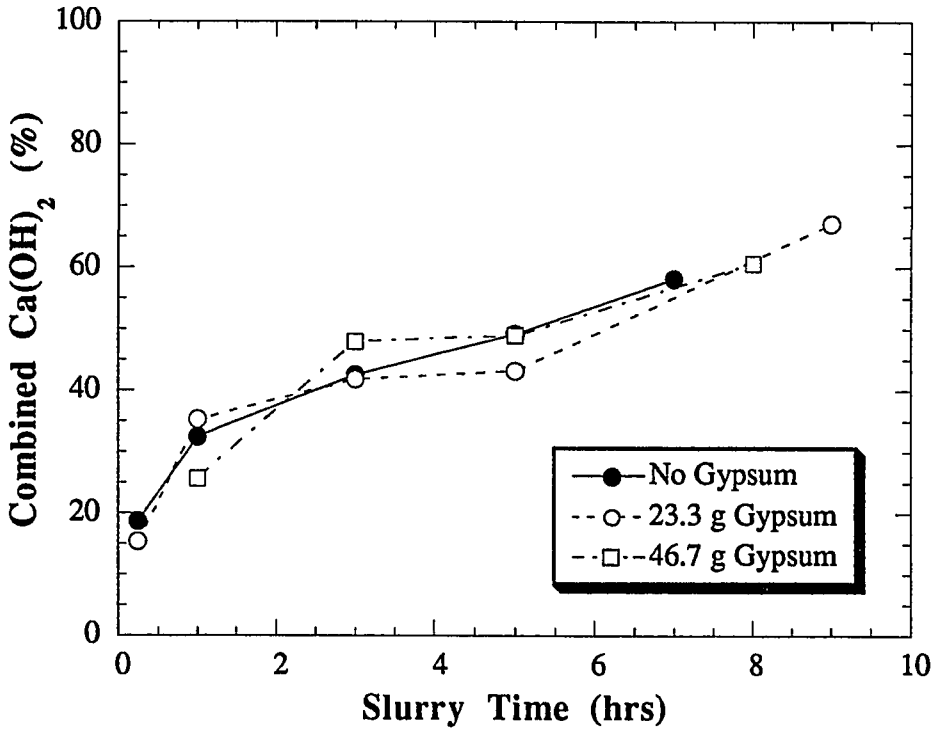

Figure 8.20 Effect of gypsum on the reaction between fly ash and $Ca(OH)_2$.

Slurry Conditions : 105 g Harrington fly ash + 35 g $Ca(OH)_2$ + 400 ml H_2O; 92 °C; 700 rpm.

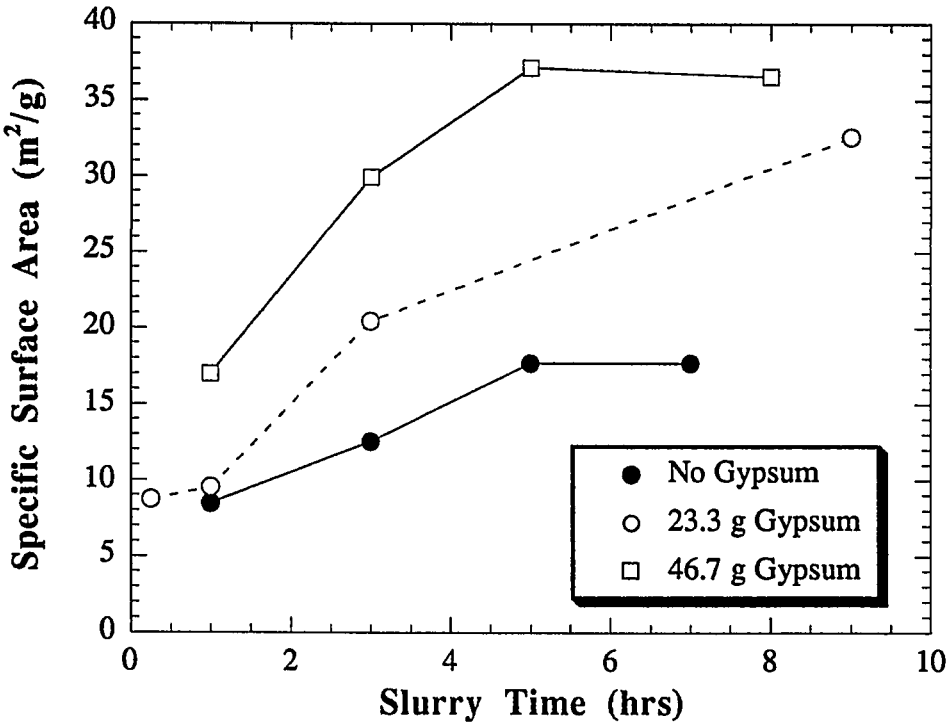

Figure 8.21 Effect of gypsum on the surface areas of lime/fly ash solids.

Slurry Conditions : 105 g Harrington fly ash + 35 g $Ca(OH)_2$ + 400 ml H_2O; 92 °C; 700 rpm.

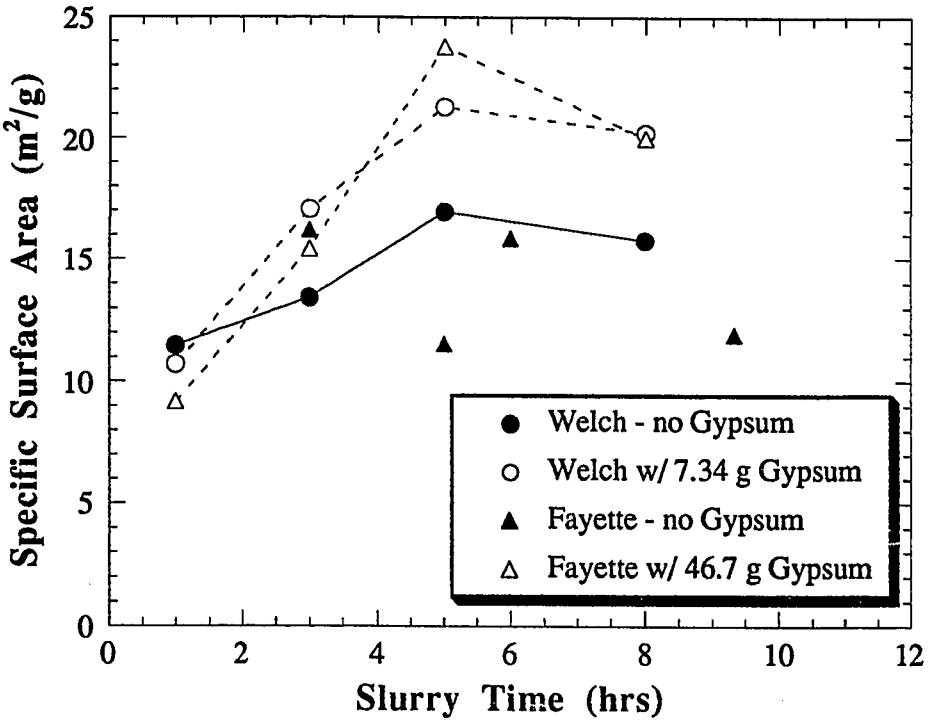

Figure 8.22 Effect of gypsum on the surface areas of lime/fly ash solids.

Slurry Conditions : 105 g high-calcium fly ash + 35 g $Ca(OH)_2$ + 400 ml H_2O; 92 °C; 700 rpm.

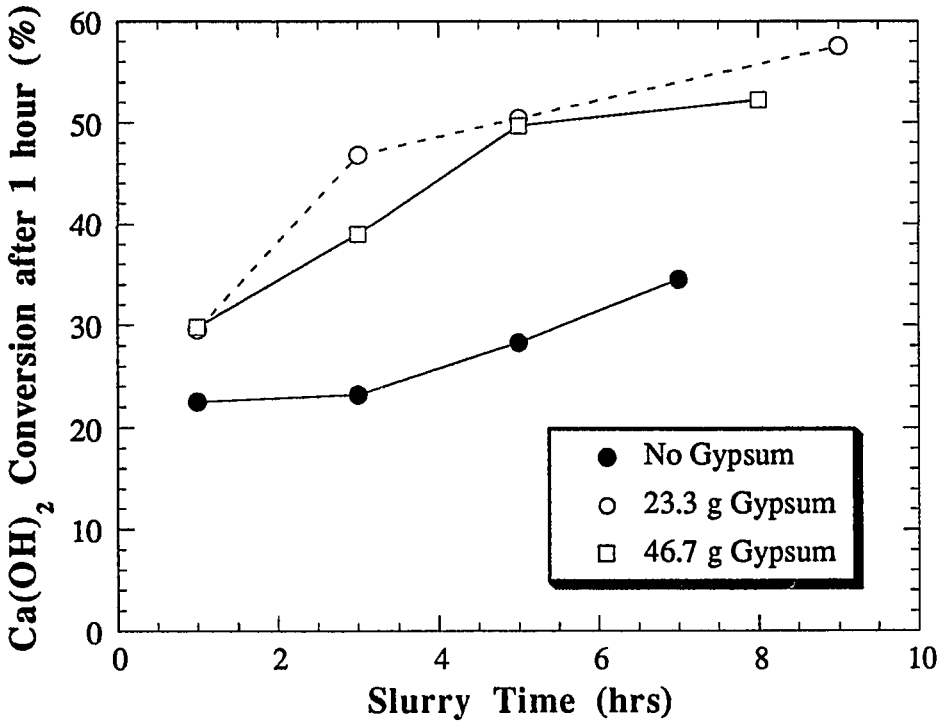

Figure 8.23 Effect of gypsum on the reactivity of lime/fly ash solids towards SO_2.

Slurry Conditions : 105 g Harrington fly ash + 35 g $Ca(OH)_2$ + 400 ml H_2O; 92 °C; 700 rpm.

dissolution on the surface of the fly ash particle. Therefore, the gypsum reacts selectively with the particles containing reactive aluminum while ignoring the other fly ash particles.

8.2.2 Effect of calcium sulfite hemihydrate

The effect of calcium sulfite hemihydrate ($CaSO_3 \cdot 0.5H_2O$) on the reaction of $Ca(OH)_2$ with fly ash was investigated using a low-calcium fly ash. In these experiments, laboratory-produced $CaSO_3 \cdot 0.5H_2O$ was slurried with Clinch River fly ash and $Ca(OH)_2$ at weight ratios of 3/1/0, 3/1/0.5, and 3/1/1 (g fly ash/g $Ca(OH)_2$/g $CaSO_3 \cdot 0.5H_2O$). The collected solids were dried and characterized using the methods described in Chapter V. The results are presented in Figure 8.24

Figure 8.24 shows that $CaSO_3 \cdot 0.5H_2O$ has a beneficial effect on the solids reactivity towards SO_2 for long slurry times, but for short slurry times there is no noticeable effect. The beneficial effect at long slurry times increases with the amount of $CaSO_3 \cdot 0.5H_2O$ present in the slurry. The data from the selective dissolution experiments shows that the presence of $CaSO_3 \cdot 0.5H_2O$ has no effect on the conversion of the silicon in the fly ash (not shown). This is expected since the presence of $CaSO_3 \cdot 0.5H_2O$ does not affect the pH of the slurry and therefore does not affect the fly ash dissolution rate.

The beneficial effect of the $CaSO_3 \cdot 0.5H_2O$ is probably not due to the $CaSO_3 \cdot 0.5H_2O$ itself, but to the small amount of gypsum which was probably present in the laboratory-produced $CaSO_3 \cdot 0.5H_2O$. It is very difficult to avoid a small amount of oxidation of sulfite to sulfate when these solids are produced in the laboratory and the small amount of gypsum present in the $CaSO_3 \cdot 0.5H_2O$ probably inhibited the formation of a small amount of calcium-aluminates. This inhibition probably increased the product solids reactivity towards SO_2.

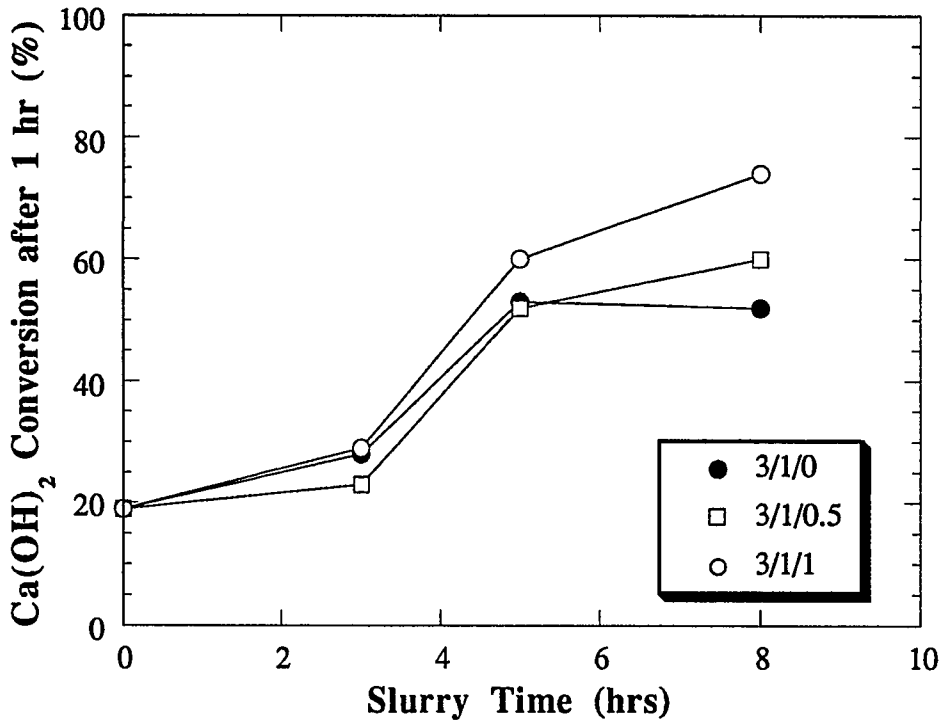

Figure 8.24 Effect of $CaSO_3 \cdot 0.5H_2O$ on lime/fly ash solids reactivity towards SO_2. Clinch River fly ash.

Slurry Conditions : 35 g $Ca(OH)_2$ + 105 g fly ash + 400 ml H_2O; 92 °C; 700 rpm.

3/1/1 = 3g fly ash/1 g $Ca(OH)_2$ /1 g $CaSO_3 \cdot 0.5H_2O$

Test Conditions : 66 °C; 51% R.H.; 4.6 l gas/min; 7 % O_2; 10 % CO_2; 83 % N_2; 450 ppm SO_2.

8.3 Effect of fly ash grinding

Grinding a fly ash before reacting it with $Ca(OH)_2$ has been shown to increase the reactivity of the resulting lime/fly ash solids towards SO_2 (Peterson et al., 1988). Experimental results presented in Chapter VI showed that the grinding process increases the dissolution rate of silica from the fly ash. This evidently increases the production rate of calcium silicates and therefore the reactivity of the lime/fly ash solids. Samples of ground low-calcium fly ash were slurried with $Ca(OH)_2$ to create lime/fly ash materials in order to complement the results from the fly ash dissolution experiments of Chapter VI. The results from these experiments are shown in Figures 8.25 through 8.29.

Figures 8.25 and 8.26 show the effect of fly ash grinding on the rate of reaction between fly ash and $Ca(OH)_2$. Figure 8.25 shows that the initial surface area of the fly ash did not markedly affect the rate or extent of the reaction between fly ash and $Ca(OH)_2$ when the fly ash loading was 2:1 (defined as grams of fly ash:g $Ca(OH)_2$ originally present in the slurry). However, when the fly ash loading was 3:1, the ground fly ash generally consumed more of the $Ca(OH)_2$ present in the slurry (Figure 8.26). These results are surprising because the data from the fly ash dissolution experiments showed that the dissolution rate of silica from the fly ash increased dramatically when the fly ash was ground from 1.9 to 26 m^2/g (Chapter VI).

The data from the surface area of the lime/fly ash solids is in much better agreement with the data from the fly ash dissolution experiments. Figure 8.27 shows the effect of fly ash grinding on the surface area of the lime/fly ash solids which were created at a fly ash loading of 2:1. The data show that the surface area of the product solids was much higher when ground fly ash was used to create the solids instead of unground fly ash, although the improvement from using the mildly-ground fly ash (5.0 m^2/g) was marginal. Figure 8.28 shows that the mildly-ground fly ash produced solids with a much higher surface area if the fly ash loading was increased to 3:1.

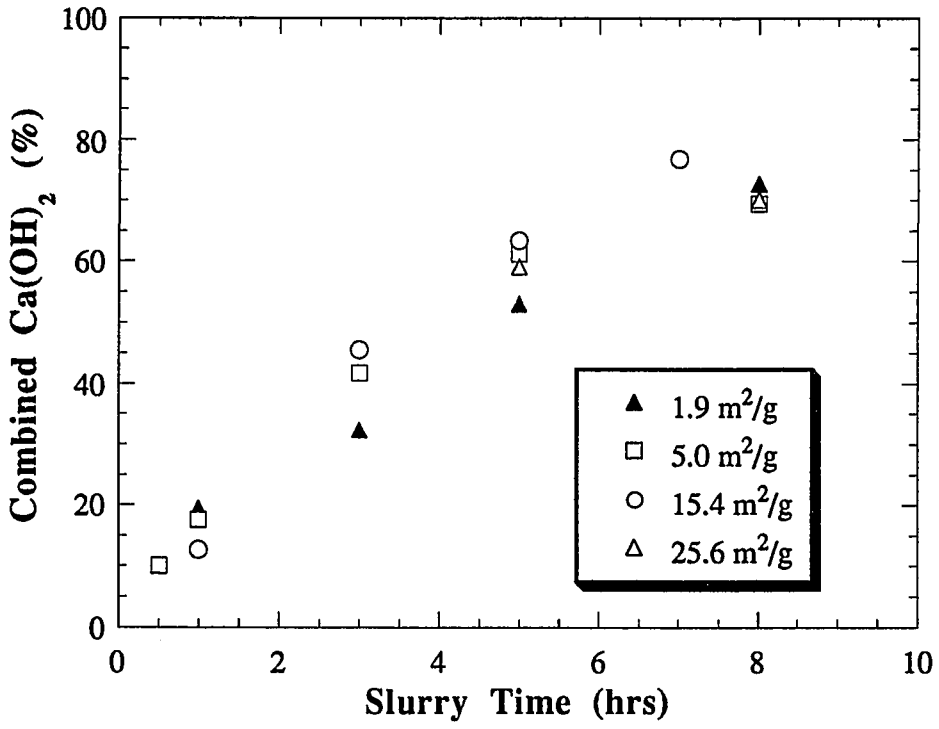

Figure 8.25 Effect of fly ash grinding on the reaction of fly ash with $Ca(OH)_2$.

Slurry Conditions : 25 g $Ca(OH)_2$ + 50 g fly ash + 400 ml H_2O;
92 °C; 700 rpm. Clinch River Fly Ash.

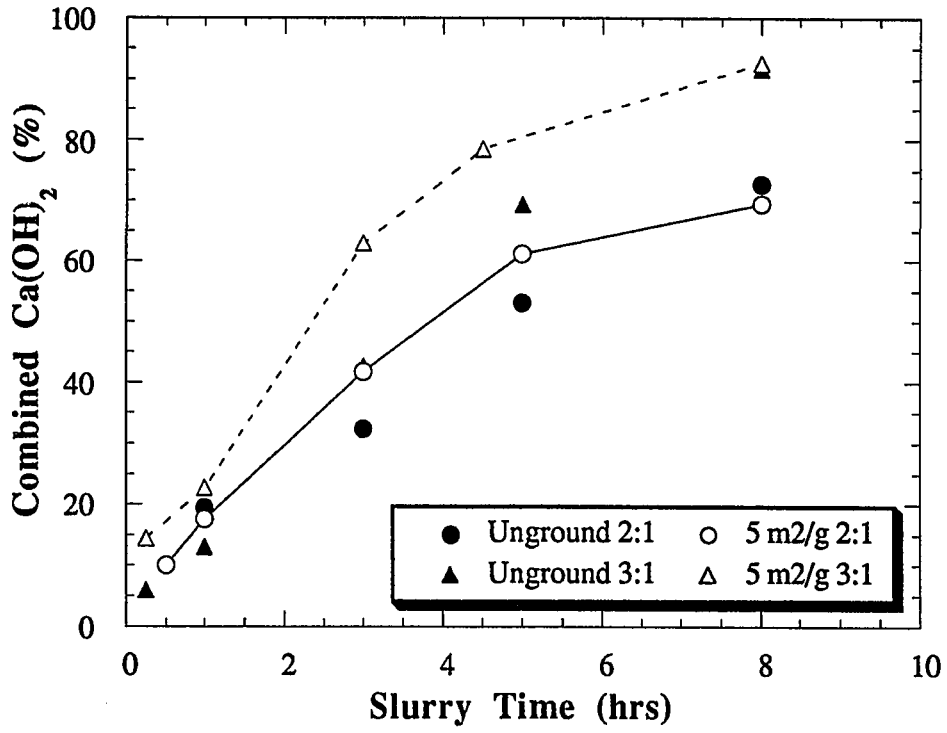

Figure 8.26 Effect of fly ash grinding on the reaction of fly ash with $Ca(OH)_2$.

Slurry Conditions : 25 g $Ca(OH)_2$ + 50 g fly ash + 400 ml H_2O; 92 °C; 700 rpm. Clinch River Fly Ash.

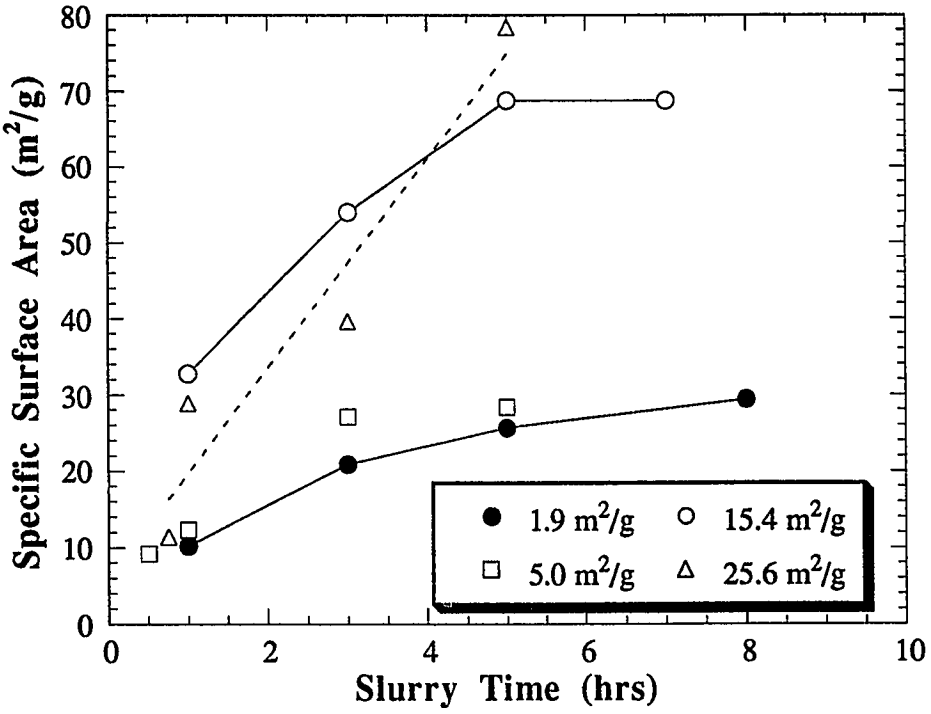

Figure 8.27 Effect of fly ash grinding on the surface area of the lime/fly ash solids.

Slurry Conditions : 25 g $Ca(OH)_2$ + 50 g fly ash + 400 ml H_2O; 92 °C; 700 rpm. Clinch River Fly Ash.

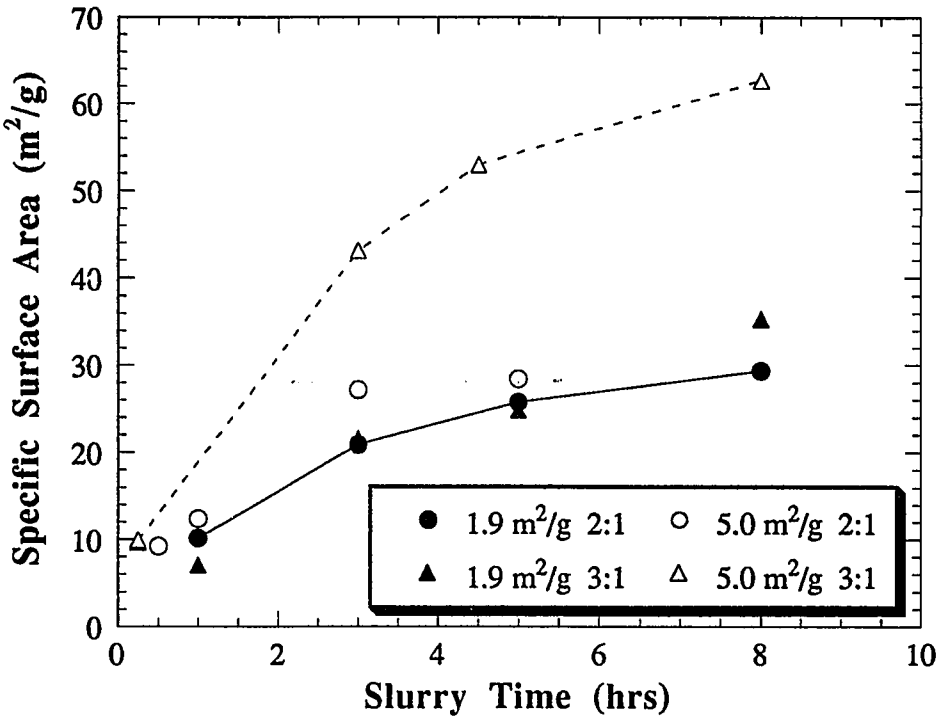

Figure 8.28 Effect of fly ash grinding on the surface area of the lime/fly ash solids.

Slurry Conditions : 25 g $Ca(OH)_2$ + 50 g fly ash + 400 ml H_2O; 92 °C; 700 rpm. Clinch River Fly Ash.

The solids created using the ground fly ash solids were tested for reactivity towards SO_2 in a sand-bed reactor. Figure 8.29 shows that the solids created using the ground fly ash were much more reactive towards SO_2 than were the solids created using the unground fly ash.

The above data show that the grinding of fly ash facilitates the production of lime/fly ash solids. The data presented in Chapter VI indicated that the reason for this improvement relates to the increased surface area of the ground fly ash : higher surface area equals higher silica dissolution rates. However, the small particle size of the ground fly ash is particularly important because of the retarding effect of the lime/fly ash product layer on the fly ash dissolution (Section 8.1.4). The relative effect of this layer would be greatly decreased when the fly ash is ground before reacting it with $Ca(OH)_2$. Both of these effects improve the production of lime/fly ash materials.

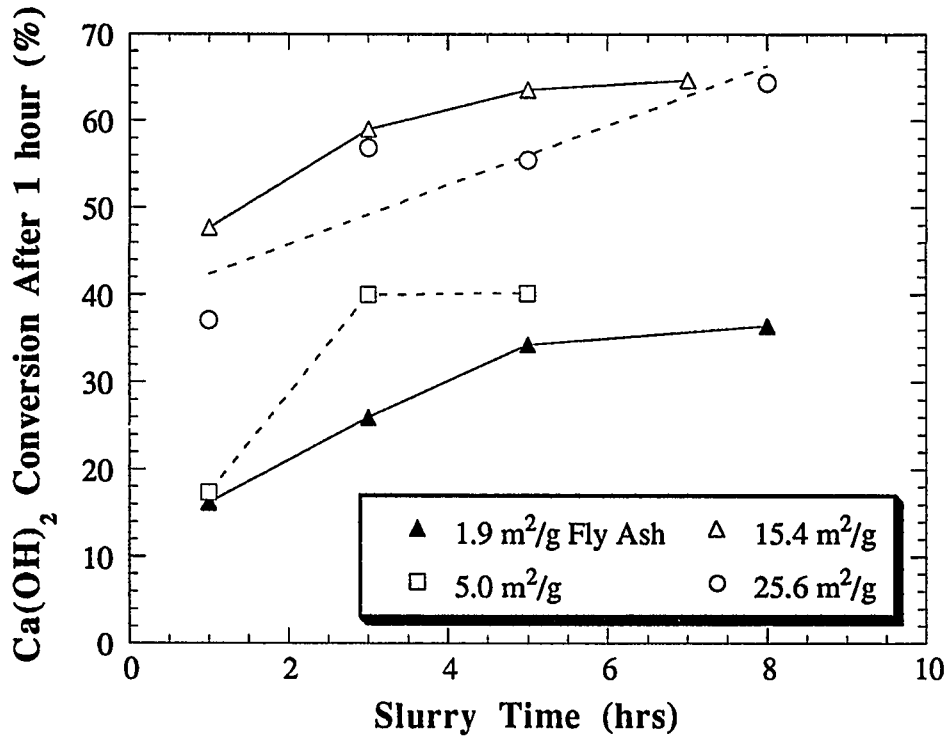

Figure 8.29 Effect of fly ash grinding on the reactivity of the lime/fly ash solids towards SO_2.

Slurry Conditions : 25 g $Ca(OH)_2$ + 50 g fly ash + 400 ml H_2O; 92 °C; 700 rpm. Clinch River Fly Ash.

Chapter IX

Summary, Conclusions, and Recommendations

9.1 Summary

Experimental work was performed to determine the chemistry of the reactions taking place when hydrated lime is mixed with fly ash in water at high temperature. Although some of these reactions have been studied extensively by cement and concrete chemists, their experimental conditions of low temperature, low water-to-solids ratio, long reaction times, and non-agitation do not give adequate information about the reactions of interest which occur at high temperatures and relatively short reaction times in a well-mixed reactor.

The current experimental work can be broken down into three general sections. One of these sections investigated the dissolution of fly ash alone, that is, the reaction of calcium with the silica and aluminum of the fly ash was not allowed to occur. In this way, it was possible to study the effects of various operational parameters on the dissolution rate of the fly ash without the added complications of a precipitated product layer on the surface of the fly ash. This work is significant because the dissolution rate of the fly ash is the rate limiting step of the reaction of hydrated lime with fly ash.

Another major section of the experimental work used reagent chemicals to determine the relative importance of the silica and aluminum content of the fly ash. Reagent chemicals were used instead of fly ash to facilitate the interpretation of the major chemical reactions that take place in the lime/fly ash system. A sizable portion

of this section investigated the effects of recycle materials on the calcium-silica and calcium-aluminum reactions.

Finally, a number of experiments were performed using fly ashes obtained from coal-fired power plants to validate some of the results obtained from the fly ash dissolution and reagent chemical experiments. This work examined the effects of fly ash type and source, the fly ash particle size, and the effects of the presence of recycle materials on the hydrated lime/fly ash reaction.

9.2 Conclusions

Although some of the conclusions of this study relied on the results from more than one of the aforementioned sections, the conclusion section is broken into sub-sections for clarity.

9.2.1 Fly ash dissolution experiments

The fly ash dissolution experiments showed that there are basically two types of fly ash : low-calcium and high-calcium. The two medium-calcium fly ashes behaved like the low-calcium fly ashes. The low-calcium fly ashes dissolved uniformly, and released silica and aluminum into the solution at equal rates. The high-calcium fly ashes dissolved incongruently. A substantial fraction of the high-calcium fly ash dissolved instantly and the aluminum was released into solution to a greater extent than the silica.

For experiments using a low-calcium fly ash, the silica dissolution rate was found to be approximately first order in the hydroxide concentration. This compares favorably with data from previous researchers who studied the dissolution of pure silica particles, and suggests that the structure of the glass present in the low calcium fly ash is similar to that for amorphous silica.

For high-calcium fly ash the order of reaction was approximately 2.3 for the dissolution of silica from the fly ash. This data, along with x-ray diffraction data, suggest that the structure of the glass is quite different for the high-calcium fly ash

than it is for the low-calcium fly ash. The glass present in the high-calcium fly ash contains a large amount of calcium and sodium atoms which shorten the silica-aluminate chains which are present in fly ash. These shortened chains dissolve much faster and are more sensitive to the hydroxide concentration in the slurry than the longer chains present in the low-calcium fly ash.

The fly ash dissolution experiments also showed that the activation energy for silica dissolution from the low-calcium fly ash was 20.3 kcal/mol. This compares favorably with previous data for the dissolution of quartz and amorphous silica powders in alkali (18 to 26.2 kcal/mol).

Several fly ash dissolution experiments were performed with samples of ground fly ash. These experiments showed that the silica dissolution rate was a function of the fly ash particle size, but the aluminum dissolution rate was not. The data also showed that the fly ash must be ground finely to affect the silica dissolution rate. This latter result was in contrast to the results from the reactivity experiments using lime/fly ash solids created from ground fly ash. This data showed that all of the ground fly ashes, even the mildly ground fly ash, produced lime/fly ash solids which were substantially more reactive than those produced from the unground fly ash.

9.2.2 Reagent chemical experiments

The experiments using reagent chemicals to investigate the relative importance of the silica and aluminum contents of the fly ash produced very interesting results. The calcium-aluminates that were formed had a very low surface area and were unreactive towards SO_2. These were identified using x-ray diffraction as $Ca_3Al_2(OH)_{12}$ which, according to other researchers, are the only stable compounds in the calcium-aluminum-water system for temperatures below 225 °C.

The calcium-silicates were found to be markedly different from the calcium-aluminates. The silicates had a very high surface area and were very reactive

towards SO_2. Because these products were amorphous, it was not possible to identify them with x-ray diffraction. These solids were identified by combining data from the selective dissolution experiments with data from the sugar dissolution analyses. This procedure showed that the molar ratio of calcium-to-silica in the product solids was 1.34 (average of 4 analyses, standard deviation of 0.34). These data suggest that the calcium silicates were type I tobermites (i.e. amorphous calcium silicates with a calcium-to-silica ratio of less than 1.5).

The experiments using reagent chemicals also provided very interesting results on the effects of the presence of recycle materials in the slurry. These experiments were focused on the interaction of calcium with aluminum, since the sulfur species is known to influence this reaction. The data showed that calcium sulfite hemihydrate had only a minor effect on the calcium-aluminum reaction. The products were still low surface area, crystalline materials and the reaction still went to completion, but the reaction product was changed. The new reaction product was not identified by x-ray diffraction because the JCPDS files have no x-ray data for calcium-aluminum-sulfite materials.

The presence of gypsum in the slurry had a dramatic effect on the reaction of calcium with aluminum and on the reactivity of the resulting solids towards SO_2. The presence of gypsum dramatically reduced the extent of reaction between $Ca(OH)_2$ and $Al(OH)_3$, presumably by forming calcium-monosulfo-aluminate materials on the surface of the $Al(OH)_3$ particles to retard their dissolution. The gypsum did not affect the reaction between $Ca(OH)_2$ and silica fume, so it served as an additive to selectively inhibit the undesirable reaction of $Al(OH)_3$ with $Ca(OH)_2$.

9.2.3 Lime/fly ash experiments

This study broadened the total number of fly ashes tested for the production of lime/fly ash materials from seven to sixteen. With the large number of fly ashes tested, the effects of fly ash type were evident. The surface areas of the lime/fly ash materials created using low-calcium fly ashes were higher than those created using high-calcium fly ashes. The highly reactive aluminum content of the high-calcium fly ashes is responsible for the production of these lower surface area materials.

This study showed a clear effect of fly ash type on the reactivity of the lime/fly ash solids towards SO_2. If the calcium present in the fly ash was considered available for reaction with SO_2, the data clearly showed that low-calcium fly ashes produced solids which were much more reactive than the solids produced from high-calcium fly ashes. However, since some of the calcium present in the high-calcium fly ash is able to react with SO_2, there was only a minor effect of fly ash type when the lime/fly ash solids were compared on a weight basis.

The lime/fly ash experiments also confirmed the effects of recycle materials observed in the reagent chemical experiments. That is, the addition of gypsum to slurries of high-calcium fly ash and $Ca(OH)_2$ increased the surface areas and the reactivities of the resulting lime/fly ash solids. The presence of calcium sulfite hemihydrate changed the reaction product, but did not significantly increase the surface areas or the reactivities of the resulting lime/fly ash solids.

Combination of the data from the sugar dissolution analyses with those from the selective dissolution experiments allowed characterization of the lime/fly ash solids. For long slurry times, the ratio of calcium-to-total pozzolanic material was found to be 1.1 with a standard deviation of 0.1, regardless of the type of fly ash. The total pozzolanic material is defined here as the total amount of silica plus alumina and the ratio is defined on a mole basis. Although the ratio was independent of fly ash type, the relative amounts of aluminum and silica contained in the product solids were not. The solids created with the high-calcium fly ash

were richer in alumina than the solids created with the low- and medium-calcium fly ashes.

A comparison of the data from the selective dissolution experiments with the data from the fly ash dissolution experiments revealed that the lime/fly ash product layer, which forms on the surface of the fly ash particles, greatly retards the dissolution of aluminum and silica from the fly ash particle. This indicates that fly ash dissolution, per se, is not the only limiting step involved in the production of lime/fly ash materials.

9.3 Recommendations

One of the major limitations when studying the reaction of fly ash with $Ca(OH)_2$ is the diverse inter-particle nature of the fly ash material. As was discussed in Chapter III, the chemical and mineralogical compositions of the individual fly ash particles vary with particle density, which allows one to classify the fly ash. Previous researchers have also shown that the glass composition is markedly different for the different density-classified fractions. It would be interesting to separate several fly ashes into different fractions and test them for the fly ash dissolution rate and for their reactivity towards $Ca(OH)_2$. This would shed some light on which components of the fly ash glass are most desirable for the production of lime/fly ash solids.

Probably the most interesting result of this study is the effect of gypsum on the formation of the lime/fly ash solids. However, the recycle streams of the duct-injection process using lime/fly ash solids would contain mostly calcium sulfite materials and only a small amount of calcium sulfate materials. It would be interesting to determine how much oxidation of the sulfite is necessary to initiate the dramatic effect of gypsum on the reactivity of the lime/fly ash solids. The best way to approach this question would be to use actual recycle materials - either from a spray dryer system, or from a lime/fly ash demonstration pilot plant.

Another interesting research area pertaining to recycle concerns the availability of the silica present in the recycle materials. A portion of these recycle materials will be sent to the lime/fly ash slurry tank where they can react with the fresh lime slurry. If one assumes that the calcium silicate solids react with SO_2 to form calcium sulfite and silicic acid, the recycle materials should be a good source of reactive silica because silicic acid is very soluble at high pH. It would therefore be interesting to create "true" recycle materials by reacting lime/fly ash materials with SO_2 and then testing the resulting solids in the fly ash dissolution experiments and the lime/fly ash reaction experiments.

Since the presence of a product layer on the surface of the fly ash particles seems to limit the dissolution rate of silica from the fly ash, it would be interesting to test additives which would "open" the product layer to keep the fly ash dissolution rate high.

An alternative method would be to react $Ca(OH)_2$ with fly ash in a ball-mill instead of a slurry tank. Lea (1971) reports that the use of a ball-mill can reduce the time for complete hydration of tricalcium silicate from 1 year to 1 day. He states that the reduction in hydration time is due to the removal of the hydrated calcium silicates from the surface of the unhydrated tricalcium silicate particles. This exposes fresh material to water and therefore completes the hydration rapidly.

It might also be wise to select one of the National Bureau of Standards fly ashes for study in the future. These fly ashes were created under well documented conditions and a significant amount of research has already been performed to characterize these materials. With this large base of research, it would probably be easier to interpret some of the results from the lime/fly ash experiments.

An alternate material would be blast furnace slag, which has a chemical composition similar to some of the higher-calcium fly ashes. Blast furnace slags are, reportedly, more uniform than coal fly ashes and tend to vary less from day-to-day.

Previous research has shown that the addition of phosphates to slurries of $Ca(OH)_2$ and fly ash increased the reactivity of the resulting lime/fly ash materials. The phosphates presumably increase the fly ash dissolution rate and therefore increase the production of lime/fly ash materials. It would be easy to perform fly ash dissolution experiments to quantify the effect of these phosphates on the dissolution rate of fly ash.

Although the lime/fly ash solids seem to have high potential for use in FGD systems, little work has been performed to determine the disposal characteristics for the waste solids from the FGD systems. Presumably, these materials could be safely land-filled. However, these materials may have application as additives to concrete mixtures to replace part of the portland cement normally present in concrete. It would be interesting to test the performance of these waste solids in standard concrete strength development tests to determine if the waste solids have a potential commercial market.

Another pozzolan which may have potential use in the production of calcium-silicate materials for FGD is the ash produced from the burning of rice-husks, a byproduct of the rice-farming industry. In the past, these rice-husks were burned on-site in large piles, but environmental considerations will soon require these materials to be sent to an incinerator where large quantities of ash will be created and collected. These ashes are nearly pure amorphous silica and would undoubtedly combine easily with $Ca(OH)_2$ to produce solids which are very reactive towards SO_2.

Finally, another area of research concerns the recycle of container glass. Large amounts of this glass are produced and, subsequently, land-filled each year. Since these glasses contain a high amount of sodium and silica and very little aluminum, they might be suitable raw materials for the production of calcium-silicate materials for FGD.

Appendix A. Analytical Techniques

A.1 Atomic Absorption

Atomic absorption spectrophotometry is the most common method of flame spectrophotometry. The method is based on the absorption of electromagnetic radiation to induce an electronic transition for the absorbing element. The method is highly specific because the atomic absorption lines are very narrow and because electronic transition energies are unique for each element.

The most common source for atomic absorption measurements is the hollow cathode lamp, which consists of a tungsten anode and a cylindrical cathode sealed in a glass tube that is filled with neon or argon at a pressure of 1 to 5 torr. The cathode is constructed of the metal whose spectrum is desired or serves as a support for that metal.

In the analysis with atomic absorption, the liquid sample is aspirated into a spray chamber where it is thoroughly mixed with the fuel and oxidant gases. This mixture is then burned to produce a very hot flame (up to 3000°C) where a substantial fraction of the metallic elements are reduced to the elemental state. Radiation is passed through the atomized sample and into the slit of a spectrophotometer. In order to discriminate between radiation from the source and that which is emitted by the flame, it is common practice to chop the beam from the source before it reaches the flame. The detector circuitry is then designed to reject the dc output from flame emission and measure the ac absorption signal from the source and sample.

In theory, the absorbance should be proportional to concentration, but deviations from linearity often occur and empirical calibration curves must be prepared.

A Varian atomic absorption spectrophotometer (Model AA-1475-AB) was used to analyze filtrate samples from the fly ash/$Ca(OH)_2$ slurries. The samples were analyzed for dissolved calcium, aluminum, and silicon metals. Varian hollow cathode lamps were used for the analysis of the samples. All samples were analyzed using a nitrous oxide-acetylene flame to keep chemical interferences to a minimum. A background sodium concentration of 2000 ppm was used in all samples and standards to minimize the ionization of the metal species. The pH of all standards was adjusted to that of the samples to account for the change in liquid viscosity with pH. This adjustment helps keep the aspiration rate of the samples equal to that of the standards. The experimental conditions for each metal analysis are given in Table A.1

The standards for the analyses were prepared according to the methods described by Varma (1985). At the start of the study, calcium carbonate, aluminum metal, and sodium metasilicate (all from Fisher Scientific) were used to prepare 1000 ppm standards for calcium, aluminum, and silicon respectively. Atomic absorption standards were purchased from Fisher Scientific about one-fourth of the way through the study to check the laboratory prepared standards. No detectable deviation was observed, but the purchased standards were used for the rest of the study. These standards were diluted to the working range for the atomic absorption analyses.

During the analysis the spectrophotometer was calibrated with known standards at two different concentrations. The diluted samples were then analyzed. This calibration and analysis procedure was followed three times. The three experimentally determined concentrations were then averaged and multiplied by their dilution to determine the actual dissolved metal concentrations in the sample.

Table A.1 Summary of Parameters for Atomic Absorption Analysis

Element	Wavelength (nm)	Slit Width (nm)	Lamp Current (mA)	Detection Level (ppm)	Working Range (ppm)
Calcium	422.7	0.5	10	0.01	1 - 4
Aluminum	309.3	0.5	20	1.0	40 -200
Silicon	251.6	0.2	20	2.0	70 - 280

Spectrophotometer : Varian Model AA-1475-AB
Radiation Source : Varian Hollow Cathode Lamps
Fuel : Acetylene
Oxidant : Nitrous Oxide

There was little drift between calibrations and the experimentally determined concentrations were also quite reproducible.

A.2 BET Surface Area

The standard method for measuring surface area of porous solids is the Brunauer-Emmett-Teller (BET) method (Brunauer et al., 1938). The BET method is based on the physical adsorption of a gas, normally nitrogen at its boiling point (77 °K), on the surface of the solid. The method involves measuring the amount of nitrogen adsorbed (v) over a range of nitrogen pressures (p) below 1 atm.

The BET equation can be written as :

$$\frac{p}{v(p_o-p)} = \frac{1}{v_m C} + \frac{(C-1)p}{C v_m p_o} \qquad (A.1)$$

where p_0 is the saturation pressure, C is a constant for the particular temperature and gas solid system, and v_m is the volume of gas required to form a complete unimolecular adsorbed layer. A plot of $p/v(p_0 - p)$ versus p/p_0 will give a straight line. The intercept of this line (I) together with the slope of the line (S) gives v_m as :

$$v_m = \frac{1}{I+S} \qquad (A.2)$$

Once v_m is known, the surface area of the solid (S_g) can be calculated as :

$$S_g = \frac{v_m N_0 A}{v} \qquad (A.3)$$

Where :

N_0 = Avogadro's Number
v = molar volume of the gas at the conditions of v_m
A = surface area of one adsorbed molecule

The BET approach extends the Langmuir isotherm to apply to multilayer adsorption. It assumes that the rate of condensation of the gas on the bare surface is equal to the rate of evaporation from the first layer and that the heat of adsorption in layers other than the first is equal to the heat of liquefaction of the adsorbate material (i.e. Van der Waals forces of the adsorbent are transmitted only to the first layer) (Brunauer et al., 1938, Hill, 1977).

The surface area given by the BET method may not correspond exactly to the surface area of the solid, but the procedure is standardized and the results are reproducible (Smith, 1981).

The BET surface areas of lime/fly ash solids were measured in the laboratory using an Accusorb Model 2100E Physical Adsorption Analyzer. The adsorbent used was nitrogen at its normal boiling point. The experimental procedure followed was that specified in the Accusorb operations manual. The solids were evacuated overnight at 70 °C.

A.3 X-ray powder diffraction

X-ray powder diffraction was used to characterize the reactants and some of the lime/fly ash solids. The x-ray diffraction method is based on the scattering of x-rays by crystals, the scattering being caused by the electron atmosphere of the atom. When certain geometrical conditions as expressed by the Bragg law are satisfied, a diffraction pattern is produced by the scattering (Cullity, 1956).

The Bragg law states :

$$\lambda = 2\, d \sin\theta$$

Where :

λ = wavelength of the x-ray radiation
θ = diffraction angle
d = lattice spacing

The diffraction pattern can be used to identify crystalline materials and to determine their crystallline structure.

A constant-slit width, powder diffractometer was used to analyze the solids produced by the reaction of fly ash with $Ca(OH)_2$. The x-rays were produced using a copper x-ray tube operating at 35 kV and 20 mA. A graphite monochromator was used after the x-rays were deflected to pass only the copper K_α radiation. The lime/fly ash solids were mounted on glass slides using amyl-acetate, which acted as a "glue" to hold the particles to the slide. All of the samples were analyzed from 4 to 60 degrees two-theta.

The data from the x-ray analyses consisted both of a plot of intensity versus two-theta and a computer printout of the location of the diffraction peaks (i.e. the d-spacings). The on-line computer was able to distinguish most of the diffraction peaks, but many were missed and each plot was checked by hand to ensure that all peaks were catalogued. The data from these experiments are given in Appendix D.

Appendix B

Mathematical Treatment of Fly Ash Dissolution Data

To analyze the data from the fly ash dissolution experiments, a general rate expression was used :

$$\frac{dX}{dt} = k_1 * S_t * [OH]^a \qquad (B.1)$$

where :

- X = fraction of silica or aluminum that has dissolved
- t = time
- k_1 = reaction rate constant
- S_t = total surface area of the fly ash at time "t"
- $[OH]$ = concentration of hydroxide in the solution
- a = reaction order with respect to hydroxide

To simplify the analysis of the effect of fly ash surface area on the fly ash dissolution rate, the fly ash particles were assumed to be spherical particles of uniform size. This simplification was not necessary to analyze the effect of hydroxide concentration on the fly ash dissolution rate.

The total surface area of the fly ash is given by :

$$S_t = n * 4\pi * r^2_t \qquad (B.2)$$

where "n" is the number of fly ash particles and "r_t" is their radius at time "t".

The conversion of the particles is given by :

$$X = \frac{\text{Initial Mass - Final Mass}}{\text{Initial Mass}}$$

$$X = \frac{\frac{4}{3}\pi\rho r^3_o - \frac{4}{3}\pi\rho r^3_t}{\frac{4}{3}\pi\rho r^3_o}$$

$$X = \frac{r^3_o - r^3_t}{r^3_o} \qquad \text{(B.3)}$$

From (B.3), it is easy to see that the radius is a funtion of the conversion :

$$r_t = r_o*(1-X)^{1/3} \qquad \text{(B.4)}$$

Using this relationship, we can simplify (B.1) :

$$\frac{dX}{dt} = k_1*n*4\pi*r^2_o*(1-X)^{2/3} * [OH]^a \qquad \text{(B.5)}$$

By separating and re-defining constants, (B.5) becomes :

$$\frac{dX}{(1-X)^{2/3}} = k_2*S_o*[OH]^a * dt \qquad \text{(B.5)}$$

where S_o is the initial surface area of the fly ash and k_2 is a constant.

B.1 Surface area analysis

Since the hydroxide concentration in the slurry was 0.1 M for all of the experiments to determine the effect of fly ash surface area, equation (B.5) can be rewritten as :

$$\frac{dX}{(1-X)^{2/3}} = k_3*S_o * dt \qquad \text{(B.6)}$$

Integration of this equation gives :

$$3*(1-X)^{1/3} = -k_3 S_o t \qquad (B.7)$$

So a plot of $-(1-X)^{1/3}$ versus time should give a straight line with a slope proportional to the inital surface area of the fly ash. Figure B.1 shows that, for low conversions, straight lines were observed for all of the ground fly ash samples. Figure B.2 shows that the slopes of the lines in Figure B.1 are proportional to the initial surface area of the fly ash, as it should be according to (B.7).

These results show that the initial dissolution rate of the fly ash is proportional to the initial surface area of the fly ash.

B.2 Effect of hydroxide concentration

To analyze the effect of hydroxide concentration on the fly ash dissolution rate, notice that, for a given conversion (say X_0), the left hand side of equation (B.5) is a constant, so the right hand side must also be a constant :

$$k_2 * S_o * [OH]^a * t_{X_o} = \text{constant}$$

Therefore, a plot of $(1/t_{X_o})$ versus [OH] on log-log paper should be a straight line of slope "a". This was shown to be the case for the dissolution of aluminum and silicon from the low-calcium fly ash.

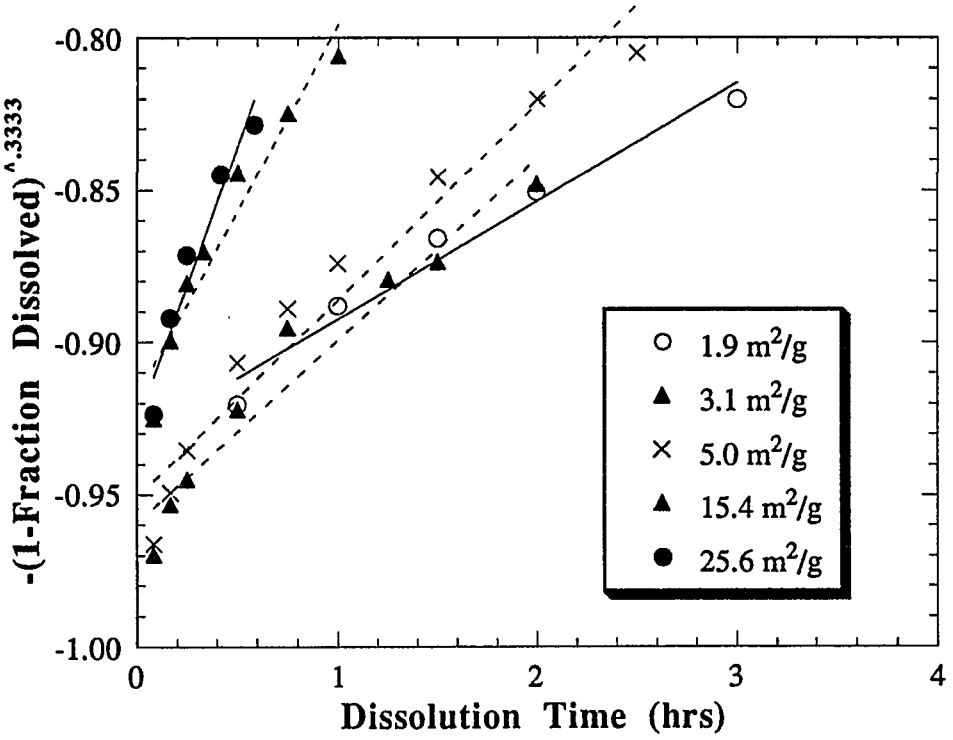

Figure B.1 Effect of initial surface area of the fly ash on the initial dissolution rate of silica from a low-calcium fly ash.

90 °C, 1.25 g Clinch River fly ash/liter; 5 g Na_2EDTA/liter;
0.1 M NaOH, stir speed : 1000 rpm.

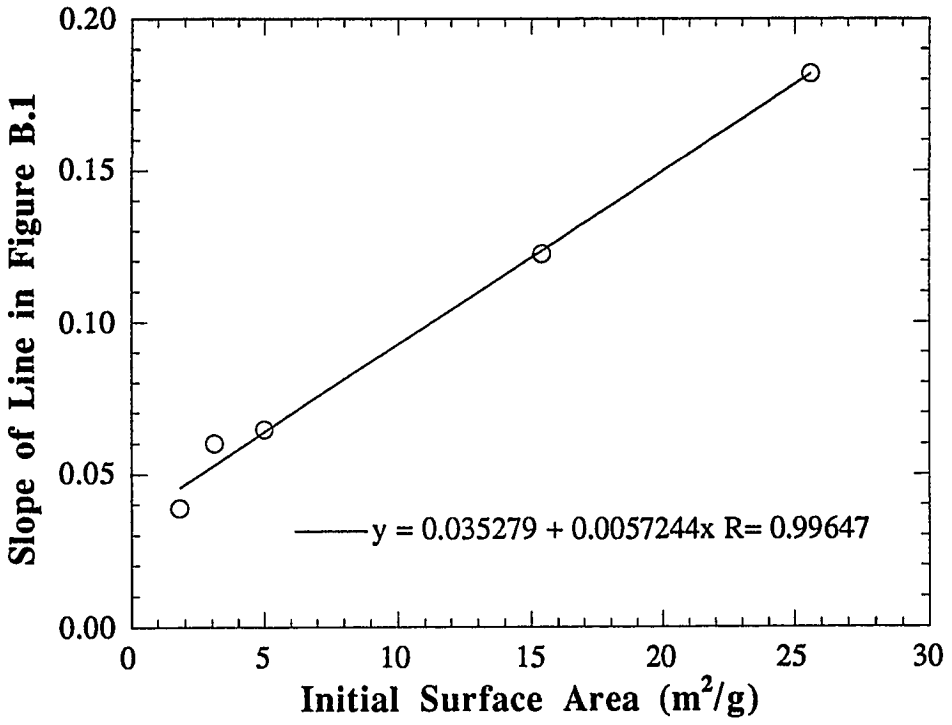

Figure B.2 Graphical analysis of effect of fly ash surface area.

REFERENCES CITED

ASTM C 219-76a, Annual Book of ASTM Standards, part 13, pp 203 - 204, Society for Testing and Materials, Philadelphia, PA, 1980.

Babu, M.,College, J., Forsythe, R., Herbert, R., Kanary, D., Kerivan, D., and K. Lee, "5-MW Toronto HALT Pilot Plant Testing - Final Test Results", DOE contract # DE-AC22-85PC81012, December, 1988.

Blythe, G., V.Bland, C. Martin, M. McElroy, and R. Rhudy. "Pilot-Scale Studies of SO_2 Removal by the Addition of Calcium-Based Sorbents Upstream of a Particulate Control Device", In: *Proceedings: Tenth Symposium on Flue Gas Desulfurization*, **2**, pp 84-105, EPA-600/9-87-004a, 1986.

Brown, P.W., and P. LaCroix, "The kinetics of ettringite formation", Cement and Concrete Research, **19**, pp 879-884, 1989.

Brunauer S., P.H. Emmett, and E. Teller, "Adsorption of Gases in Multimolecular Layers", J. Am. Chem. Soc., **60**, pp 309-319, 1938.

Burnett, T.A., L. Larkin, and R.L. Torstrick, "Economic Analysis and Comparison of Wet and Dry Scrubbing for Utility Application," Presented at the *Seminar on Dry Scrubbing Sponsored by Joy Industrial Equipment, Western Precipitation Division/Niro Atomizer*, Minneapolis, MN, 1981.

Cabrera, J.G.,C.J. Hopkins, G.R. Woolley, R.E. Lee, J. Shaw, C. Plowman, and H. Fox, "Evaluation of the properties of British pulverized fuel ashes and their influence on the strength of concrete", In : *Proceedings of the Second International Conference on Fly Ash, Silica Fume, Slag, and Natural Pozzolans in Concrete*, Madrid, Spain, 1986.

Chang, J.C.S., and C.B. Sedman, "Scale-Up Testing of the ADVACATE Damp Solids Injection Process", In :*Proceedings of the First Combined FGD and Dry SO_2 Control Symposium*, St. Louis, MO, October, 1988.

Chu, P., and G.T. Rochelle, "Removal of SO_2 and NO_x from Stack Gas By Reaction with $Ca(OH)_2$ Solids", M.S. Thesis, The University of Texas at Austin, 1986B.

Chu, P., and G.T. Rochelle. "SO_2/NO_x Removal by $Ca(OH)_2$", ,In: *Proceedings: Tenth Symposium on Flue Gas Desulfurization*, **2**, 50-58, EPA-600/9-87-004a, 1986A.

Cummins, A.B., and L.B. Miller, "Diatomaceous earth", Ind. and Eng. Chemistry, **26**, pp 688-693, 1934.

Cullity, B.D., Elements of X-ray Diffraction, Addison-Wesley, Reading, Massachusetts, 1956.

Drabkin, M., and E. Robison, "Spray Dryer FGD Capital and Operating Cost Estimates for a Northeastern Utility", In: *Proceedings: Symposium on Flue Gas Desulfurization*, **2**, pp 731-760, EPA-600/9-81-019b, (NTIS PB81-243164), 1981.

Drummond, C.J., Babu, M., Demian, A., Henzel, D.S., Kanary, D.A., Kerivan, D., Lee, K., Murphy, K.R., Newman, J.T., Samuel, E.A., Statnick, R.M., and M.R. Stouffer, "Duct Injection Technologies for SO_2 Control", In : *Proceedings of the First Combined FGD and Dry SO2 Control Symposium*, St. Louis, MO, October, 1988.

Edgar, Thomas F., Coal Processing and Pollution Control, Gulf Publishing Company, Houston, 1983.

Gooch, J.P., E.B. Dismukes, R.S. Dahlin, M.G. Faulkner, M.G. Klett, T.L. Buchanan, and J.E. Hunt, "Scaleup tests and supporting research for the development of duct injection technology : Literature Review", Prepared for the U.S. Department of Energy, May, 1989.

Greenberg, S.A., and T.N. Chang, "Investigation of the colloidal hydrated calcium silicates. II. Solubility relationships in the $CaO\text{-}SiO_2\text{-}H_2O$ system", J. Phys. Chem., **69**, pp 182-188, 1965.

Greenberg, S.A., "The depolymerization of silica in sodium hydroxide solutions", J. Phys. Chem., **61**, pp 960-965, 1957.

Greenberg, S.A., "Thermodynamic Functions for the Solution of Silica in Water", J. Phys. Chem., **61**, pp 196-197, 1957.

Greenberg, S.A., T.N. Chang, and E. Anderson, "Investigation of Colloidal Hydrated Calcium Silicates. I. Solubility Products", J. Phys. Chem., **64**, pp 1151-1157, 1960.

Hemmings, R.T., and E.E. Berry, "On the glass present in coal fly ashes : Recent advances", Materials Research Society Symposia Proceedings, **113**, pp 3-38, 1989.

Hemmings, R.T., and E.E. Berry, "Speciation in size and density fractionated fly ash", Materials Research Society Symposia Proceedings, **65**, pp 91-104, 1986.

Hill, C.G., An Introduction to Chemical Engineering Kinetics and Reactor Design, John Wiley & Sons, Inc., 1977.

Iler, R.K., "Effect of Adsorbed Alumina on the Solubility of Amorphous Silica in Water", J. of Colloid and Interface Science, **43**, pp 399-408, 1973.

Iler, R.K., The Chemistry of Silica, John Wiley & Sons, New York, 1979.

Ireland, P.A., G.D. Brown, W.F. Frazier, and P.T. Radcliffe, "Site Specific Evaluation of Six Sorbent Injection Processes", In : *Proceedings of the First Combined FGD and Dry SO_2 Control Symposium*, St. Louis, MO, October, 1988.

Jankura, B.J., J.B. Doyle, and T.J. Flynn, "Dry Scrubber, Flue Gas Desulfurization on High-Sulfur, Coal-Fired Steam Generators: Pilot Scale Evaluation," In: *Proceedings: Eighth Symposium on Flue Gas Desulfurization*, EPA Report 600/9-84-017b,NTIS PB84-226646, 1984.

Jozewicz, W., J.C.S. Chang, C.B. Sedman, and T.G. Brna, "Silica-enhanced sorbents for dry injection removal of SO2 from flue gas", JAPCA , **38**, 1027-1034, 1988A.

Jozewicz, W. and G.T. Rochelle, "Dry Scrubbing: Flyash Recycle," Final Draft Report for EPA Cooperative Agreement CR 81 1531, Washington, D.C., 1986B.

Jozewicz, W. and G.T. Rochelle, "Fly Ash Recycle in Dry Scrubbing," J. Env. Prog., **5**, pp 218-223, 1986A.

Jozewicz, W., C. Jorgensen, J.C.S. Chang, C.B. Sedman, and T.G. Brna, "Development and Pilot Plant Evaluation of Silica-Enhanced Lime Sorbents for Dry Flue Gas Desulfurization", In: *Proceedings: Tenth Symposium on Flue Gas Desulfurization*, **2**, pp 123-144, EPA-600/9-87-004a, 1986A.

Jozewicz, W., J.C.S. Chang T.G. Brna, and C.B. Sedman, "Reactivation of Solids from Furnace Injection of Limestone for SO_2 Control", Environ. Sci. Technol., 1987, **21**, pp 664-670.

Jozewicz, W., J.C.S. Chang, C.B. Sedman, and T.G. Brna, "Characterization of Advanced Sorbents for Dry SO_2 Control," Reactivity of Solids, **6**, pp 243-262, 1988B.

Jozewicz, W., J.C.S. Chang, T.G. Brna, and C.B. Sedman, "Reactivation of Solids from Furnace Injection of Limestone for SO_2 Control," In : *Proceedings of the Second Joint Symposium on Dry SO_2 and Simultaneous SO_2/NO_x Control Technologies*, Raleigh, North Carolina, 1986B.

Karlsson, H.T., J. Klingspor, M. Linne, and I. Bjerle, "Activated Wet-Dry Scrubbing of SO_2," APCA Journal, **33**, pp 23 - 28, 1983.

Lea, F.M., The Chemistry of Cement and Concrete, Chemical Publishing Company, New York, New York, 1971.

Manz, O.E., and G.J. McCarthy, "Effectiveness of Western U.S. high-lime fly ash for use in concrete", In : *Proceedings of the Second International Conference on Fly Ash, Silica Fume, Slag, and Natural Pozzolans in Concrete*, Madrid, Spain, 1986.

McCarthy, G.J., F.P. Glasser, D.M. Roy, Materials Research Society Symposia Proceedings, **65**, December, 1985.

McCarthy, G.J., O.E. Manz, D.M. Johansen, S.J. Steinwand, and R.J. Stevenson, "Correlations of chemistry and mineralogy of Western U.S. fly ash",Materials Research Society Symposia Proceedings, **86**, December, 1986.

McCarthy, G.J., K.D. Swanson, L.P. Keller, and W.C. Blatter, "Minerology of Western Fly Ash", Cement and Concrete Research, **14**, pp 471-478, 1984.

Mehta, P.K., "Pozzolanic and Cementitious By-Products in Concrete --- Another Look", In : *Proceedings of the 3rd International Conference on : Fly Ash, Silica Fume, Slag, and Natural Pozzolans in Concrete*, Trondheim, Norway, 1989.

Mehta, P.K., "Pozzolanic and Cementitious Byproducts as Mineral Admixtures for Concrete - A Critical Review", ACI, **SP-79**, pp. 1- 46, 1983.

Melia, M.T., R.S. McKibben, and F.M. Jones, "Trends in commercial applications of FGD", In: *Proceedings: Tenth Symposium on Flue Gas Desulfurization*, EPA-600/9-87-004a, 1986.

O'Conner, T.L., and S.A. Greenberg, "The Kinetics for the Solution of Silica in Aqueous Solutions", J. Phys. Chem., Vol.68, 1195-1198, 1958.

Petersen, T.P., J.R. Peterson, H.T. Karlsson, and I. Bjerle, "Physical and Chemical Activation of Fly Ash to Produce Reagent for Dry FGD Processes", In : *Proceedings of the First Combined FGD and Dry SO_2 Control Symposium*, St. Louis, MO, October, 1988.

Peterson, J.R., M.D. Durham, and N.S. Vlachos, "Fundamental Investigation of Duct/ESP Phenomena", Prepared for the U.S. Department of Energy, Contract AC22-88PC88850, May, 1989.

Peterson, J.R., and G.T. Rochelle, "Aqueous Reaction of Fly Ash and Ca(OH)2 to Produce Calcium Silicate Absorbent for Flue Gas Desulfurization", J. of Envir. Sci. and Tech., **22**, 1988A.

Peterson, J.R., and G.T. Rochelle,"Production of lime/fly ash absorbents for flue gas desulfurization" , In : *Proceedings of the First Combined FGD and Dry SO_2 Control Symposium,* St. Louis, MO, October, 1988B.

Quian, J.C., and F.P. Glasser, "Bulk Composition of the Glassy Phase in some Commercial PFA's", Materials Research Society Symposia Proceedings, **113**, 1988.

Quian, J.C., E.E. Lachowski, and F.P. Glasser, "The Microstructure of National Bureau of Standards Reference fly ashes", Materials Research Society Symposia Proceedings, **136**, 1989.

Raask, E., and M.C. Bhaskar, "Pozzolanic activity of pulverized fuel ash", Cement and Concrete Research, **5**, pp. 363-376, 1975.

Robards, R.F., R.W. Aldred, T.A. Burnett, L.R. Humphries, and M.J. Widico, "High-sulfur spray dryer evaluations," In: *Proceedings: Ninth Symposium on FGD*, pp 621-642, EPA-600/9-85-033b, 1985.

Smith, J.M., Chemical Engineering Kinetics, McGraw-Hill, Inc., 1981.

Stevenson, R.J., and T.P. Huber, "SEM Study of Chemical Variations in Western U.S. Fly Ash", Materials Research Society Symposia Proceedings, **86**, December, 1986.

Taylor, H.F.W., "Hydrated Calcium Silicates. Part I. Compound Formation at Ordinary Temperatures", Chemical Society Journal, pp 3682-3689, 1950.

Taylor, H.F.W., The Chemistry of Cements, **1**, Academic Press, New York, 1964.

Tikalsky, P.J., Dissertation, The University of Texas at Austin, 1989.

Varma, A., Handbook of Atomic Absorption Analysis, CRC Press, 1985.

Wilkinson, J.M., and D.P. Tonn, "Baghouse vs. Precipitator for Dry Scrubber Systems - Pilot Study Results", In : *Proceedings : Coal Technology Conference*, Houston, November 17-19, 1981.

VITA

Joseph Roger Peterson was born in Belvidere, Illinois, on June 2, 1963, the son of Mary Margaret Peterson and Gerald Roger Peterson. After graduating from Belvidere High School, Belvidere, Illinois (1981), he entered The University of Illinois in Champaign-Urbana, Illinois. He received a Bachelor of Science in Chemical Engineering from The University of Illinois in May, 1985. In September, 1985, he entered The Graduate School of The University of Texas. He worked under the supervision of Dr. Gary Rochelle and received a Masters of Science in Chemical Engineering in August of 1987. From Austin he traveled to Lund, Sweden, where he worked for six months under the supervision of Dr. Ingemar Bjerle in the Department of Chemical Engineering at the University of Lund. In March of 1988 he returned to The University of Texas to enroll in the doctoral program in chemical engineering. In January of 1989 he started working part-time for Radian Corporation in Austin as he continued his PhD studies. Upon completion of requirements for the Ph.D. in Chemical Engineering, he will work as a Staff Engineer for the Process Engineering Department at Radian Corporation in Austin, Texas.

Permanent Address: 1001 E. Lincoln
Belvidere, Illinois 61008

This dissertation was typed by Joseph Roger Peterson.